Active Vibration Control of Flexible Structures under Input Saturation through Delay-Based Controllers and Anti-Windup Compensators

Ricardo Falcón-Prado

université PARIS-SACLAY

NNT : 2023UPASG042

Active Vibration Control of Flexible Structures under Input Saturation through Delay-Based Controllers

Thèse de doctorat de l'Université Paris-Saclay
École doctorale n°580 Sciences et Technologies de l'Information et de la Communication (STIC)
Spécialité de doctorat: Automatique Graduate School : Informatique et Sciences du Numérique.

Référent : Faculté des Sciences d'Orsay
Thèse préparée dans l'unité de recherche Laboratoire des Signaux et Systèmes (Université Paris-Saclay, CNRS, CentraleSupélec), sous la direction d'**Islam BOUSSAADA**, Professeur des Universités, et le co-encadrement de **Sami TLIBA**, Maître de Conférences.

Thèse soutenue à Paris-Saclay, le mercredi 7 juin 2023, par

Ricardo FALCÓN-PRADO

Composition du Jury :

Salah LAGHROUCHE Professeur des Universités, Université de Technologie de Belfort-Montbéliard (FEMTO-ST)	Rapporteur
Mohamed DJEMAI Professeur des Universités, Université Polytechnique Hauts-de-France (LAMIH)	Rapporteur
Sihem TEBBANI Professeur des Universités, CentraleSupélec (L2S)	Examinatrice
Ali EL ATI Enseignant-Chercheur, Institut Polytechnique des Sciences Avancées (IPSA)	Examinateur
Juan Antonio ESCARENO Maître de Conférences, Université de Limoges (XLIM)	Examinateur
Kaïs AMMARI Professeur des Universités, Université de Monastir (FSM)	Invité

Université Paris-Saclay

université PARIS-SACLAY
ÉCOLE DOCTORALE
Sciences et technologies de l'information et de la communication (STIC)

Titre: Contrôle actif de vibration d'une structure flexible soumise à une saturation d'entrée par contrôleur basé retard et compensateur anti-windup

Mots clés: systèmes à retard, contrôle de vibration, structures flexibles, command $\mathcal{H}_\infty$, analyse spectrale, approche par LMI, systèmes des données echantillones

Résumé: Dans ce travail, on traite le problème du commande actif des vibrations robustes pour une structure mécanique flexible à travers des techniques pour des systèmes à dimensions infinis et finis. Les approches abordées sont reglées pour une commande à retour de sortie basée sur une commande aux actions retardées proportionelles, par une approche basée sur quasipolynomials, et une commande synthétisée par la méthode $\mathcal{H}_\infty$ avec une approche par LMIs. Le but c'est l'analyse de ses capabilités pour amortisser les modes vibratoires dans une bande passante d'intérêt, et éviter les effets dénommés de phénomène "spillover". Cettes commandes sont sythétisés à travers d'un modèle de dimensions finies, dérivé à partir d'un analyse des dimensions finies des structures mécaniques, combiné avec des methodes de réduction.
Les structures flexibles envisagées ici sont, d'abord, une poutre flexible d'aluminium à la configuration Euler-Bernoulli, dont un bout est encastrée et l'autre libre, deuxièmement, une membrane axisymmetrique. Chaque système est instrumenté d'un capteur et d'un actionneur piézoélectrique, ils sont bien soumises à chaque coté des structures et elles sont bien placées. Notre intention est d'examiner les performances susmentionnés par les environnements de simulation numérique et la mise en œuvre à titre expérimental.

Title: Active Vibration Control of Flexible Structures under Input Saturation through Delay-Based Controllers and Anti-Windup Compensators

Keywords: time-delay systems, vibration control, flexible structures, $\mathcal{H}_\infty$ control, spectral analysis, LMI approach, sampled-data systems

Abstract: In this work, the problem of active vibration control of flexible mechanical structures is addressed through infinite and finite dimensional techniques. The compared approaches are adjusted for an output feedback controller based on delayed proportional actions, through a quasipolynomial-based approach, and an optimal $\mathcal{H}_\infty$ controller design computed with an LMI approach. They are shown in order to analyze their capabilities to damp some vibrational modes in the frequency bandwith of interest, and to avoid the so called "spillover" phenomenon. These controllers are synthetized through a finite dimensional model, derived from a finite element analysis of the mechanical structure, combined with some reduction methods.
The flexible structures considered here are, firstly, a flexible aluminium beam in the Euler-Bernoulli configuration, and secondly, an axysimmetric membrane. Both of them are equipped with two piezoelectric patches that are bounded and collocated on each face of the structure. We intend to examine and discuss the aforementioned performances in both simulation and experimental environments.

Université Paris-Saclay
Espace Technologique / Immeuble Discovery
Route de l'Orme aux Merisiers RD 128 / 91190 Saint-Aubin, France

To my wife Rihab and my son Youssef Alexander,

without whom this work would have never been completed.

Acknowledgements

I want to show my gratitude and my sincerest recognition to my supervisors, Islam BOUSSAADA and Sami TLIBA, for giving me the opportunity to learn and collaborate at their side, for choosing such an interesting and broad subject, and for providing a very excellent guidance throughout the years working together. I would like to thank Daniel ALAZARD and Elena PANTELEY for their insightful comments and their interesting questions and remarks during my midterm evaluation. I want to specially thank Silviu NICULESCU for receiving me in his research group.

I extend my sincere gratitude to the rapporteurs of my manuscript, Professor Salah LAGHROUCHE and Professor Mohamed DJEMAI, whose valuable insights, meticulous observations, and thoughtful annotations contributed to enhancing the readability and organization of this manuscript. I would like also to express my thanks to the members of my thesis defense jury, Professor Sihem TEBBANI, Professor Juan Antonio ESCARENO and Professor Kais AMMARI, for their insightful questions and observations during the defense which contributed to the discussion.

I am also thankful to Alejandro MARTÍNEZ GONZÁLEZ and Enrique HERNÁNDEZ DIEZ for their advices, insightful conversations and their dedication to their own thesis. In particular, I want to thank Diego TORRES GARCÍA for the good chats and his unwavering support during the final months of my thesis road.

And to my beloved wife, Rihab, your boundless encouragement and enduring love have been the cornerstone of my motivation and the driving force behind my achievement. Thank you for being my constant and endless source of inspiration.

Introduction en français

Le contrôle actif des vibrations des systèmes flexibles pose de sérieux problèmes dans de nombreux domaines industriels et scientifiques. Dans la littérature, nous pouvons trouver de tels problèmes, qu'ils ont tendance à apparaître dans une grande variété de systèmes, comme les ponts, les grues [161], les bâtiments [169, 160], les véhicules [69], les avions [131, 45, 75], etc. Tous ces systèmes ont tendance à être exposés à des vibrations, et s'ils ne sont pas construits pour supporter ces environnements extrêmes (vent, traversée de turbulences atmosphériques, moteurs en marche), ils peuvent les faire tomber en panne à cause de la fatigue, l'usure des connecteurs électriques, la fissuration de certaines pistes de cuivre, etc. De fortes contraintes peuvent apparaître dans les composants lors des pics de résonance si plusieurs pièces possèdent les mêmes fréquences de résonance. Normalement, lorsqu'un ingénieur doit concevoir des composants, il est primordial de connaître l'environnement dans lequel il va travailler. L'ingénieur doit posséder des compétences de grande valeur afin de mettre en œuvre les simulations pour émuler les phénomènes qui agiront sur les composants. L'amortissement actif des vibrations [141] est un outil particulier qui, avec des capteurs et des actionneurs appropriés, peut permettre de manipuler une structure mécanique flexible comme un système dynamique d'entrée-sortie de dimension infinie. Ce problème peut être résolu avec des outils tels que Méthode des Éléments Finis [110], pour approcher un système donné en un système linéaire de dimension finie.

Le contrôle actif de vibrations, qui aussi sont appelés d'isolation active des vibrations ou d'annulation active des vibrations, sont les systèmes qui réagissent, de façon dynamique, c'est-à-dire, sont capables de capter et de réagir à ces vibrations en conséquence. L'amortissement des vibrations c'est la réduction des pics de résonance par la dissipation de l'énergie vibratoire, ce qui peut être réalisé avec la conception d'un contrôleur qui stabilise l'approximation linéaire de la dynamique de la structure flexible [141]. L'isolation des vibrations c'est où l'origine de l'excitation vibratoire et les parties sensibles du système à être isolées sont séparées avec des dispositifs auxiliaires qui sont appellés des isolateurs de vibrations ou des montures d'isolateurs de vibrations [146]. Par ailleurs, il y a deux types généraux des systèmes d'annulation des vibrations : les systèmes de commande prédicitive et ceux pour retour de sortie [123, 104]. Les systèmes de commande prédictive sont programmés spécifiquement pour compenser les vibrations périodiques régulières, de tel façon que, cette méthode peut anticiper et corriger les vibrations avant leur production. Les systèmes de rétroaction détectent et réagissent en permanence aux vibrations entrantes, en ajustant les erreurs au fur et à mesure qu'elles se produisent. Typiquement ils ont un mécanisme qui détecte les vibrations d'entrée et un actionneur qui réagit par conséquence, soit par le réglage d'un

isolateur pour réduire les vibrations, ou bien, soit par la création d'un signal qui les réduit [154].

Les structures flexibles ont plusieurs avantages par rapport a celles des systèmes rigides. Parmi ceux-ci, nous retrouvons la légèreté, la vitesse de fonctionnement plus élevée et le moindre coût. Peu de systèmes possèdent les particularités d'être l'archétype général des structures flexibles. C'est le cas d'une poutre flexible ou d'une membrane axisymétrique, qui appartiennent à ce type de structures. Leur étude et leur analyse illustrent, clairement, les avantages offerts susmentionnés [76]. De plus, une révision extensive à propos des méthodes de modélisation, des analyses dynamiques, et des techniques de commande utilisées pour les manipulateurs flexibles, en incluant deux liens, est presentée en [111]. L'étude des structures flexibles s'applique dans les domaines industriels [43], comme les manipulateurs flexibles utilisés dans la chirurgie medical [109], avec les robots à roues [203], c'est aussi possible de les utiliser dans l'orbite terrestre [153], dans les oléoducs de haute mer[86, 186], des tubes prolongateurs pour le transport du pétrole [82], des câbles de grue pour le positionnement des charges [128], dans les avions à ailes battantes [77], pour les secours en cas d'incendie à échelle pivotante [53], dans les tours éoliennes [1], entre autres. Un obstacle qui se manifeste pour ces structures, est causé par les vibrations inattendues.

De plus, les effets des vibrations sont connus comme un obstacle pour le comportement des systèmes, qui conduissent vers une basse productivité et qui créent des ruptures par fatigue. Le contrôle vibratoire a été un sujet attirant pendant les dernières années par les communautés scientifique et industrielle. Des approches différentes ont été utilisé pendant les dernières décennies pour contrôler l'amortissement des modes de vibration dans les structures flexibles. Par exemple, en [125] diverses techniques sont rassemblées en utilisant des transducteurs piézoélectriques "shunt", qui sont encastrés dans les structures flexibles. Ils peuvent être utilisés comme des capteurs ou des actionneurs. Aussi une approche passive qui utilise des transducteurs piézoélectriques "shunt" pour réduire la vibration dans une roue d'un train a été utilisé en [115]. Les accéléromètres piézoélectriques sont très populaires mais ils ne peuvent pas mesurer les composantes continues [141]. Un autre exemple de cette démarche est la conception des lois de commande dans les cas des capteurs et des actionneurs non-colocalisés pour les structures flexibles, où il existe un nombre infini de modes de vibration. Leur points nodaux se trouvent entre les emplacements des capteurs et des actionneurs. Par conséquence les fréauences des modes du système se dirigent vers la partie droite du plan complexe [198].

Les techniques de placement de pôles sont utilisées dans des problèmes de contrôle très divers [159]. Le comportement robuste des systèmes dynamiques est souvent un sujet d'intérêt par le fait que les incertitudes sont inévitables. Sous une allocation des valeurs propres par régions, le comportement robuste peut être accompli. L'amortissement en boucle fermé peut être réalisé en forçant les emplacements des pôles dans les régions stables souhaitées du plan complexe, c'est-à-dire, à n'importe quelle région dans la partie gauche ouverte du plan complexe. Cette idée est une approche qui peut être réalisée en prenant en considération les contrôleurs $\mathcal{H}_\infty$, et en utilisant les inegalités de matrices linéaires (LMIs) pour spécifier une région exponentiellement stable (c'est-à-dire $\{s \in \mathbb{C} : \mathcal{R}(s) < 0\}$, où s répresente la variable complexe de Laplace) sur le plan complexe. Ces LMIs sont résolus avec l'utilisation de la méthode du point intérieur, efficace pour l'optimisation convexe. Une caractérisation des LMIs pour des régions convexes générales du plan complexe pour la synthèse du contrôleur $\mathcal{H}_\infty$ a été montré en [39]. Par ailleurs, des résultats importants de la stabilité-$\mathcal{D}$ avec régions

définies par LMIs, avec des incertitudes paramétriques suivies par des exemples illustratifs pour la conception dynamique des contrôleurs par retour de sortie sont traités en [40], où les pôles de la boucle fermée sont assignés à l'intérieur des régions spécifiques.

Le problème de la commande $\mathcal{H}_\infty$ a été initialement mis en évidence par les travaux de Zames [205], incluant plusieurs aspects englobés dans la sensibilité d'un système de rétroaction aux perturbations pour améliorer sa robustesse. Le problème de sensibilité minimale indiqué dans [205] s'est avéré comme un problème d'interpolation de Nevanlinna-Pick. Aussi, dans [7], pour placer les pôles à l'intérieur d'une région circulaire dans la moitié gauche du plan complexe.

Autre approche consiste à attribuer de manière robuste les valeurs spectrales dans la moitié gauche du plan complexe. Il s'agit essentiellement d'un problème des valeurs inverses propres, à la recherche d'une immunité contre les perturbations du système. Une mesure du conditionnement optimale auquelle on peut s'attendre pour un système particulier avec un ensemble donné des pôles pour évaluer l'application de ces derniers attribués est donnée dans [93]. L'affectation d'une structure robuste a été analysée dans [87], où un théorème d'analyse du retour de sortie dynamique a été proposé.

En raison des modes de vibration haute fréquence non modélisées qui apparaissent dans l'analyse fréquentielle des structures flexibles, les approches robustes ont tendance à être plus attirantes. Une autre approche qui utilise des patchs piézoélectriques a été montrée dans [177]. Dans [178], une amélioration pratique a été incluse dans le système où la préoccupation concernant la limitation des actionneurs est prise en compte.

Une façon de simmuler le comportement de ces systèmes d'ordre élevé consiste à utiliser des retards temporels, car il est possible de les réduire avec des variables d'état de dimension finie, voir [67]. D'autres références qui s'y trouvent, soulignent l'application des systèmes retardés dans de nombreuses disciplines comme l'ingénierie de contrôle : les procédés de fabrication (voir [83]), le moteur à combustion interne (voir [42]), la simplification et la réduction d'équations aux dérivées partielles (EDP) (voir [158]), les retards de communication dans la télécommande et le réseau par exemple un système de téléopérateur maître-esclave pour un robot est illustré dans [5] et une recherche sur les téléopérateurs bilatéraux se trouvent dans le survey [134], etc. Néanmoins, il est communément admis que les retards peuvent entraîner des effets déstabilisants sur la dynamique qu'ils impliquent, pour les systèmes sans retards il est possible d'utiliser des retards dans les actions de contrôle pour rétroaction pour atteindre l'objectif spécifié. L'un des premiers articles montrant cela, indiquait l'utilisation d'un contrôleur basé sur le retard pour améliorer la stabilité des systèmes avec un comportement oscillatoire et un faible amortissement dans [166]. Les propriétés concernant les fonctionnalités utiles des contrôleurs basés sur le retard ont été traitées récemment. Par exemple, une propriété appelée la dominance induite par la multiplicité (MID) a été prouvée et utilisée dans plusieurs applications de suppression des vibrations dans des travaux pionniers récents, voir [27].

Dans des travaux antérieurs, il a été montré que la multiplicité d'une valeur spectrale peut être bornée par une borne générique, que nous noterons B_{PS} tout au long de ce document. Aussi, il a été souligné que l'attribution exacte des B_{PS} valeurs spectrales différentes pour les systèmes à retard d'ordre inférieur, sans aucune exigence supplémentaire de multiplicité entre eux, garantit la dominance de ces modes non oscillants. Logiquement, si ces racines assignées sont négatives, la stabilité exponentielle du système est garantie. Dans le cas d'un système de deuxième ordre, la propriété de

dominance a été démontrée analytiquement avec une conception de placement des pôles pour le contrôle actif des vibrations dans [29], voir aussi [31]. En [17], un critère qui permet de caractériser l'effet stabilisateur donné par la coexistence des modes pour les équations différentielles retardées linéaires d'ordre n est donné. La stabilité et les performances des systèmes à retards ont une importance théorique et pratique. Par conséquent, l'analyse de stabilité est effectuée par des approches dans le domaine fréquentiel.

Nous considérerons ci-après deux approches de commande différentes pour un contrôle de dimension finie robuste des systèmes à paramètres distribués : une approche $\mathcal{H}_\infty$ optimale basée sur l'optimisation des LMI et une approche basée sur le retour de sortie proportionnel-retardé. La première implique l'analyse et la synthèse des techniques de placement de pôles robustes à l'aide des inégalités matricielles linéaires, atteignant une stabilité quadratique grâce à la synthèse de contrôleurs $\mathcal{H}_\infty$ [40]. La deuxième est basée sur des actions proportionnelles et retardées de la sortie mesurée et des signaux de commande [180]. Les deux approches sont spécifiques aux systèmes linéaires assurant les emplacements des pôles dans la moitié gauche du plan complexe, soit dans une région prescrite spécifique, ou bien soit dans des valeurs négatives spécifiques ponctuelles. Dernièrement, un grand intérêt s'est manifesté pour comprendre le comportement des retards en tant que paramètre de conception dans le contrôle des systèmes dynamiques.

Objectifs

Le sujet principal de cette thèse se divise en deux grandes parties. Premièrement, la description des structures flexibles soumis à des lois de la commande proportionnel-retardé et la commande $\mathcal{H}_\infty$ basée sur les LMIs, dans le domaine frequentiel et temporel. Deuxièmement, la conception du contrôle pour placement des pôles des systèmes à retard, où un contrôleur pour rétroaction est conçu de telle manière que les performances en boucle fermée du modèle de synthèse (d'ordre inférieur que le système d'origine), comprenant jusqu'aux trois premiers modes de vibration des structures flexibles considérées, seront bien amorties. De plus, la boucle fermée doit être robuste et stable face aux dynamiques non modélisées.

Avec la commande quasi-polynômial, nous mettons l'accent sur la synthèse et la conception des contrôleurs conus grâce à la connaissance de la racine la plus placée à droite dans le spectre des pôles du système. Au cours de cette thèse, nous envisageons à approfondir les connaissances de ces techniques émergentes. L'objectif géneral se développe en sous-objectifs qui se présentent comme suit :

Objectif 1. L'étude approfondie de lacommande linéaire, robuste et optimale, en se concentrant sur la technique de placement des pôles dans les régions convexes du plan complexe, et décrites par inégalités matricielles linéaires (LMI) pour les systèmes linéaires avec des incertitudes statiques sur la matrice d'état. Nous appliquons le résultat déduit pour la conception d'un correcteur dynamique pour rétroaction attribue d'une manière robuste les pôles du système dans une région LMI prédéfinie du plan complexe et minimise un coût $\mathcal{H}_\infty$.

Objectif 2. L'approche de modélisation des structures mécaniques minces, de type plaque, permet l'utilisation des modèles

mathématiques linéaires et de dimension finie et sa réduction modale correspondante pour la synthèse du contrôleur.

Objectif 3. L'analyse de ces systèmes de synthèse d'ordre inférieur que les systèmes d'analyse qui permet la synthèse des correcteurs et l'exploitation d'avantage de leur application pour les systèmes de dimension finie d'ordre supérieur dans une gamme de fréquences plus large.

Objectif 4. L'effet de pôles réels dans le plan complexe, qui sont une conséquence directe des quasi-polynômes et leur impact dans le contrôle actif de vibrations de structures mécaniques flexibles considérés. Nous nous intéressons à la racine dominante d'un quasi-polynôme, qui est caractérisée soit par la coexistence des racines réelles différentes, ou soit par la multiplicité de racines réelles dans la moitié gauche du plan complexe.

Dans un effort pour atteindre ces objectifs énumérés ci-dessus, nous envisageons une analyse dans le domaine fréquentiel. Pour l'application de tels correcteurs, nous devons nous assurer que leur ordre est relativement bas. Pour cela, nous utilisons un modèle de synthèse des structures flexibles considérées, qui est obtenu à partir d'un modèle d'analyse par des techniques de réduction bien connues. Cela introduit une autre exigence de stabilité robuste, où le contrôleur d'un modèle d'ordre inférieur doit garantir le bon contrôle lorsqu'il est appliqué au modèle d'ordre supérieur de la structure flexible, appelé " modèle d'analyse ", et qui décrit les structures mécaniques flexibles dans une plage de fréquences plus large. Quant à la contribution principale liée à l'approche basée sur les quasi-polynômes, nous étudions sa version en temps discret avec un retard proportionnel au temps d'échantillonnage.

Structure du manuscrit

Le présent travail est organisé comme suit. Les résultats de base sont rassemblés dans le chapitre 2. Le chapitre 3 introduit les prérequis et décrit les systèmes flexibles que nous considérons. Un contrôleur $\mathcal{H}_\infty$ optimal est présenté au chapitre 4. La méthodologie récente qui induit le placement des pôles dominants non oscillants dans l'axe réel négatif est explorée dans le chapitre 5. La conception de compensateurs anti-windup, dont le but est de peaufiner les contrôleurs linéaires, ce qui agrandit l'ordre du système en boucle fermée, qui permettent de réduire les saturations du système, et les résultats des simulations numériques appliquées au problème de suppression des vibrations d'une poutre flexible sont exprimés au chapitre 6. Enfin, dans le chapitre 7 les remarques et observations finales sont discutées.

Contents

List of Figures

List of Tables

Chapter 1

Introduction

This chapter serves as an introduction to the manuscript and sets the stage for the subsequent chapters. In this first chapter, firstly we introduce the motivation of this research, secondly the objectives proposed for this dissertation are outline, and finally the manuscript structure is presented. We then outline the structure of the manuscript and conclude by listing the publications that have contributed to this work.

In Section 1.1, we discuss the context and motivation for the research. We highlight the current state of the field, identify gaps in knowledge, and articulate the research questions that this study aims to address. We also discuss the significance of the study and its potential impact.

In Section 1.2, we lay out the specific objectives of the research. We describe the research questions that we aim to answer and the methods that we will use to achieve our objectives.

In Section 1.3, we provide an overview of the structure of the manuscript. We describe each chapter's content, and the methods used. This overview will help readers navigate the manuscript and understand how the different chapters contribute to the overall research objectives.

In final Section 1.4, we list the publications that have contributed to this work. These publications have provided the foundation for the research and have been used to support the arguments made in this manuscript.

Overall, this introduction chapter sets the tone for the rest of the manuscript and provides a comprehensive overview of the research. It outlines the context and motivation, research objectives, manuscript structure, and list of publications that have contributed to the study.

Contents

1.1 Context and motivation

The active vibration control of flexible systems causes serious problems in many industrial and scientific fields. In the literature we can find such problems, and they tend to appear in a wide variety of systems, as bridges, cranes [161], buildings [169, 160], vehicles [69], airplanes [131, 45, 75], etc. All these systems tend to be exposed to vibrations, and if they are not constructed to endure these extremes environments (wind, crossing of atmospheric turbulences, working engines), they can cause them to fail due to fatigue, wearing away the electrical connectors, cracking some copper tracks, etc. High stresses can appear in components during the resonance peaks if several parts own the same resonant frequencies. Normally, when an engineer needs to design components, it is of paramount importance to know the environment in which it will work. The engineer needs to possess high valuable skills in order to set the correct initial conditions in the simulations to emulate the phenomena that will be acting on the component. Vibration damping is a particular tool that, with appropriate sensors and actuators, can allow to manipulate a mechanical flexible structure as an input-output dynamical system of infinite dimension. This problem can be tackled with tools such as the Finite Element Method [110], to approximate a given system into a linear system of finite dimension.

Active vibration control systems, also called active vibration isolation or active vibration cancellation, are isolation systems that dynamically react to incoming vibrations, e.i., they sense incoming vibrations and react to them. Different approaches for achieving this vibration reduction can be considered, where we can find vibration stiffening, damping and isolation as the most common ones. Vibration stiffening involves shifting the resonance frequencies of the flexible structure under consideration out of the range of the frequency span of interest [183]. Vibration damping is founded on reducing the resonance peaks by dissipating the vibration energy, which can be performed through the design of a stabilizable controller for the linear approximation of the flexible structure dynamics [141]. Vibration isolation is where the origin of vibration excitation and the sensitive parts of the system to be isolated are separated by auxiliary devices called vibration isolators or vibration isolating mounts [146]. Additionally, there are two general types of active vibration cancellation systems: feedforward and feedback systems [123, 104]. Feedforward systems are specifically programmed to compensate for regular periodic vibrations, this way, this method anticipates and corrects the vibrations before they happen. Feedback systems continually sense and react to incoming vibrations, adjusting the errors as they take place. Typical feedback systems have a sensing mechanism which senses incoming vibrations and an actuator which reacts to these vibrations, either by tuning an isolator to reduce the incoming vibrations or creating a signal which reduces them out [154].

Flexible structures have several advantages over those rigid-body structures. Among those we find the lightweight, higher operation speed and lower cost. Few systems have the particularity of being the touchstone of a general archetype of structures. This is the case of the flexible beam system, which belongs to this class of structures, and its study and analysis illustrates, clearly, the advantages mentioned above [76]. Moreover, an extensive review on the modeling methods, dynamical analyses and control techniques employed for flexible manipulators including two links is presented in [111]. The study of these flexible structures finds applications in, industrial as well as scientifical areas [43], such as flexible

manipulators used in surgical procedures [109], wheeled robots [203], it finds also Earth's orbital utility [153], deep-sea oil pipelines [86, 186], marine mooring lines for station keeping [193, 78], marine risers for oil transportation [82], crane cables for positioning the payload [128], the flapping-wing robotic aircraft [77], the fire rescue turntable ladder [53], the wind turbine tower [1], among other systems. Also, severe hindrance in the performance of such structures is caused due to undesired vibrations.

Moreover, since vibration effects are known to be a system performance hindrance, leading to low productivity and provoking early fatigue failures, vibration control has been a topic that gets a lot of attention during the last years by the scientific and industrial communities. Different approaches to the damping control of vibration modes in flexible structures have been used through the last decades. In [125] a number of techniques are collected using "shunted" piezoelectric transducers, which are embedded into the flexible structures, and can be used either as sensors or actuators. A passive approach using "shunted" piezoelectric transducers to mitigate vibration in a train wheel was used in [115]. Piezoelectric accelerometers are very popular but they cannot measure a D.C. component [141]. Another example of this procedure is the fact of designing controllers for the case of non-collocated, either sensors or actuators, in flexible structures, in which exist an infinite number of modes whose nodal points fall between the sensor and actuator locations, consequentely moving some of the system's eigenvalues into the right-half of the complex plane, [198].

Pole placement techniques are used in different control problems [159]. Robust behavior of dynamical systems is often a topic of interest due to the fact that uncertainties are inevitable. There exist several controller design methods which work with the assignment of a finite spectrum, such as, for example, the Linear-Quadratic regulator (LQR) controller, which sets a quadratic performance index to be minimized on the states and control input, the Linear-Quadratic Gaussian (LQG) controller, which takes into account the presence of measurement noise and disturbance inputs, but we choose to treat the $\mathcal{H}_\infty$ controller, which provides an intuitive framework for achieving a certain performance and robustness, altogether with computational efficiency, using LMIs. Systems' performance can be measured through different norms such as the $\mathcal{H}_2$ and the $\mathcal{H}_\infty$ norms [64]. Under an adequate regional or pointwise eigenvalue structure assignment this can be achieved. Closed-loop damping can be achieved by forcing the poles into a desired stable region of the complex-plane, i.e. any region in the open left-half side of such plane. This idea is an approach that can be done through the consideration of $\mathcal{H}_\infty$ controllers, the use of Linear Matrix Inequalities (LMIs) to specifie a certain exponentially stable region (i.e. $\{s \in \mathbb{C} : \Re(s) < 0\}$, where s stands for the complex variable) in the complex-plane. These LMIs are solved using efficient interior-point methods for convex optimization. An LMI characterization for general convex regions of the complex-plane for the $\mathcal{H}_\infty$ controller synthesis has been shown in [39]. Important results over $\mathcal{D}$-stability with LMI regions with parametric uncertainties followed by illustrative examples for designing dynamic output-feedback controllers are discussed in [40], where the closed-loop poles are robustly assigned into an specified region.

The $\mathcal{H}_\infty$ problem was initially pointed-out by the work of Zames [205], including several aspects encompassed within the sensitivity of a feedback system with disturbances for improving its robustness. The minimum sensitivity problem pointed-out in [205] turned out to be a Nevanlinna-Pick interpolation problem. Lately, in [7], the Nevanlinna-Pick interpolation

problem is used for robust stabilisation, placing the poles inside a circular region in the left-half of the complex-plane.

Other approaches consist on robustly pointwise assigning the spectral values in the left-half of the complex-plane. This is essentially an inverse eigenvalue problem, looking for immunity against system perturbations. A measure for the optimal conditioning that may be expected for a particular system with a given set of poles to evaluate the applicability of the assigned poles is given in [93]. Robust eigenstructure assignment has been analysed in [87], where a theorem for the analysis of the dynamic output-feedback was proposed.

Due to the unmodeled high-frequency vibration modes that appear in the frequency analysis of flexible structures, robust approaches tend to be more appealling. Other approach using piezoelectric patches was shown in [177]. In [178], a practical improvement was included in the system where concern about the actuators' limitation is taken into account.

A way to simulate the behavior of these high-order systems is using time-delays, as it is possible to simplify them with finite dimensional state variables, see [67] and the references therein, where it is stressed the applicability of such delayed systems in many disciplines besides control engineering, e.g. the manufacturing processes (see, e.g., the thesis dissertation [83]), the internal combustion engine (refer to the survey paper [42]), the simplification and reduction of partial differential equations (PDEs) (in [158] the growth-rate model for the Covid-19 is estimated), communication delays in remote control and network (a master-slave teleoperator system for a robot is shown in [5] and a survey on the bilateral teleoperators can be found in [134]), among others. Nonetheless, it is a common belief that time-delays may lead to destabilizing effects on the dynamics that they are involved, for systems without delays it is possible to use time-delays in feedback control actions to achieve the specified objective. One of the first papers showing this stated a delay-based controller used for improving the stability of systems with oscillatory behaviour and small damping in [166]. Properties about the useful features of delayed-based controllers have further been treated recently, e.g. a property called Multiplicity-Induced Dominancy (MID) has been proven and used in several vibration suppression applications in recent pioneering works, see for instance [27]. The first time where multiple zero frequency imaginary roots were characterized with a general formula for the LU-factorization was in [24].

In previous works, it has been showed that the multiplicity of a spectral value can be bounded by a generic bound, that we will denote as B_{PS} throughout this document. Besides, it has been pointed out that assigning exactly B_{PS} different spectral values for low-order time-delay systems, without any further requirement of multiplicity among them, guarantees the dominancy of such non-oscillating modes. In [17], where the coexistence of real spectral values is proven as an effective approach. Logically, if these assigned roots are negative, exponential stability of the system is guaranteed. In the case of second-order systems, the dominancy property has been analitically shown altogether with a pole placement design for the active vibration control in [29], see also [31]. In [17], a criterion that allows the characterization of the stabilizing effect given by the coexistence of non-oscillating modes for n-order linear delayed-differential equations is given. The stability and the performance of the systems with time-delays are of theoretical and practical importance. Therefore, the stability analysis is done through frequency-domain approaches.

We will consider hereafter two different control approaches for robust finite-dimensional control of thin mechanical

structures: an optimal $\mathcal{H}_\infty$ LMI-based approach and an output-feedback proportional-delayed-based approach. The former implies analysis and synthesis for robust pole placement techniques using Linear Matrix Inequalities, arriving to a quadratic stability and $\mathcal{D}$-stability through the synthesis of $\mathcal{H}_\infty$ controllers [40]. The latter based on proportional and delayed actions of the measured output and control law's signals [180]. Both approaches are customized for linear systems assuring the poles locations in the left-half of the complex-plane, either in a specific prescribed region, or in pointwise specific negative values.

1.2 Objectives

Lately a big interest has arisen to understand the behavior of time-delays as a design parameter in the control of dynamical systems. The main topic of this thesis is the frequency-domain analysis and pole placement control design of time-delay systems, where an output-feedback controller is designed in such a way, that the closed-loop performance of the low-order synthesis model, which for the studied case includes the first three vibration modes of the flexible structures under consideration, will be well-damped. Also, the closed-loop should be robustly stable against unmodelled dynamics.

With the quasipolynomial-based control, we make emphasis on the synthesis and controllers design based on the knowledge of the rightmost root in the spectrum of the system's poles. During this dissertation we aim to deepen in the application of these emergent techniques, and understanding the usage and the design of such techniques. The sub-objectives noted to be developed during this research are presented as follows:

Objective 1. Study and familiarization with linear, robust and optimal control, focusing in a technique for pole placement in convex regions of the complex plane, described by Linear Matrix Inequalities (LMI) for linear systems with static uncertainties on the state matrix. We apply this result for the design of a dynamic output-feedback controller that robustly assigns the system's poles in a predefined LMI region of the complex plane.

Objective 2. The modelling approach involving thin mechanical structures allows to use finite-dimensional linear mathematical models and its corresponding modal reduction for their controller synthesis.

Objective 3. The investigation and analysis of these low-order systems to allow the optimization of controller's parameters for the controller synthesis, and to further explore their applicability for the high-order finite-dimensional systems that approach these thin mechanical structures in a wider range of frequency.

Objective 4. The effect of the poles among the infinite spectral values in the complex plane, which are a direct consequence of quasipolynomials and their impact in the active vibration control of the thin mechanical structures under consideration. We are interested on the dominant root of a quasipolynomial, which is characterized by the coexistence of different real roots in the left-half of the complex plane.

In an effort to meet these listed objectives above, we consider a frequency domain analysis. For the application of such controllers we have to ensure that their order is relatively low. For this purpose, we are using a synthesis model of the considered flexible structures, which is obtained from an analysis model through some reduction techniques that are well known. This introduces another robust stability requirement, where a low-order model's controller has to guarantee the proper control when it is applied to the high-order model of the flexible structure, called as "analysis model", and that describes the thin mechanical structures in a wider range of frequency. As for the main contribution related to the quasipolynomial-based approach, we study its discrete-time version with a commensurate delay w.r.t. the time-sampling.

1.3 Structure of the manuscript

The present work is organized as follows. Basic results are gathered in the Chapter 2. The Chapter 3 introduces the prerequisites and describes the flexible systems that we consider. An optimal $\mathcal{H}_\infty$ controller is outlined in Chapter 4. The recent methodology that induces dominant non-oscillating poles placement in the negative real axis is explored in Section 5. Approaches for designing anti-windup compensators, whose purpose is to tweak linear controllers, which enlarges the order of the closed-loop system, which enable the reduction of the saturations in the system, and results from numerical simulations applied on the vibration suppression problem of a flexible beam are expressed in Chapter 6. Finally, in Chapter 7 closing remarks and observations are discussed.

1.4 List of Publications

The following list is a list of the publications we worked on during the course of this research project.

- S. Tliba, I. Boussaada, S.-I. Niculescu, and R. Falcon Prado. Delayed Control Design of a Vibrating Thin Membrane via a Partial Pole Placement [180]
- R. Falcón-Prado, S. Tliba, I. Boussaada, S.-I. Niculescu. Active Vibration Control of Axisymmetric Membrane through Partial Pole Placement. IFAC-PapersOnLine, 54(18):58-63, 2021. [51]
- Tliba, S., Boussaada, I., Niculescu, S.I. and Falcón Prado, Ricardo. An MID-based Control of a Vibrating Axisymmetric Membrane using Piezoelectric Transducers. In ENOC 2021-10th European Nonlinear Dynamics Conference, 2021. [181]
- Tliba, S., Boussaada, I., Niculescu, S.I. and Falcon Prado, RicardoDesign of Quasipolynomial-based Controllers with Dynamical Parameters-Application to Active Vibration Damping. In Joint IFAC Conference: SSSC-TDS-LPVS, 2022. [182]

Chapter 2

Background

In this particular chapter, we focus to analyse several properties and characteristics of time-delay systems. This sets the stage for a formal introduction in much generality, introducing functional differential equations as representations of time-delay systems. Linear delay systems are discussed deeply with the frequency-domain methods. It provides background knowledge required to understand the subsequent chapters. It covers linear differential-difference equations in Section 2.1.1, we treat the frequency domain analysis of LTI systems in Section 2.1.2, design of delayed feedback stabilizing controllers in Section 2.1.3, some convex optimization problems and examples in Section 2.2, and provides some notes and references for further reading in Section 2.3.

Contents

2.1 Retarded Differential equations' problems

This section gathers important theorems and some examples of delay-differential equations of retarded type.

2.1.1 Linear differential-difference equations

Ordinary differential equations (ODE's) are equations involving functions on a temporal continuous argument, and time-derivatives of such a function. These equations can be written as

$$f\left(t, x, \frac{d\,x}{dt}, \cdots, \frac{d^n\,x}{dt^n}\right) = c$$

which can be also well written simply as $f(t, x, \dot{x}, \cdots, x^{(n)}) = c$, where t represent the time argument, the variable $x \in \mathbb{R}^n$ indicate an unknown function, the dots and powers among parenthesis indicate time-derivatives, and the constant c, that may be scalar or vector variables, and should have the same dimension. When these equations involve current and past values of the states, they are called time-delay systems.

Time-delay systems (often called TDS) are dynamical systems modelled through differential equations that depend on current and past values of the states. They are often called *functional differential equations* (FDEs), are also known as *differential equations with deviating arguments*, due to their evaluation on arguments that are distributed over some intervals in the past.

Time-delay systems are systems that include in their dynamics the effect of a deferral during a certain amount of time. This entails the involvement, not only of the current states' values, but also about its past values. The previously mentioned systems are also called hereditary systems, systems with time-lag, systems with aftereffect, systems with dead times, equations with deviating argument, or differential-difference equations, among others. Their presence proliferates among different natural systems, including a wide variety of fields spanning along biosciences (dynamics of populations' heredity [102]), physics, chemistry (dynamics in chemical kinetics [151]), economics (dynamics of bussiness cycles [88]), social behaviors, etc. An example of their study and analysis has become largely interesting due to its repercussion rate of contagions that can arise after an extensive virus oubreak [191]. As a matter of fact, TDS were first introduced in order to describe the behavior of biological systems, and later their consideration was found useful in many engineering systems, such as mechanical transmissions, fluid transmissions, manufacturing processes, nuclear reactors, and so on and so forth.

Normally, the study and design of control laws can be compared and tested using practical methods, adjusting gains, modifying parameters, or augmenting the system with the addition of compensators, like the anti-windup compensators, which can enhance and improve its behavior. Nonetheless, in the case when these systems are challenging, expensive or dangerous, experimental implementation should be compared with data obtained from digital computer simulations performed in advance.

The stability analysis of time-delay systems has aroused so much interest in recent years, but among its difficulties

is that, contrary to the linear systems of finite dimension where Routh-Hurwitz stability criterion is available [13], there is no simple known criterion for determining the asymptotic stability of a general linear time-delay system based only on its coefficients and delays [118]. Several methodologies capable of synthetizing controllers of a similar order than the system are available, including but not limiting to approaches through the finite spectrum assignment, $\mathcal{H}_2$ and $\mathcal{H}_\infty$ control synthesis schemes, and Linear Matrix Inequalities based controllers. Despite their usefullness, these approaches are often of difficult implementation into high-order systems. Due to this reason, most of the cases low-order controllers are chosen over high-order ones.

It can be considered that many of the effects often studied in systems dynamics, are the reactions of given systems to real exogenous actions, as well as their satisfactory or insatisfactory behaviour when stabilized with a control law. The reason of this delay can be attributed to many reasons, but specially due to the transport and the propagations phenomena, often intrinsically present in the systems' dynamics. Once more, the study of TDS becomes important.

In the forthcoming sections, and without loss of generality, we will briefly introduce the reader to some basic aspects of time-delay systems represented by functional differential equations (FDEs).

A thoroughly study of the real world systems inevitablely compels one to take into account that the rate of change of physical systems involve present states, as well as past states. As it was discussed in the introduction (Chapter 1), one way to tackle phenomenons involving delayed signals is to include the information relating the past states values in the computed model of the systems' dynamics. These model's differential equations, where a time-delay is involved and, thus, the present value is a function that is evaluated with present and past values, which lay in a solution interval, are called functional differential-difference equations. When the theory of linear differential-difference equations is discussed, what is intended is to recall in a comprehensible way a unified theory for different classes of ordinary differential equations (see e.g. [116], [73]).

There are classes of systems that involve time-delays in the derivatives, which include many of these special types, are called neutral functional differential equations (NFDE). Other interesting case of ODE's is the case when there are equations with no delays in the derivatives and a past-dependence only on the state variable, which are called retarded functional differential equations (RFDE).

Retarded Functional Differential Equations

The functional differential equations of retarded type can be considered as

$$\begin{cases} \dot{x}(t) &= f(t, x_t(\theta)), & t &\geq t_0, \\ x_{t_0}(\theta) &= \phi(\theta), & \forall\, \theta &\in [-\tau, 0] \end{cases} \tag{2.1}$$

where $x_t(\cdot)$, for a given $t \geq t_0$, denotes the restriction of $x(\cdot)$ to the interval $[t-\tau, t]$ translated to $[-\tau, 0]$, i.e.

$$x_t(\theta) = x(t+\theta), \quad \forall\, \theta \in [-\tau, 0]$$

It is assumed that $\phi \in \mathcal{C}^v_{n,\tau}$ and the map $f(t,\phi) : \mathbb{R}_+ \times \mathcal{C}^v_{n,\tau} \mapsto \mathbb{R}^n$ is continuous and Lipschitzian in ϕ and $f(t,0) = 0$. The scope of this thesis constraints itself to the linear case of these type of equations, which is presented below.

The characteristic equation for an homogeneous linear differential equation with constant coefficients (2.2) is obtained by looking for its nontrivial solutions of the form $c\,e^{\lambda t}$, where c is either a real constant or an n-vector, i.e. $c \in \mathbb{R}^n$.

$$\dot{x}(t) = A_0\, x(t) + A_1\, x(t-\tau) \tag{2.2}$$

where $A_0 \in \mathbb{R}^{n\times n}$ is a squared matrix, the n-dimensional state vector $x(t) \in \mathbb{R}^n$, and τ is the time-delay [120], with a characteristic equation given by the roots of the right-hand side of the function

$$h(s) \stackrel{\text{def}}{=} \det\{s\,\mathbb{I} - A_0 - A_1\, e^{s\tau}\} \tag{2.3}$$

has non-trivial solutions $f(t) = c\,e^{st}$ with $i = 1, \ldots, n$. As this thesis deals partly with the poles of infinite dimensional systems, a useful theorem capable of predicting an upper-bound on the number of zeros in an horizontal strip is given by the Polya-Szegö theorem, which is summarized as follows:

Theorem 1. *([140, pp. 144-145]) Let $\tau_1, \tau_2, \ldots, \tau_N$ denote real numbers such that*

$$\tau_1 < \tau_2 < \cdots < \tau_N$$

and let $m_1, m_2, \ldots, m_\ell$ be positive integers such that

$$m_1 \geq 1, \ldots, m_\ell \geq 1, \quad m_1 + m_2 + \cdots + m_N = D.$$

Let $f_{i,j}(s) = s^{i-1}\, e^{\tau_j s}$, for $1 \leq i \leq d_j$ and $1 \leq j \leq N$. Let PS_b be the number of zeros of the function

$$f(s) = \sum_{\substack{1\leq j\leq N \\ 1\leq i\leq d_j}} c_{i,j}\, f_{i,j}(s) \tag{2.4}$$

that are contained in the horizontal strip

$$\alpha \leq \Im(s) \leq \beta$$

Assuming that

$$\sum_{1\leq k\leq d_1} |c_{k,1}| > 0 \quad \textit{and} \quad \sum_{1\leq k\leq d_n} |c_{k,N}| > 0$$

then

$$\frac{(\tau_N - \tau_1)\,(\beta-\alpha)}{2\,\pi} - D + 1 \leq PS_b \leq \frac{(\tau_N - \tau_1)\,(\beta-\alpha)}{2\,\pi} + D + N - 1. \tag{2.5}$$

Setting $\alpha = \beta = 0$, the above theorem yields $PS_b \leq D + N - 1$ where D stands for the sum of the degrees of the polynomials involved in the quasipolynomial function $f(s)$ and N denotes the associated number of polynomials. This gives a sharp bound for the number of real roots of $f(s)$.

Neutral Functional Differential Equations

The delayed differential equations of neutral type are generalizations of differential equations that describe

$$\dot{x}(t) - \sum_{i=1}^{m} D_i\,\dot{x}(t-\tau_i) - \sum_{i=0}^{m} A_i\,x(t-\tau_i) = 0, \tag{2.6}$$

with $x(t) \in \mathbb{R}^n$ are the state variables, A_i and D_i are square real matrices of dimension n and τ_i, with $i = 1, \ldots, m$, are constant delays. The characteristic equation of the NFDE is described in the frequency domain as

$$h(s) = \det\left(s\,\mathbb{I} - \sum_{i=1}^{m} D_i\,s\,e^{-s\tau_i} - \sum_{i=0}^{m} A_i\,e^{-s\tau_i}\right), \tag{2.7}$$

where $\tau_0 = 0$. When we consider these systems in the scalar case with a single delay, the general function of NFDE in (2.6) is rewritten as

$$\dot{x}(t) - d\,\dot{x}(t-\tau) - a\,x(t-\tau) = 0 \tag{2.8}$$

The characteristic equation is rewritten as

$$h(s) = s - (d\,s + a)\,e^{-s\tau} = 0 \tag{2.9}$$

As the stability of the solutions of differential equations lies on the roots' locations of its characteristic equation, an important result to take into consideration when dealing with neutral functional difference equations is expressed in the next theorem.

Theorem 2. *([56, Theorem 2.1]) In the equation (2.8), if $|d_m| > 1$, then for all $\tau > 0$, there is an infinite number of roots of equation (2.9) where the real parts are positive.*

We can say then, that if in equation (2.9) we set $|d_m| > 1$, then the trivial solution of the system described by the NFDE (2.8) is unstable for all $\tau > 0$.

Example 1. We illustrate the analysis of a scalar neutral time-delay equation with the following system

$$\dot{x}(t) - d\,\dot{x}(t-\tau) = a\,x(t) \tag{2.10}$$

from this last equation, its characteristic function is given by a quasipolynomial of the form

$$h(s) = s\,(1 - d\,e^{-\tau s}) - a$$

From this last characteristic function, if $|d| < 1$, then the solution is stable. Nonetheless, there exist an infinite number of roots. □

Example of time-delay systems

Time-delay systems belong to the class of infinite dimensional systems, which are different from ordinary differential equations (ODE), whose dimension is finite. In modelling physical processes, a classical hypothesis taken is that we can predict the future behavior of a deterministic system by taking into account the present state of the system. But in time-delay systems, we can suppose that the past states also affect the system future responses.

Example 2. Proportional Minus Delay (PMD) controller

Usually, the presence of time-delays in industrial processes can represent a big challenge, so many efforts have been done in order to minimize the effect of such problems. Generally, the presence of time-delays on stabilizing feedback structures will induce a destabilizing effect. Nonetheless, they are not necessarily destabilizing, as it has been pointed by [16] with a single-species equation.Besides that, there has also been proposed to use those time-delays in the controller design to improve the systems' performances [165]. Time-delays incorporated in conventional controllers can result convenient (see, e.g. [201], where it is shown that time-delays can result beneficial for energy harvesting performance).

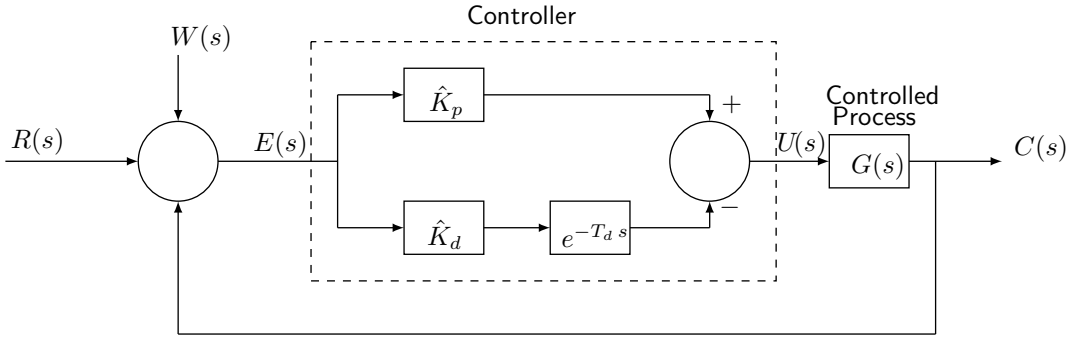

Figure 2.1. Proportional Minus Delay controller.

Considering the closed-loop system of Figure 2.1 in the Laplace domain, the control law has the form

$$U(s) = \left(\hat{K}_p - \hat{K}_d\,e^{-\tau s}\right) E(s) \tag{2.11}$$

where $\hat{K}_p > 0$ and $\hat{K}_d > 0$ are parameters to adjust and τ is the controller's delay. The effect of this controller is equivalent to the PD-controller's effect. To show this, from (2.11) we have

$$\begin{aligned} u(t) &= \hat{K}_p\, e(t) - \hat{K}_d\, e(t-\tau), \\ &= \left(\hat{K}_p - \hat{K}_d\right) e(t) + \tau\, \hat{K}_d \left[\frac{e(t) - e(t-\tau)}{\tau}\right] \end{aligned} \tag{2.12}$$

One can state that

$$\frac{1}{\tau}\left[e(t) - e(t-\tau)\right] = \frac{1}{\tau}\int_{t-\tau}^{t} \dot{e}(t)\, dt. \tag{2.13}$$

From (2.12)-(2.13), and letting $K_p = \hat{K}_p - \hat{K}_d$, and $K_d = \tau\, \hat{K}_d$, we write

$$u(t) = K_p\, e(t) + K_d \left[\frac{1}{\tau}\int_{t-\tau}^{t} \dot{e}(t)\, dt\right]. \tag{2.14}$$

Therefore, it is possible to perform the action of the PD controller averaged over a very short period of time τ, adjusting the gains K_p and K_d as the proportional and derivative gains.

Simulation of the PMD controller For illustration purposes, a simulation of a first order system given by $G(s) = \frac{1}{s+1}$ is performed, with a reference signal $r(t)$ and a perturbation signal $w(t)$ chosen as

$$\left.\begin{aligned} r(t) &= 1.5\,(1 - e^{-6t}), \qquad t \geq 0, \\ w(t) &= 0.2\,\sin(100t), \quad 0 \leq t \leq 5. \end{aligned}\right\} \tag{2.15}$$

The addition of the signals $r(t)$ and $w(t)$ is plotted on Figure 2.2a. The gains are chosen as $K_p = 1$ and $K_d = 4$, the time-delay is chosen as $\tau = 0.314$, and the response $c(t)$ of the system is shown in Figure 2.2b, where we appreciate how the proportional minus delay control law is appropriately responding against a noisy input.

□

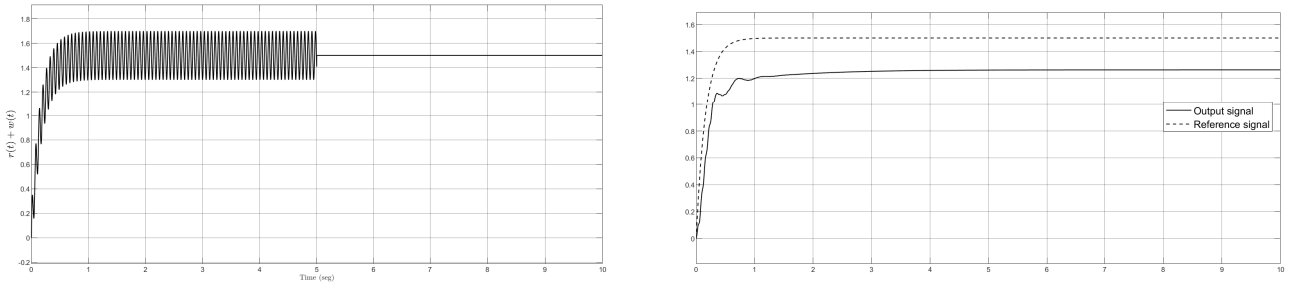

(a) Reference signal plus perturbation (2.15). (b) Output response for the PMD-controller.

Figure 2.2. Noisy reference input and PMD-controller action.

2.1.2 Frequency-domain analysis

Despite that in this work, we deal exclusively with linear time-invariant (LTI) systems, we are focused in studying and achieving conditions that ensure the stabilisation of time-delay systems with a small amount of conservatism. The LTI-delay systems are discussed in greater length with frequency domain descriptions [68].

Different kind of systems are analyzed in the time-domain by means of the convolution. To perform a similar analysis through the frequency domain, we use the Fourier transform. In this way, every input signal is represented as an addition of cosine waves, and each of them having a specific amplitude and phase.

Recalling, the convolution is the standard tool for the analysis of LTI systems. The impulse response, $h(t)$, of a given system, is the only knowledge required from such system to compute its response $y(t)$ to different inputs $x(t)$, and it is represented as

$$y(t) = x(t) * h(t), \tag{2.16}$$

where the symbol $*$ represent the convolution operation $\int_0^t x(t-\tau)\, h(\tau) d\tau$. As a way to elude a difficult operation as the convolution, it results highly advantageous to analyse the system in the frequency domain applying a Fourier transform to the LTI system. The Fourier transform permits to obtain the ouput of the LTI system performing a simple multiplication instead of the difficult convolution, as it is shown below, in equation (2.17), where $Y(\omega)$, $X(\omega)$ and $H(\omega)$ denote the Fourier transforms of the system's output $y(t)$, the LTI system state $x(t)$, and the impulse input $h(t)$, respectively.

$$Y(\omega) = X(\omega)\, H(\omega), \tag{2.17}$$

As we can say that the Fourier transform is a subset of the Laplace transform, this frequency-domain analysis approach is commonly referred as the Laplace-domain approach [47].

A common method for defining stability relies in the fact that, for any given system that may be described by the convolution operation (2.16) is *bounded-input, bounded-output* (BIBO) stable if any bounded input $u(t)$ results in a bounded output $y(t)$. Additionally, the steady-state solution of a LTI system also is said to be stable if, and only if, all the roots of its characteristic quasipolynomial (polynomial for the non-delayed case) have negative real part, i.e. $\Re(s) < -\alpha$ for $\alpha > 0$.

The retarded-type time-delay systems are written as

$$\dot{x}(t) - \sum_{i=0}^{m} A_i\, x(t-\tau_i) = 0, \tag{2.18}$$

where $A_i \in \mathbb{R}^{n\times n}$ are given matrices of appropriate dimensions, and τ_i are constant delays. Its characteristic equation is written as

$$\Delta(s) = \det\left(s\,\mathbb{I} - \sum_{i=0}^{m} A_i\, e^{-s\tau_i} \right), \tag{2.19}$$

where $\tau_0 = 0$ [116].

For example, we can consider the scalar case of a linear retarded differential equation as

$$\dot{x}(t) = a_0\, x(t) + a_1\, x(t-\tau), \tag{2.20}$$

where the constant coefficients a_0 and a_1 are real and the time-delay $\tau > 0$ is positive. We see that the quasipolynomial of this function is written as

$$\Delta(s) = s - a_0 - a_1\, e^{-\tau s} = 0. \tag{2.21}$$

The difference from systems without delays is that, the characteristic equation $\Delta(s) = 0$ from Eq. (2.21) has an infinite number of solutions. This corresponds to the infinite-dimensional property of the time-delay systems. Since the quasipolynomial (2.21) is an entire function [81], it cannot have an infinite number of zeros within any compact set $|s| \leq c$, $\forall c > 0$. A consequence of this is that most of the characteristic roots tend to infinity.

The loci of these roots can be explained in the following way. Let

$$|s| \leq |a_0| + |a_1|\, e^{-\tau \Re(s)} \tag{2.22}$$

be the upper bound for the absolute value of the characteristic roots. As the left-hand side of (2.22) approaches infinity, i.e. $|s| \to \infty$, in the right-hand side approaches infinity. As a consequence we have

$$\lim_{|s|\to\infty} \Re(s) = -\infty.$$

Therefore, there is a finite number of zeros to the right of any line parallel to the real-axis [57].

The effect of time-delays across the different areas may have different behaviours, either stabilizing or destabilizing effects. This notion can be studied through the frequency domain. For example, the system

$$\ddot{x}(t) + x(t) - x(t-\tau) = 0 \tag{2.23}$$

will be unstable for a time-delay $\tau = 0$, but it is asymptotically stable for $\tau = 1$ [57]. This damping effect can be explained by the approximation

$$\frac{d}{dt}x(t) \simeq \frac{1}{h}\left[x(t) - x(t-\tau)\right].$$

Just as for the ODEs are asymptotically stable if, and only if, all the characteristic roots have negative real parts, it is the same case when dealing with LTI TDS. It is worth noting that for linear TDS, as in Eq. (2.23), asymptotic stability and exponential stability are equivalent.

2.1.3 Delayed feedback stabilizing design

Straightaway we address the behavior of the generic delay-differential equations of the form

$$y^{(n)}(t) + a_{n-1}\, y^{(n-1)}(t) + \cdots + a_0\, y(t) + \alpha_{n-1}\, y^{(n-1)}(t-\tau) + \cdots + \alpha_0\, y(t-\tau) = 0, \tag{2.24}$$

where $y(t)$ is the time-dependent function, $n > 0$ is a positive integer, $a_k \in \mathbb{R}$ and $\alpha_k \in \mathbb{R}$ are the constant coefficients, for $k0,\, 1,\, \ldots,\, n-1$, and $\tau > 0$ is a real-valued time-delay. The delay-differential equations of retarded type, or retarded functional differential equations (RFDE) subsumes the highest derivative in the non-delayed polynomial, being this highest derivative given by $y^{(n)}(t)$ in equation (2.24).

A way that illustrates the reason for the study of this time-delay systems is that a delayed-state-feedback control law under the form

$$y^{(n)}(t) + a_{n-1}\, y^{(n-1)}(t) + \cdots + a_0\, y(t) = u(t-\tau), \tag{2.25}$$

where $u(t-\tau)$ is the delayed-state-feedback control input, chosen in a specific way for getting a specific closed-loop behaviour of the equation (2.25). In the non-delayed case, i.e. when $\tau = 0$, an effective choice that properly assigns all eigenvalues of the system accordingly to the coefficients' values is taken as $u(t) = -\beta_{n-1}\, y^{(n-1)}(t) - \cdots - \beta_0\, y(t)$, resulting in dynamics that behave following

$$y^{(n)}(t) + (a_{n-1} + \beta_{n-1})\, y^{(n-1)}(t) + \cdots + (a_0 + \beta_0)\, y(t) = 0. \tag{2.26}$$

The stabilization methodology discussed for arriving to the equation (2.26) is called pole placement [137], and it does not hold in the delay-based case described here. An important diffficulty in the analysis of the asymptotic behaviour of (2.24) is that, contrarily to the situation for (2.26), the corresponding characteristic function has infinitely many roots. Going back to our discussion about time-delay systems, the stability of the RFDE (2.25) can be analyzed through the characteristic quasipolynomial's roots, thus

$$\Delta(s) = s^n + \sum_{k=0}^{n-1} a_k\, s^k + \sum_{k=0}^{n-1} \beta_k\, s^k\, e^{-\tau s}. \tag{2.27}$$

The function in equation (2.27) is defined for the Laplace variable $s \in \mathbb{C}$, where $\Delta : \mathbb{C} \mapsto \mathbb{C}$ [118]. The stability properties analysed from the characteristic roots' placement on equation (2.26), will be asymptotically stable if each spectral value $s_i < 0$ is a negative real pole, with $i = 0,\, 1,\, \ldots,\, n$. Moreover, the dynamics behaviour of (2.25) is determined by the spectral abcissa, that is the dominant root of this quasipolynomial (2.27), i.e. the root with the largest real part.

Multiplicity Induced-Dominancy

The interesting idea of controlling systems through a partial pole placement with a multiple dominant root (MID) has been treated in recent works, as in [32, 33, 28], among others, where a generic quasipolynomial of retarded type, as given in equation (2.27) are used, and a given real negative value s_0 can be a multiple root of the characteristic quasipolynomial of the closed-loop system. When this multiplicity reaches its maximal value for its given quasipolynomial, it can be portrayed as an integral representation, as it is shown in the next theorem from [182]:

Theorem 3. *([182, Thm 2.3]) Let $\tau > 0$, a real scalar $s_0 \in \mathbb{R}$, and consider the quasipolynomial $\Delta(s)$ from (2.27). The number s_0 is a root of $\Delta(s)$ with multiplicity of at least $n+m$ if, and only if, there exists a constant $a \in \mathbb{R}$, s.t.*

$$\Delta(s) = \frac{\tau^m\,(s-s_0)^{n+m}}{(m-1)!} \cdot \int_0^1 t^{m-1}\,(1-t)^{n-1}\,(1-a\,t)e^{-t\tau(s-s_0)}\,dt \tag{2.28}$$

Another way to show the characterization of real roots of maximal multiplicity for the quasipolynomial $\Delta(s)$ and their dominance on the dynamics of (2.25) is portrayed in the theorem depicted forthwith.

Theorem 4. *([118, Thm 3.1]) Consider the quasipolynomial $\Delta(s)$ given by the equation (2.27). Let s_0 be the root of highest multiplicity. Then, the root s_0 holds a multiplicity $2n$ in the quasipolynomial $\Delta(s)$, if and only if, for every $k = 0,\,1,\,\ldots,\,n-1$, the parameters a_k and α_k denoted in equation (2.27) are given by*

$$\left.\begin{aligned} a_k &= \binom{n}{k}(-s_0)^{n-k} + (-1)^{n-k} + (-1)^{n-k}\,n!\,\sum_{j=k}^{n-1}\binom{j}{k}\binom{2n-j-1}{n-1}\frac{s_0^{j-k}}{j!\,\tau^{n-j}}, \\ \beta_k &= (-1)^{n-1}\,e^{s_0\tau}\,\sum_{j=k}^{n-1}\frac{(-1)^{j-k}\,(2n-j-1)!}{k!\,(j-k)!\,(n-j-1)!}\,\frac{s_0^{j-k}}{\tau^{n-j}}, \end{aligned}\right\} \tag{2.29}$$

then, if the requisites in the equations (2.29) hold, the spectral value s_0 is strictly the dominant root of the quasipolynomial $\Delta(s)$ in equation (2.27). Moreover, if the coefficient $a_{n-1} > -\frac{n^2}{\tau}$, then the trivial solution of (2.24) is exponentially asymptotically stable.

Proof. See [118, §4].

Thanks to this last theorem, a system's spectral values of maximal multiplicity are necessarily dominant for retarded delay-differential equations.

Coexistence of real roots

The best way to explain this procedure, is applying into a simple systems portrayed by delay-differential equations. Theorems showing properties on first-order and second-order retarded time-delay equation with a single time-delay, i.e. a scalar

differential equation with only one delay. A retarded differential equation involving a single delay constant term can serve as a mathematical model for many different phenomena.

The first-order DDE is governed by

$$\dot{x}(t) + a\,x(t) + b\,x(t-\tau) = 0. \tag{2.30}$$

This model represents a biological model which was discussed in [18, Eq. (3.5.3), p.382]. A contagious disease is spread throughout a community by people coming into contact with other people. Let the state $x(t)$ represent the population size at time t, $b > 0$ denotes the contact rate between infected and uninfected populations [152, Ch. 8, § 7]. The characteristic equation associated to equation (2.30) is

$$\Delta(s,\tau) = s + a + b\,e^{-\tau s}. \tag{2.31}$$

The value of a time-delay τ in equation (2.30) that adequately places two negative real spectral values, assuring a delay independent exponential asymptotic stable solution, can be given as long as the parameters values a and b meet some requirements, whose requirements can be summarized in the next theorem:

Theorem 5. *([3, Thm 2]) For a given time-delay $\tau > 0$, the first-order delay-differential equation (2.30) has two distinct negative real spectral value at s_1 and s_2, where $s_2 < s_1$, if and only if*

$$\begin{aligned} a = a(s_1, s_2, \tau) &:= \frac{s_2\,e^{-\tau s_1} - s_1\,e^{-\tau s_2}}{e^{-\tau s_2} - e^{-\tau s_1}}, \\ b = b(s_1, s_2, \tau) &:= \frac{s_1 - s_2}{e^{-\tau s_2} - e^{-\tau s_1}}. \end{aligned} \tag{2.32}$$

Also, the spectral values s_1 and s_2 from the equation (2.30) are negative, if and only if $a(s_1, s_2, \tau) = 0$ with a positive time-delay $\tau > 0$. The spectral value s_1 is the spectral abcissa in the complex-plane.

Second-order RDE Consider the detailed procedure for a scalar second-order delay differential equation, which can provide insight into the dynamic behaviour of wide variety of many natural phenomena. However there are some inherent limitations to this approach. The equation for this kind of systems is given as follows

$$\ddot{x}(t) + a\,\dot{x}(t) + b\,x(t) + \alpha\,x(t-\tau) = 0. \tag{2.33}$$

The characteristic equation related to the equation (2.33) is

$$\Delta(s,\tau) = s^2 + a\,s + b + \alpha\,e^{-\tau s}. \tag{2.34}$$

Then, we gather results allowing delay-dependent stability on a scalar second-order retarded-differential equation in the next theorem.

Theorem 6. *([3, Thm 4]) The RDE (2.33) permits three different negative real poles in the spectral plane s_i with $i = 1, 2$ and $s_i < s_{i+1}$, if and only if the parameters a, b and α satisfy*

$$\left.\begin{aligned} a &= a(s_1, s_2, s_3, \tau) := \tfrac{1}{Q} \sum_{\substack{i,j,k\in\Lambda \\ i<j,\, i\neq j\neq k}} (-1)^{i+j} \left(s_i^2 - s_j^2\right) e^{-\tau s_k}, \\ b &= b(s_1, s_2, s_3, \tau) := -\tfrac{1}{Q} \sum_{\substack{i,j,k\in\Lambda \\ i<j,\, i\neq j\neq k}} (-1)^{i+j}\, s_i\, s_j \left(s_i - s_j\right) e^{-\tau s_k}, \\ \alpha &= \alpha(s_1, s_2, s_3, \tau) = -\tfrac{1}{Q} \prod_{\substack{i,j\in\Lambda \\ i<j}} (s_i - s_j). \end{aligned}\right\} \tag{2.35}$$

where $\Lambda = \{1, 2, 3\}$ and

$$Q := Q(s_1, s_2, s_3, \tau) = \sum_{\substack{i,j,k\in\Lambda \\ i<j,\, k\neq i,\, j}} (-1)^{i+j} \left(s_i - s_j\right) e^{-\tau s_k}.$$

In this case, α is necessarily negative. The spectral value s_1 is negative, if and only if there exists $\tau_0 > 0$ that solves the equation

$$a(s_1, s_2, s_3, \tau_0) + s_2 = 0,$$

which guarantees the asymptotic stability of the system. Furthermore, the root s_1 is the spectral abscissa of (2.33).

Remark 2.1. *For higher-order retarded delay systems, the procedure is to assign a number N of negative spectral values ($N \leq PS_b$) allowing to get conditions on the parameters. Once the parameters' values are set, one shows the dominancy of the assigned spectral values, either by using the principle argument or using the quasipolynomial factorization proposed in [3].*

2.2 Convex optimisation problems

This section recollects some fundamental proofs and reasonings that structure the robust control field.

2.2.1 Pole placement

Pole placement techniques are ideal when dealing with robustness issues. The unstructured uncertainties can be represented as in Figure 2.3, where Δ stands for an uncertainty operator of the system, and $G(s)$ is the nominal model of the system. These poles can be assigned either to specific points or to a whole region. These regions can be described appropriately with the help of Linear Matrix Inequalities (LMIs). Methods involving LMIs have become wide popular for designing regional eigenvalues' assignment controllers through efficient optimisation algorithms nowadays widely available, see [11], [149], and for discrete time [148].

In addition, robust pole placement fits in an excellent way to treat different control objectives, thus giving a multiobjective performance. Particularly, the $\mathcal{H}_\infty$ approach involves frequency-domain aspects that guarantee that the $\mathcal{H}_\infty$ norm

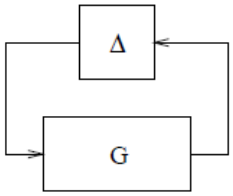

Figure 2.3. System interconnection with the neglected dynamics.

between the controlled output and the external disturbance achieves satisfactorily frequency response in closed-loop.

The time performance of a given system is directly related to the location of its poles in the complex plane. In closed-loop, we can force the system's poles to be constrained in a previously specified and adequated region of the complex plane. Many different kinds of regions have been already considered, such as α-stability regions, vertical strips, horizontal strips, circular regions, and more general convex regions [70].

For every pole of an LTI system $s \in \mathbb{C}$, we can specified several parameters of its behavior in relation to its location, which are defined as follows

$$\begin{aligned} \omega_n &= |s|, \qquad \omega_d = \Im(s) \\ \alpha &= -\Re(s) \quad \zeta = \frac{\alpha}{\omega_n}, \end{aligned} \tag{2.36}$$

where ω_n and ω_d stand for the undamped and damped natural frequencies respectively, α represents the decay rate and ζ serves as the modal damping ratio [135].

2.2.2 Robust stability analysis

Let us consider the autonomous Linear Time-Invariant system described by

$$\dot{x}(t) = A\,x(t), \text{ with } x(0) = x_0 \in \mathbb{R}^n \tag{2.37}$$

where square matrix $A \in \mathbb{R}^{n\times n}$ is the coefficient matrix, the state-vector $x(t) \in \mathbb{R}^n$ and $x_0 \in \mathbb{R}^n$ the initial condition. Asymptotic stability of this system is achieved when

$$\lim_{t\to\infty} x(t) \to 0, \quad \forall\, x(0) \in \mathbb{R}^n. \tag{2.38}$$

In this last case, the system is said to be (asymptotically) stable. Analysing the stability of a closed-loop system, where the stabilization property of a control law designed for a given system is effective, is of paramount importance. If a practical system of interest can be modeled simply as in Eq. (2.37), its stability analysis is straightforward [105], [48]. Let all the eigenvalues of the system (2.37) be on the open left-half part of the complex plane (denoted by $\mathbb{C}_{neg}$), then the matrix A

is said to be Hurwitz stable.

Nonetheless, due to inevitable parametric uncertainties [54], it is difficult (if no impossible) to model a pragmatic system with precision as depicted in Eq. (2.37). For these kind of problems, commonly it is used a "model set", that is written as

$$\dot{x}(t) = A(\theta)\, x(t), \tag{2.39}$$

where the ℓ-parameters $\theta \in \mathbb{E}^\ell$ are contained in a simplex set, which is defined as

$$\mathbb{E}^n := \{\theta \in \mathbb{R}^n : \theta \geq 0,\, \mathbf{1}^T \theta = 1\}.$$

with $\mathbf{1}$ representing a vector of appropriate dimensions with all its components one. Then, $\mathbb{E}^n$ is said to be a standard simplex set on $\mathbb{R}^n$. Therefore, the matrix A is linear in θ, and it is given by

$$A(\theta) := \sum_{j=1}^{\ell} \theta_j\, A_j,$$

where the matrices $A_j \in \mathbb{R}^{n\times n}$ (with $j = 1, \ldots, \ell$) are known matrices.

It is required to mention that the value of the parameter θ is time-invariant, but its exact value is unknown. In other words, the only available information on these parameters θ is that they belong to the simplex set $\mathbb{E}^\ell$.

Now, if all the eigenvalues of a simple depicted system, as in Eq. (2.37), are contained in the left-half part of the complex plane, the uncertain system (2.39) is said to be robustly stable. A way of dealing with the little variations of the eigenvalues of $A(\theta)$, with $\theta \in \mathbb{E}^\ell$, thoroughly, is with the next theorem.

Theorem 7. *([48, Thm 2.1]) If there exist a real matrix $P = P^T > 0$ symmetric and positive definite, such that*

$$P\, A + A^T\, P < 0, \tag{2.40}$$

then, the system (2.37) is Hurwitz-stable.

Thus, we can use this last Theorem 7 to analyse the robust stability of the uncertain system (2.39).

Theorem 8. *([48, Thm 2.2]) If there exists a real matrix $P = P^T > 0$ such that*

$$\sum_{j=1}^{\ell} \theta_j\, (P\, A_j + A_j^T\, P) < 0 \tag{2.41}$$

or equivalently, $P\, A(\theta) + A(\theta)^T\, P < 0$. Then the system (2.39) is stable for all $\theta \in \mathbb{E}^\ell$.

2.2.3 Some Linear Matrix Inequalities Problems with Analytic Solution

Problems involving LMI can vary in a wide range, we focus into three different problems, the feasibility problem, the linear optimization problem, and the generalized eigenvalue minimization problem.

The feasibility problem

The feasibility problem consists in determining the variable $x \in \mathbb{R}^m$ such that the matrix $F(x) < 0$ hold.

For example, let a linear time-invariant (LTI) system be given by $\dot{x}(t) = A\,x(t)$, the convergence of the trajectories $x(t) \to 0$ (i.e. asymptotic stability) is ensured by the existence of a positive quadratic function $V(x) = x^T(t)\,P\,x(t)$ if, and only if its time-derivative along all trajectories of the system is negative, i.e. $\dot{V}(x) = \dot{x}^T\,P\,x + x^T\,P\,\dot{x} < 0 \quad \forall\, x, \dot{x}$ [48].

It is possible to derive LMI formulas to the problem given above, by replacing $\dot{x}$ by its value $A\,x$, and thus, resulting into the next matrix-valued functions inequalities

$$P > 0, \quad A^T\,P + P\,A < 0$$

where the symbols > 0 and < 0 stand for positive and negative definiteness, respectively. Using the standard definition

$$F(x) \triangleq F_0 + \sum_{i=1}^{m} x_i\,F_i > 0, \tag{2.42}$$

we can redefine the latter example, given two matrices $A = A^T$, $P = P^T \in \mathbb{R}^{2\times 2}$ as

$$A = \begin{bmatrix} a_1 & a_2 \\ a_2 & a_3 \end{bmatrix}, \quad \text{and} \quad P = \begin{bmatrix} x_1 & x_2 \\ x_2 & x_3 \end{bmatrix}$$

where the variables x_1, x_2 and x_3 are the design parameters. Thus, we write the LMI problem as

$$A^T\,P + P\,A = x_1 \begin{bmatrix} 2\,a_1 & a_2 \\ a_2 & 0 \end{bmatrix} + x_2 \begin{bmatrix} 2\,a_2 & a_1 + a_3 \\ a_1 + a_3 & 2\,a_2 \end{bmatrix} + x_3 \begin{bmatrix} 0 & a_2 \\ a_2 & 2\,a_3 \end{bmatrix}. \tag{2.43}$$

This results in a standard feasibility problem.

Minimisation of a linear objective under LMI constraints

The problem of the minimisation of a linear objective under LMI constraints is stated as follows:

$$\min_{x \in \mathbb{R}^m} \; c^T x$$

$$\text{such that } F(x) < 0$$

where $c \in \mathbb{R}^m$ is a given vector, and $x \in \mathbb{R}^m$ is the vector of decision variables.

As an example, we will consider a $\mathcal{H}_2$ control problem. We assume the system described by

$$\begin{cases} \dot{x}(t) &= A\,x(t) + B\,w(t), \\ y(t) &= C\,x(t) \end{cases} \tag{2.44}$$

where $w(t)$ represents the disturbance with unit covariance. Suppose the $\mathcal{H}_2$ performance is given by

$$\|\mathcal{H}\|_2^2 = \lim_{t \to \infty} \mathbb{E}\left(\frac{1}{t}\int_0^t y^T(s)\,y(s)\,ds\right),$$

So, the optimal $\mathcal{H}_2$ performance is given by

$$\|\mathcal{H}\|_2^2 = \min\left\{tr(C\,P\,C^T) : A\,P + P\,A^T + B\,B^T < 0\right\}.$$

This optimization problem is equivalent to minimize $tr(Q)$ subject to

$$A\,P + P\,A^T + B\,B^T < 0, \tag{2.45}$$

$$C\,P\,C^T \leq Q. \tag{2.46}$$

Using the Schur complement (discussed after the following example **??**), (2.46) is equivalent to

$$\begin{bmatrix} -Q & C\,P \\ P\,C^T & -P \end{bmatrix} < 0.$$

Schur complement A simple way to solve a set of n linear equations is using what is known as Schur complement. It consists simply of the row reduction involved in a coefficient matrix of dimension 2×2 that renders the given matrix into the upper triangular form.

In the homogeneous case, let

$$\Delta = \begin{bmatrix} A & B \\ C & D \end{bmatrix}$$

and suppose that $A \in \mathbb{R}^{n\times n}$ is non-singular, $B \in \mathbb{R}^{n\times 1}$, $C \in \mathbb{R}^{1\times n}$ and $D \in \mathbb{R}^{1\times 1}$. Now define the vector $v = \begin{bmatrix} x_1 & x_2 \end{bmatrix}^T$ and let

$$\begin{aligned} \Delta\, v &= 0, \\ \begin{bmatrix} A & B \\ C & D \end{bmatrix} \begin{bmatrix} x_1 \\ x_2 \end{bmatrix} &= 0, \end{aligned}$$

that describes a system of $n = 2$ linear equations, given by

$$A\, x_1 + B\, x_2 = 0, \tag{2.47}$$

$$C\, x_1 + D\, x_2 = 0. \tag{2.48}$$

Multiplying (2.47) from the left by $(-C\, A^{-1})$ and adding one equation to the other we get

$$\begin{aligned} -C\, A^{-1}\, A\, x_1 - C\, A^{-1}\, B\, x_2 + C\, x_1 + D\, x_2 &= 0, \\ \underbrace{(D - C\, A^{-1}\, B)}_{(M/A)}\, x_2 &= 0. \end{aligned} \tag{2.49}$$

reducing the original problem (2.47) into solving a single linear equation.

Now, let's consider the non-homogeneous case for a system of linear equations given by

$$\begin{bmatrix} A & B \\ C & D \end{bmatrix} \begin{bmatrix} x_1 \\ x_2 \end{bmatrix} = \begin{bmatrix} u \\ v \end{bmatrix} \tag{2.50}$$

Following the same procedures as before, we write

$$\underbrace{(D - C\, A^{-1}\, B)}_{(M/A)}\, x_2 = u - C\, A^{-1}\, u \tag{2.51}$$

and now the solution of the variable x_2 can be represented in function of the Schur complement as

$$x_2 = (D - C\, A^{-1}\, B)^{-1}\, (u - C\, A^{-1}\, u).$$

This basic property, introduced by the mathematician Issai Schur (1875-1941) in 1917 [156], allows to represent a system of linear matrix inequalities as a single inequality [206]. From this last result, it is deduced the next lemma.

Lemma 2.2.1. *[59, Lemma 3.2] The block matrix*

$$\begin{bmatrix} P & M \\ M^T & Q \end{bmatrix}$$

is negative definite, if and only if

$$\begin{cases} Q & < & 0, \\ P - M\,Q^{-1}\,M^T & < & 0 \end{cases} \tag{2.52}$$

Besides, $P - M\,Q^{-1}\,M^T$ is referred as the Schur complement of Q.

2.2.4 Singular value decomposition

Here we recall some notions about the singular value decomposition (SVD), which is part of some approximation methods for model order reduction. It is an important tool in the analysis of linear time-invariant systems and has paramount importance in the robust stability issue. For that, the next Lemma guarantees the existence of the SVD.

Lemma 2.2.2. *([66, Lemma 2.2.1]) For any $m \times p$ complex matrix Q, there exist $m \times m$ and $p \times p$ unitary matrices Y and U, and a real matrix Σ, such that*

$$Q = Y \begin{bmatrix} \Sigma & 0 \\ 0 & 0 \end{bmatrix} U^* \tag{2.53}$$

in which $\Sigma = \mathrm{diag}(\sigma_1, \ldots, \sigma_r)$ with $\sigma_1 \geq \sigma_2 \geq \cdots \geq \sigma_r > 0$ and $\min(m, p) \geq r$. When Q is real, Y and U may be chosen orthogonal. The equation (2.53) is called a singular value decomposition (SVD) of Q.

The singular values of the matrix Q, given by $\sigma_1, \sigma_2, \ldots, \sigma_r$, are obtained through the computation of the square roots of the positive eigenvalues of $Q^*\,Q$ or $Q\,Q^*$.

The set of all singular values, the maximum singular value and the minimum singular value of a given matrix $(\cdot)$ will be written as

$$\begin{aligned} \sigma(\cdot) &= \{\sigma_i : i = 1, \ldots, p\}, \\ \bar{\sigma}(\cdot) &= \sigma_1, \\ \underline{\sigma}(\cdot) &= \sigma_p. \end{aligned}$$

Some important inequalities worth to mention, are

$$\begin{aligned} \bar{\sigma}(Q+R) &\leq \bar{\sigma}(Q)+\bar{\sigma}(R), \\ \bar{\sigma}(QR) &\leq \bar{\sigma}(Q)\,\bar{\sigma}(R). \end{aligned}$$

This is due to the fact that the maximum singular value defines an induced norm [66].

2.2.5 LMI Regions

A region of the complex plane described by linear matrices inequalities (LMI) can be either an open half plane, or a disk, or a conic sector, among other convex sets. It is often represented by the letter $\mathcal{D}$ and can be written as

$$\mathcal{D} = \left\{ z = s + s^* \in \mathbb{C} | L + s\,M + s^*\,M^T < 0 \right\}$$

where L and M are both real, and $L^T = L$. Next, we will list some elementary LMI regions commonly used in the pole placement approach [40] :

Open Half Plane. For the open left-half-plane $Re(z) < -\alpha$

$$F_{\mathcal{D}}(z) = f_{\mathcal{D}}(z) = s + s^* + 2\,\alpha < 0.$$

Centered Disk. For a disk centered on the real-axis at $(-q, 0)$ with radius r

$$F_{\mathcal{D}}(z) = \begin{bmatrix} -r & q+s \\ q+s^* & -r \end{bmatrix} < 0.$$

Conic Sector. For conic sectors with apex at the origin and inner angle $2\,\theta$

$$F_{\mathcal{D}}(z) = \begin{bmatrix} \sin(\theta)\left[z+z^*\right] & \cos(\theta)\left[z-z^*\right] \\ \cos(\theta)\left[z^*-z\right] & \sin(\theta)\left[z+z^*\right] \end{bmatrix}.$$

Along these elementary LMI regions mentioned above, it is worth to mention some basic properties of these LMI regions (see [105] for further details).

- **Symmetry:** LMI regions are symmetric with respect to the real axis.
- **Convexity:** LMI regions are convex.

- **Intersection:** Given two LMI regions $\mathcal{D}_1$ and $\mathcal{D}_2$ with characteristic functions $f_{\mathcal{D}_1} = L_1 + s\,M_1 + s^*\,M_1^T$ and $f_{\mathcal{D}_2} = L_2 + s\,M_2 + s^*\,M_2^T$, respectively, then the intersection $\mathcal{D}_1 \cap \mathcal{D}_2$ is another LMI region with a characteristic function given by $f_{\mathcal{D}_T} = L_T + s\,M_T + s^*\,M_T^T$, where $L_T = \operatorname{diag}\{L_1, L_2\}$ and $M_T = \operatorname{diag}\{M_1, M_2\}$.

- **Density:** LMI regions are dense in the set of convex regions that are symmetric with respect to the real axis.

- **Openness:** If $s \in \mathcal{D}$ and $f_{\mathcal{D}} < 0$, then the openness of the set of negative definite matrices implies that

$$L + (s + \Delta s)\,M + (s + \Delta s)^*\,M^T = f_{\mathcal{D}} - \left[\Delta s\,M + (\Delta s)^*\,M^T\right] < 0$$

  for small $|\Delta s|$. Therefore, LMI regions are open.

- **Invariance:** The LMI regions are invariant under congruence transformation of the characteristic function with a non-singular matrix, i.e. the LMI regions remains the same.

2.3 Notes and references

The efforts done along the years in the study of functional differential-difference equations has been as broad as it is long. For a wider introduction on the theory of functional delay-differential equations, from which the time-delayed differential equations form a special class, can be regarded in [18], [72] and [73].

We introduce the class of DDEs called linear time-delay system of retarded type, whose equations largely appear when modelling biological or physical systems, among others. For further references on these kind of systems see [98], [97].

The section recalling the convex optimisation methods is based on [34], where different tools for optimising control loops were recalled, such as the "Linear Matrix Inequalities", the Shur complement, among others.

We outlined the spectral properties of the time-delay systems. We will deepen more in the recent results involving the partial pole-placement for linear time-invariant systems with time-delays in the Chapter 5. The results presented in the following chapters are treated with frequencey-domain concepts to analyse their stability.

Chapter 3

Flexible systems under consideration

This chapter is concerned with the study of flexible structures and its state of the art in the Section 3.1. Then, we begin in Section 3.2 by exploring the different vibration modes on these structures, followed by Section 3.3 on the use of piezoelectric devices in such systems. We will then delve into the model order reduction technique in Section 3.4, which plays a critical role in our analysis. Afterward, in Section 3.5 we will introduce the statement of the control problem, which we aim to address in this study. In Section 3.6 and Section 3.7, we will provide an overview of the characteristics of the two flexible structures that we work with, which are the flexible beam, which is located at the *Laboratoire des Signaux et Systèmes (L2S)* in the *Université Paris-Saclay*, in Paris, France, and the flexible axisymmetric membrane, respectively, essential to understanding the results of our analysis. Finally, we will summarize the key points covered in this chapter in Section 3.8.

Contents

3.1 Introduction

During the last several years, the use of the flexible beam structure has been widely spreaded throughout the world due to its advantages, such as the evolution of smart materials, actuators, control strategies, but mainly to the development of computational tools [2]. In [2] a comparative analysis is done through several control strategies for the vibration control of civil structures, including classical (Proportional-Integral-Derivative (PID) [71], Positive Position Feedback (PPF) [197], Integral Force Control (IFC) [107], Pole Placement Control (PPC) [19], Velocity Feedback Control [200]) and modern (Linear Quadratic Gaussian (LQG) regulator [129], $\mathcal{H}_\infty$ [163], Sliding Modes Control (SMC) [37], $\mathcal{H}_2$ [21], fuzzy logic [199]) control strategies.

The beam represents the transposition of a 2-dimensional plate in a 1-dimensional space. As the beam's dynamics can be quite well described by only one dimension when only the flexion movement is considered, as can be seen in Figure 3.5. It is a well known dynamical model, widely used in the literature related to the active vibration control. The performance of several control strategies on different models of the flexible beam have been evaluated in past works (see for instance [15], [52], [185], [95] and [8], among others), but the topic of the time-delay based controllers has not been yet studied deeply.

As a matter of fact, flexible structures are systems whose models exist under the influence of an infinite number of vibration modes. Their behavior is studied with the description of a truncated model, which are finite-dimensional models. Using these models, it is possible to compute and synthetize feedback control laws. Usually, the dynamics that stay outside the bandwidth of interest are called the out of bandwidth modes, and they are neglected during the controller synthesis. Often, their vibrations are attenuated with the implementation of piezoelectrical structures, creating in this way the termed *"smart structures"*. Due to their characteristics, smart materials have been used for several years in fields as civil engineering, where the structures' deformation is isolated and attenuated [20].

3.2 Vibration Modes

When we consider flexible structures, we need to considerate specific features intrinsic on them. Resonance is a phenomenon which consists in the amplification of the motion at a specific frequency. The flexible structures resonate at certain frequencies, whose movements are harmonic, or sinusoidal, and it keeps the same pattern of deformation. These patterns are called mode shape, or simply mode [62]. The set of equations forming the general representation of all the individual components of the dynamics of a flexible structure with a finite number of modes, where n is the number of degrees of freedom, is

$$M\,\ddot{x}(t) + C\,\dot{x}(t) + K\,x(t) = f(t), \tag{3.1}$$

where $x(t) \in \mathbb{R}^n$ is the vector that denotes all the displacements of the corresponding outputs to be controlled, $f(t) \in \mathbb{R}^n$ is a vector of all the equivalent forces and torques, $M = M^T > 0 \in \mathbb{R}^{n \times n}$ is the mass matrix, $C \geq 0 \in \mathbb{R}^{n \times n}$ is the damping matrix and $K \geq 0 \in \mathbb{R}^{n \times n}$ is the stiffness matrix, respectively. These matrices come from the linear approximation of the infinite-dimensional model, often done through the finite elements analysis [141]. The damping matrix C stands for various dissipation mechanisms whose meticulously modeling is not an easy task. Therefore, the Rayleigh damping assumption is often used and corresponds the choice of a damping matrix written as a linear combination of the mass and stiffness matrices, given as $C = \alpha\, M + \beta\, K$, where the parameter α and β are selected empirically. The displacement trajectories can be found by solving equation (3.1). Nonetheless, the number of vibration modes in the whole frequency span of the system is n, which is roughly equal to infinity, and it is too large for practical engineering applications. One popular approach, is the use of the modal analysis technique (or superposition technique) [110]. In order to apply the aforementioned technique, we need to analyse the homogeneous equation of (3.1), i.e. when the forces applied to the system $f(t) = 0$ are equal to zero, which is also called free response of an undamped system, or free vibration analysis, and it is written as

$$M\, \ddot{x}(t) + K\, x(t) = 0. \tag{3.2}$$

where $x(t)$ is the vector that denotes all the displacements, $M > 0$ is the mass matrix and $K \geq 0$ is the stiffness matrix. The befitting trajectory to this late equation is expressed as

$$x = \phi_i\, e^{j\omega_i t}, \tag{3.3}$$

where ϕ_i and ω_i are the amplitude of the modal displacement, i.e. the corresponding mode shape, and the natural frequency of the free vibration mode, respectively. These parameters must satisfy the Equation (3.4), shown as

$$(K - s_i\, M)\, \phi_i = 0 \tag{3.4}$$

which was obtained after substituting the corresponding solution (3.3) into (3.2). The number of modes is equal to the number of degrees of freedom, $x \in \mathbb{R}^n$. Due to the fact that the matrices $M = M^T > 0$ and $K = K^T \geq 0$, the eigenvalue $s_i = \omega_i^2$, must be real and non-negative [141]. In most of the literature is common to find the vibration modes ordered by increasing frequency, i.e. $\omega_1 \leq \omega_2 \leq \cdots \leq \omega_n$. Solving Equation (3.4) for a mode shape $\phi_i \neq 0$ different from zero, the determinant of the left-hand side of its equation must be equal to zero, i.e.:

$$\det(K - s\, M) = 0, \tag{3.5}$$

that being developed, we get a polynomial on s of order n, meaning that we have n roots, whose eigenvalues are solved as $s_1 \leq s_2 \leq \cdots s_n$, and ϕ_i is the eigenvector or mode shape, associated to the mode i ($i \in [1, \ldots, n]$, with the

aforementioned n being the size of the system).Orthogonality relations among the eigenmodes of different eigenfrequencies exist, and in case of M-normalised eigenmodes, it leads to the relations given as

$$\left.\begin{aligned} \phi_i^T\, M\, \phi_j &= \delta_{ij}, \\ \phi_i^T\, K\, \phi_j &= \omega_j^2\, \delta_{ij}, \end{aligned}\right\} \tag{3.6}$$

where the Kronecker delta function $\delta_{ij} = 0$ if $i \neq j$ and $\delta_{ij} = 1$ if $i = j$ [150, Ex. 13.6]. Given that the eigenvectors ϕ_i are independent and orthogonal, they form a basis T spanning the n-dimensional space in which, the solution vector is the summation of the products between the i eigenvectors ϕ_i and the modal coordinates $\mathcal{X}_i(t)$, which have a unique expansion and is given by

$$U(t) = \sum_{k=1}^{n} \phi_k\, \mathcal{X}_k(t) \tag{3.7}$$

where $\mathcal{X}_k$ stand for the modal coordinates,

For succesful active vibration control, identification of these resonance frequencies is very important. This oscillation phenomenon is introduced for several components in the mechanical devices. If a structure is excited by a signal with a frequency given as either one of its natural frequencies, it can be subjected to acute aggressive vibrations. The identification of this natural frequencies can lead to the detection of structural damage, as it is shown in the survey [196] with the analysis of some recent resonance frequency detection technologies, and a method where first, an eigensolution is identified and used together with properties of the eigenvalue problem to detect damaged components is given in [14]. The corresponding eigenvalue equation (3.5) is said to have m multiple eigenvalues if there are m vectors satisfying this equation.

3.3 Piezoelectric devices

The coupling between the electrical energy and mechanical energy is done, for example, through the piezoelectric effect, which is present in certain materials. When a mechanical stress is exerted into the piezoelectric material, a potential difference is produced as a consequence. This phenomenon, called direct piezoelectric effect, was discovered in quartz by Pierre and Jacques Curie in 1880 [100]. The converse piezoelectric effect was discovered by Gabriel Lippmann in 1881. This is, when a potential difference is applied into some of such materials, this electrical energy is visible in the device through a mechanical effect. When the electrical energy is set across a piezoelectric device, the polarized charges of the material try to align themselves along the potential's electric field, which causes the mechanical deformation that we perceive as the effect of this potential. Following this line, the fact that a voltage is generated within these devices was thought as a very convenient way to measure the strain applied to some structures [46].

Among the wide and useful applications of the piezoelectric devices, there are the piezoelectric ceramics, which are PZT (lead-zirconate-titanate) ceramics that act, either, as mechanical sensors, or actuators. These PZT composites act

when vibration is transmitted to the piezoelectric material, and in this way it is converted into electrical energy, and vice versa.

The characteristics of different piezoelectric materials, such as the Quartz or the PZT, make them relevant for different applications. Quartz crystals are ideal as timing devices, due to their minimal temperature effects and high quality factor. Piezoelectric ceramics as the PZT, gives a better performance when is used as a transducer, due to its higher dielectric constant and higher coupling factor. These characteristics are grouped in Table 3.1.

Table 3.1. Piezoelectric material characteristics.

	Symbol	Units	Quartz	PZT
Dielectric constant	K^T		4.5	1,800
Coupling factor	k_{33}		0.09	0.66
Charge constant	d_{33}	$C/N \times 10^{-12}$	2.0	460
Voltage constant	g_{33}	$\mathrm{Vm/N} \times 10^{-3}$	50	28
Quality factor	Q		10^5	80

More details about the characteristics of piezoelectric materials can be found in [141], [142], [187], etc.

3.4 Model Order Reduction

The flexible mechanical structures' dynamics contain both PDEs and ODEs, making it difficult to control for engineers due to its infinite dimensionality. Several methods have been developed to improve the frequency response estimation [150]. The main tool used to construct models, in a reduce frequency range, capable of describing the system behaviour in a finite-frequency span is called finite element analysis. Particularly, the structures involving elastic properties tend to need a large number of degrees of freedom in finite element models, leading to high-order finite systems, in such a way that they get realistic predictions of their dynamic behaviours. As we consider structures that can be called flexible systems, which are distribute parameter systems, and whose state-space is infinite-dimensional.

These systems have an infinite number of degrees of freedom due to the distributed feature of their variables. Several lightly damped vibration modes are susceptible of being very close one to each other. Differences between the full-order and the low-order mathematical model still exist, and both approximated models still keep important differences with the real structure. Modelling methods should stand for the controller robustness and performance characteristics based on the model design, as model inaccuracies or uncertainties.

The design of robust dynamic controllers that succesfully stabilize flexible structures cannot be expected to lead to low-order controllers [23]. However, we are interested in low order vibration modes, typically spanning from $[1\text{–}700]\,\mathrm{Hz}$.

As we can observe in the bode diagram of the Figure 3.1, the magnitude and phase frequency response are shown for the undamped flexible beam's analysis model in black solid lines, which spans along $[0-1,300]\,\mathrm{Hz}$. We are interested in

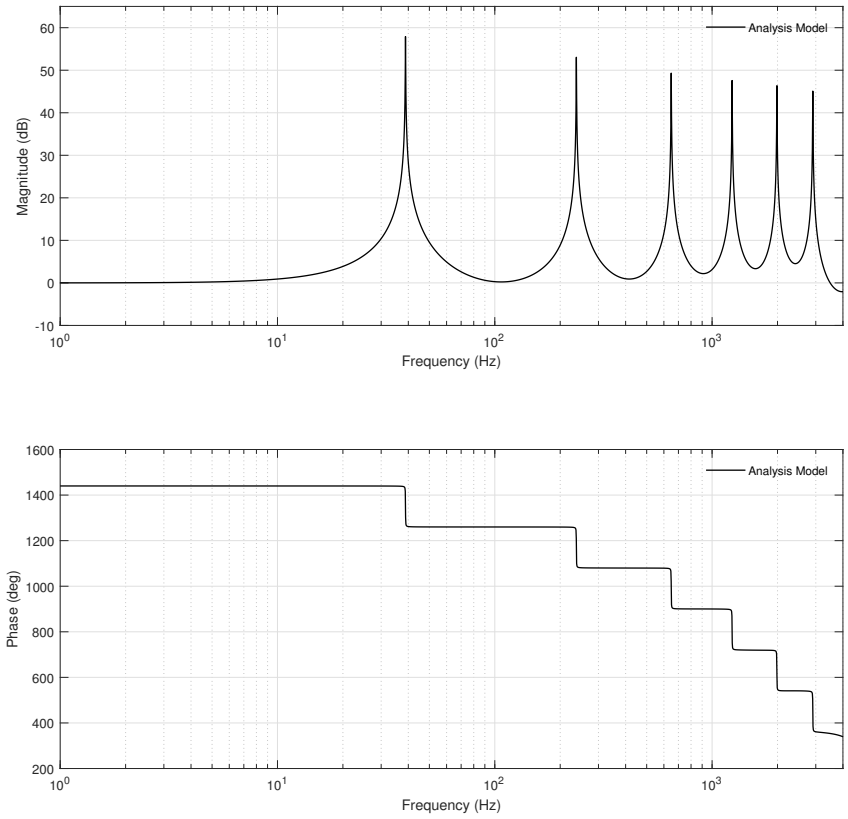

Figure 3.1. Undamped response from $w(t)$ to controlled output $z_a(t)$ of the flexible beam's analysis model.

a mathematical model that appropriately describes the flexible beam's range of frequency that we are interested on. So we use a low-order synthesis model for the controller synthesis. This low-order synthesis model describes a SISO system, (i.e. Single-Input Single-Output system), and it is used for computing a plant's controller whose input is the measured output z_a of the flexible structure, and its output is the control input u of the system, which are the position at the tip of the beam and the PZT actuator, respectively.

A model that correctly describes the dynamics of our flexible systems with n degrees of freedom, which at the same time is a good approximation of an infinite dimensional system (as the distributed parameter systems treated here), is an acceptable approximation, only if n is big enough [35]. Using numerical discretization techniques, such as the Finite Element Method, the PDEs that describe our flexible system are deciphered into n first-order ODEs. When we consider that the lower-frequency vibration modes of a flexible system are the most easily excitable ones, they become the most significant to the global response of the system [185]. When it comes to the choice of the coordinates to be used for the system's representation, the most commonly used are the nodal and modal coordinates. The nodal coordinates are defined with the displacements and velocities of particular structural locations, which are called nodes. The modal coordinates are defined through the displacements and velocities of structural (or natural) modes. In the following we consider the

modal model of the considered systems. Through the use of modal coordinates, the following state-space representation is obtained [62, Ch. 2]:

$$A = \begin{bmatrix} \mathbf{0}_{n_c \times n_c} & \mathbf{1}_{n_c} \\ -\Omega^2 & -2\,Z\,\Omega \end{bmatrix}, \tag{3.8}$$

$$B_u = \begin{bmatrix} 0 & b_u \end{bmatrix}, \quad B_w = \begin{bmatrix} 0 \\ b_w \end{bmatrix}, \tag{3.9}$$

$$C = \begin{bmatrix} c_y & 0 \end{bmatrix}, \tag{3.10}$$

where $\mathbf{0}_{n_c}$ is a zero matrix of dimensions n_c by n_c, the element $\mathbf{1}_{n_c}$ is the identity matrix of dimensions n_c by n_c, the element $\Omega = \operatorname{diag}(\omega_1, \omega_2, \ldots, \omega_n) \in \mathbb{R}^{n \times n}$ represents the natural frequencies of each mode in a diagonal matrix, and the element $Z = \operatorname{diag}(\xi_1, \xi_2, \ldots, \xi_n) \in \mathbb{R}^{n \times n}$ represents the damping coefficients of each mode in a diagonal matrix; the vectors $b_u = \begin{bmatrix} b_1 & b_2 & \cdots & b_n \end{bmatrix}$ and $b_w = \begin{bmatrix} \beta_1 & \beta_2 & \cdots & \beta_n \end{bmatrix}$. If any of the values of, either $b_i = 0$ or $\beta_i = 0$, with $i = 1, 2, \ldots, n$, then the mode i is uncontrollable by the control input u. The vector $c_y = \begin{bmatrix} c_1 & \cdots & c_n \end{bmatrix}$, where if any of its elements $c_i = 0$, with i defined above, then the mode i is not observable by the output variable z_a.

3.5 Statement of the control problem

We are interested in a **mathematical model** describing **low-frequencies** of interest, i.e. in the range of $[1\,\mathrm{Hz} - 1100\,\mathrm{Hz}]$. The complete model used for the system's analysis is called "analysis model", which involves a high-order dimension, including the displacements and velocities of the structural modes in a large span of frequency. Nonetheless, for the controller synthesis we used the so-called "synthesis model", which implies a lower or equal order than the former discussed analysis model, given that the range of frequency of interest spans through the vibration modes of interest, which go from low-frequency modes to high-frequency modes. The equations (3.11) stand for the state-space representation of a system, and it permits to get its input-output frequency response, whose dimensions may vary according to the flexible structure to be modelled, and the dimensions of the real matrices A, B_u, B_w, C_y,, D_y, C_z and D_z are $2n_c \times 2n_c$, $2n_c \times 1$, $2n_c \times 1$, $1 \times 2n_c$, 1×2, $6 \times 2n_c$ and 6×2, respectively. The state vector x arranges the second-order dynamics of the n_c vibration modes. One output corresponds to the measurement of the deformation of the piezoelectric sensor $y \in \mathbb{R}$, and the vector $z = [z_d, z_v, z_a, z_{d_1}, z_{v_1}, z_{a_1}] \in \mathbb{R}^6$ is the controlled output, which in the case of the flexible beam, it is composed of 6 measurements of position, velocity and acceleration at two different places in the beam.

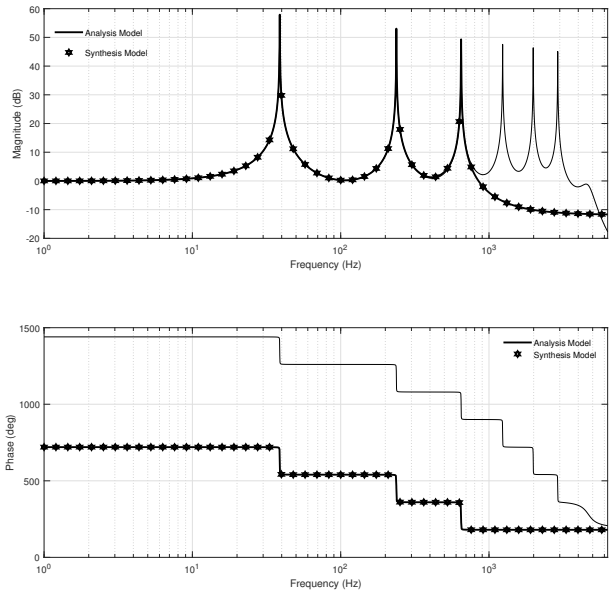

(a) Bode diagram from w to z_a.

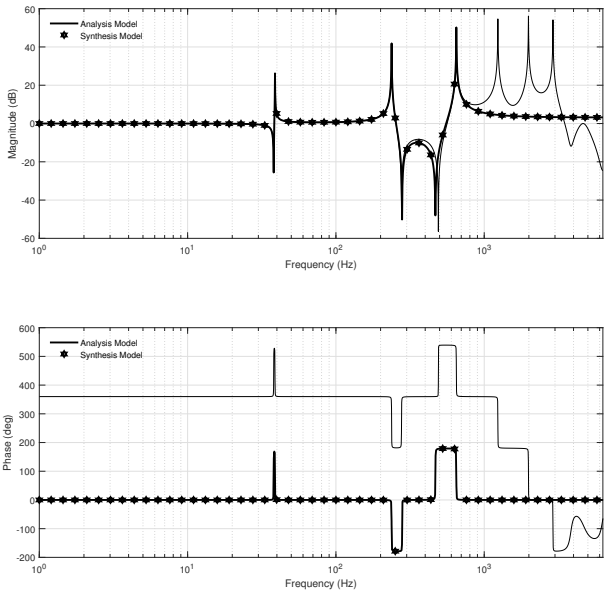

(b) Bode diagram from u to z_a.

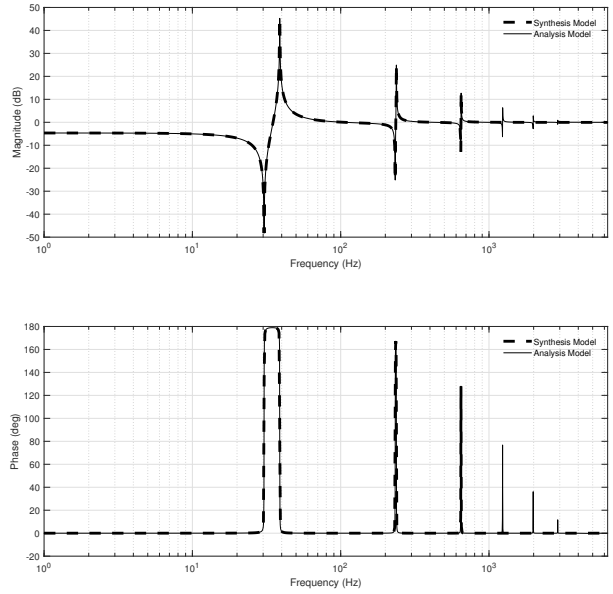

(c) Bode diagram from w to y.

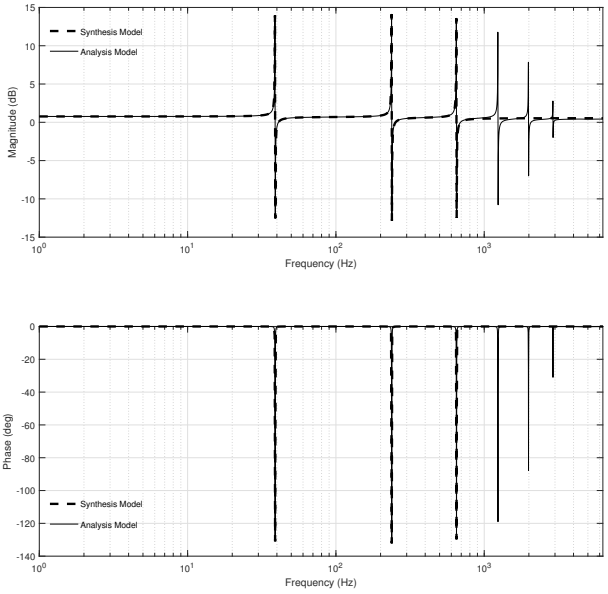

(d) Bode diagram from u to y.

Figure 3.2. Bode diagrams of the flexible beam from the perturbation w and the control input u to the measured output y and the controlled output z_a.

$$\begin{cases} \dot{x}(s) &= A\,x(s) + B_u\,u(s) + B_w\,w(s), \\ y(s) &= C_y\,x(s) + D_{yw}\,w(s) + D_{yu}\,u(s), \\ z(s) &= C_z\,x(s) + D_{zw}\,w(s) + D_{zu}\,u(s) \end{cases} \tag{3.11}$$

We reduce our model even further to describe just the low order frequencies that we are interested to control with the active vibration control. In the Figure 3.2, we can observe the bode diagrams of the model that we obtain from the numerical technique of the finite element model in solid lines, and the bode diagrams of the low-order model describing just the first three vibrating modes in dashed-starred lines. In the Subfigure 3.2a we see the Analysis-model vs. Low-Order model magnitude in the bode diagram from w to z_a. Similarly, in Subfigures 3.2b and 3.2c, we see the uncontrolled response between the inputs u and w, and the outputs z_a and y, respectively. Moreover, the Subfigure 3.2d, we see the bode plot response between the input u and the measured output y. The damping factor on each mode of the system is given by $\xi = 1 \times 10^{-3}$. In practical systems, some level of damping is usually present due to factors like friction, air resistance, or material properties. This damping helps dissipate energy and prevents the oscillations from continuing indefinitely. However, in idealized mathematical models without damping, the damping ratio is zero, and the oscillations persist without any loss of energy. With the active vibration control techniques we purport to increase this damping factor for the vibration modes of interest (in this case, the interest befalls on the first three controllable and observable vibration modes). Thus, we use a low-order mathematical model describing the first three vibrating modes plus the low-pass filters W_1 and W_2, with cutoff frequencies of $950\,\mathrm{Hz}$ each one, and the high-pass filter W_3, which concerns the robustness with respect to the neglected modes of high frequencies in the synthesis model, with a cutoff frequency of $900\,\mathrm{Hz}$. Using weighting filters, we allow the bandwidth of interest to be analysed by isolating low-order frequencies from the high-order frequencies.

Evaluation of frequency responses along all the high-order analysis model, may not be benefical for the controller synthesis intended for the flexible structure. Instead, these controllers can be efficiently computed through reduced low-order models.

3.6 Characteristics of the flexible beam

Several types of models for flexible structures can be found among the vast existing literature, as the non-linear models with partial differential equations were compared in [23] for the Euler-Bernoulli beam theory with structural and viscous damping, or in [147] where the mathematical modelling of the flexible beam is acquired for the Timoschenko beam theory as well as for the Euler-Bernoulli beam theory.

As it can be inferred by the title of this dissertation, we intend to adequately damp the vibrating modes of interest inside a frequency range in a generic flexible structure. The techniques treated in the following chapters deal with state output-feedback control laws, as a linear optimal-based $\mathcal{H}_\infty$, and a quasi-polynomial-based controller. These will be designed from a low-order model lumped from the controllable and observable modes included in the high-order model. This synthesis model is obtained from the selected n modes of the system, in such n modes will be controlled. The energy of the uncontrollable and observable modes, and the modes outside the range of frequency is ignored during the controller synthesis. Nonetheless, the case where the actuator(s) action(s) render these ignored vibration modes instable can happen,

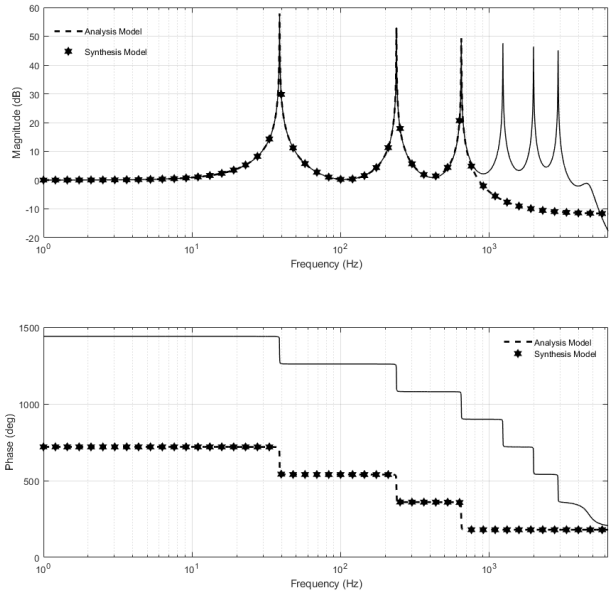

(a) Bode diagram from w to z_a.

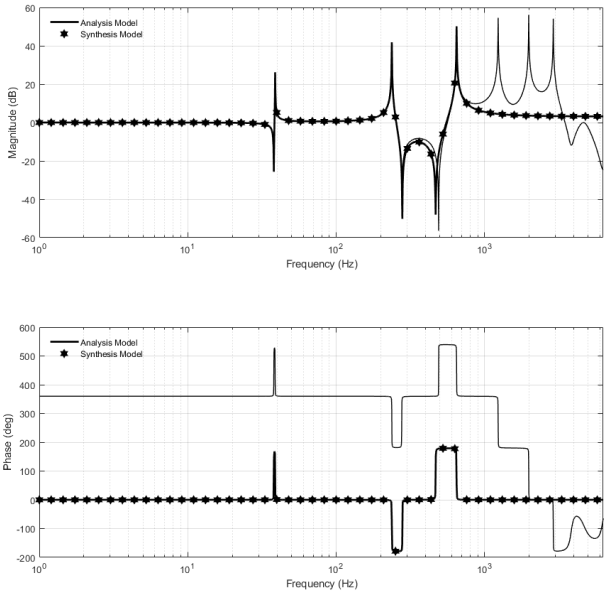

(b) Bode diagram from u to z_a.

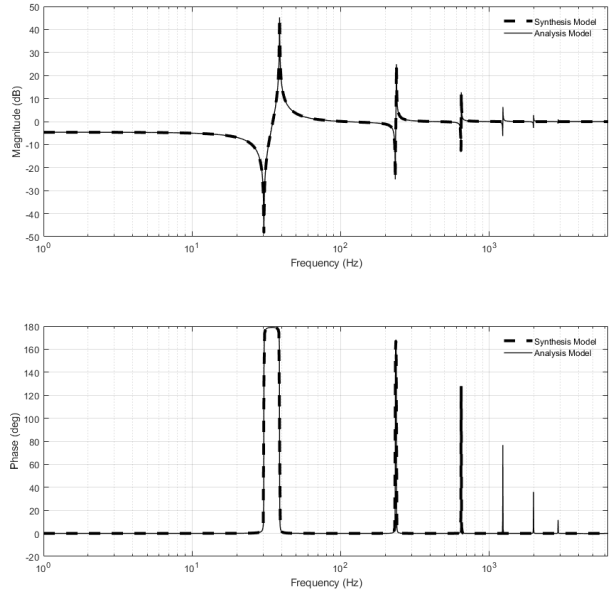

(c) Bode diagram from w to y.

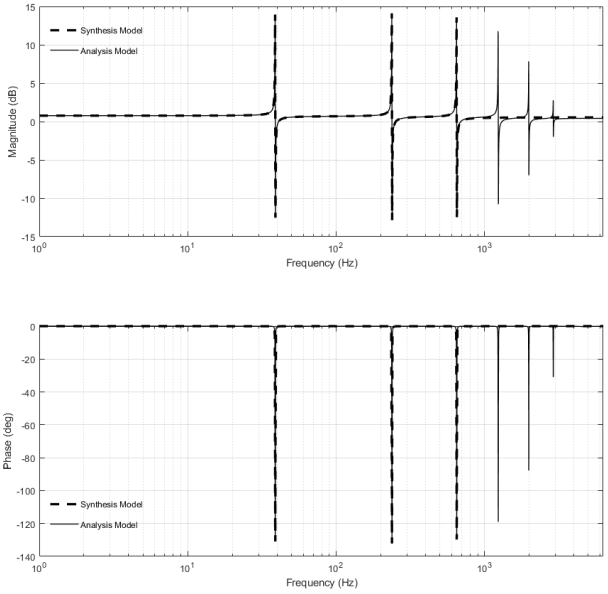

(d) Bode diagram from u to y.

Figure 3.3. Bode diagrams of the flexible membrane from the perturbation w and the control input u to the measured output y and the controlled output z_a.

and it is known as a controller "spillover" [12].

Below, the flexible structures under consdieration in the frequency range of interest that we intend to use (for the controllers' synthesis in future chapters) are considered.

The models considered here were obtained through the Finite Element Method (FEM) and they can be expressed

in state-space form or through transfer functions. The main difference of this order reduction is the presence of direct feedforward elements in the measured output, i.e. $y(t) = C_y\, x(t) + D_{yw}\, w(t) + D_{y\,u}\, u(t)$. Following the model's truncation up to the vibration modes involved in the frequency range of interest, we end up with a finite-dimensional model. Since the controllers treated in this work are designed for tackling vibration perturbations in finite-dimensional systems, this is appropriate for our purposes. For this case, the frequency range that best suits will be with the first three controllable and observable vibration modes, which implies a range of frequency spanning among $[0\text{—}700\,]Hz$ for the flexible beam, and $[0\text{—}1200\,]Hz$ for the flexible axisymmetric membrane. A methodology for measuring the energy contained in each mode was proposed in [176].

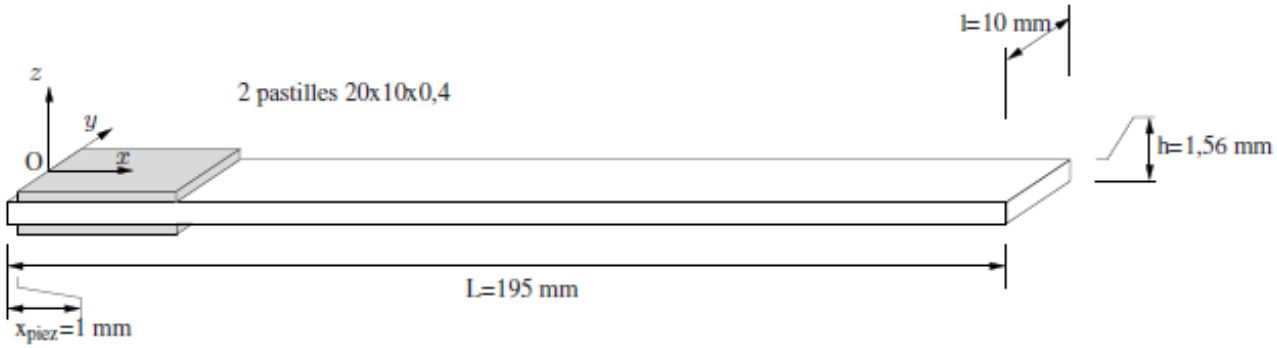

Figure 3.4. Flexible beam.

3.6.1 State-space representation of the flexible beam

In this part we describe the structure of the system under consideration, i.e. the flexible beam. In the mechanical engineering area, as a result of the robotics technology development with high speed, high precision and lightweight, flexible arms are being used for industrial purposes, instead of rigid arms [76].

The flexible beam is a mechanical system with an aluminium based structure, clamped into a stiff movable support from one side subjected to an irregular thrust, meant to act as a perturbation input-signal $w(t)$ aligned vertically (i.e. along the z-axis), holding the other side of the beam loose. It is equipped with two piezoceramic lead zirconate titanate (PZT) collocated patches, one of them is used as an actuator with a $0.4\,\mathrm{mm}$ thickness and the other is used as a sensor with a $0.7\,\mathrm{mm}$ thickness. An analysis including the reason that the sensor's thickness must be greater than the actuator's thickness can be found in [172].

The first six vibrating modes inside the range of frequency that awares interest to our control purposes are represented from the Figures 3.6.a to 3.6.f, that spans from $0\,\mathrm{Hz}$ to $700\,\mathrm{Hz}$, and all are controllable and observable, controllable by the actuators and observables by the sensor.

There are other modes that are not controllable and not observable at all. In the Figures 3.7.a to 3.7.c are the first three modes that are not controllable and observable, and that lie inside our frequency range of interest.

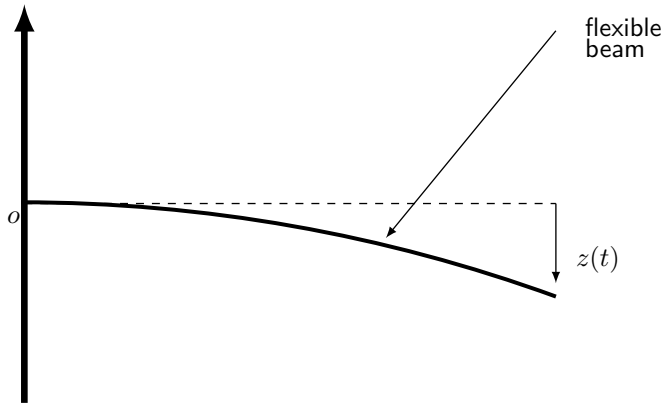

Figure 3.5. Flexible beam diagram.

The state variables in a system's model possess an engineering meaning, they are the canonical set of conserved extensive quantities in the system [74]. The flexible beam considered here is endowed with the first 10 vibrating modes, from which 2 are static modes (1 for every system's input). Finally, this model is composed of 12 modes, i.e. 12 pairs of complex poles, $A \in \mathbb{R}^{2n_c \times 2n_c}$, where $n_c = 12$ represents the number of vibration modes. The two inputs are formed by one matching the actuator's voltage through the matrix $B_u \in \mathbb{R}^{2n_c \times 1}$, and the other matches the imposed acceleration to the embedded device (in m/sec^2), through the matrix $B_w \in \mathbb{R}^{2n_c \times 1}$.

This model is also made by 7 outputs, from which one corresponds to the piezoelectric sensor's deformation measurement, it is the output used for the computation of the control law, seen through observation matrix $C_y \in \mathbb{R}^{1 \times 2n_c}$, and a feedforward matrix $D_y \in \mathbb{R}^{1 \times 2}$. Three outputs allow to recover the cinematic characteristics along the vertical axis (z-axis) of a point located at the beam's loose end (z_d, z_v & z_a), and other three at a point located at the beam's center (z_{d1}, z_{v1} & z_{a1}).

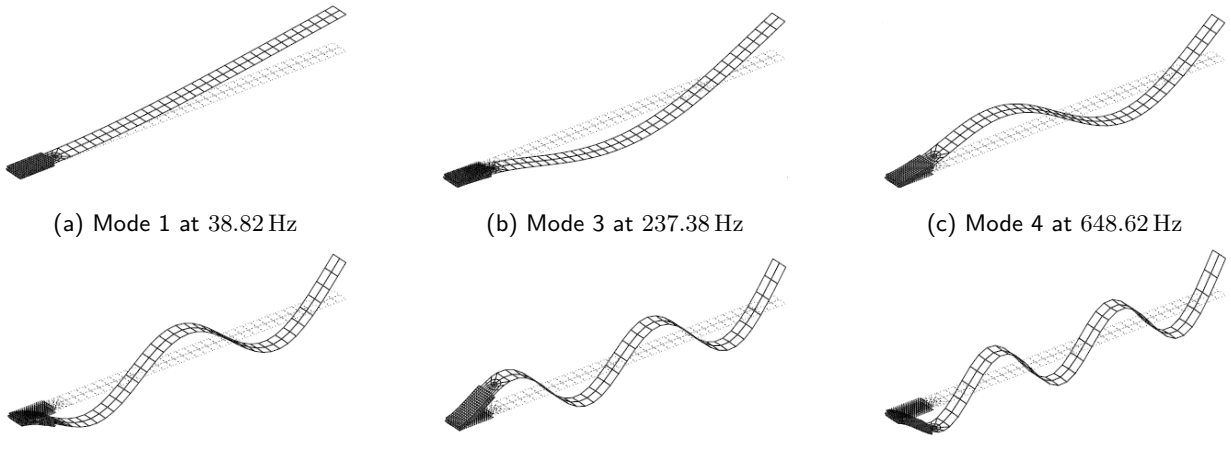

(a) Mode 1 at $38.82\,\mathrm{Hz}$ (b) Mode 3 at $237.38\,\mathrm{Hz}$ (c) Mode 4 at $648.62\,\mathrm{Hz}$

(d) Mode 5 at $1,236.05\,\mathrm{Hz}$ (e) Mode 8 at $1,986.94\,\mathrm{Hz}$ (f) Mode 9 at $2,907.37\,\mathrm{Hz}$

Figure 3.6. Controllable and observable modes in the range of frequency of interest.

These devices are often called *smart structures*, which are structures that can adapt automatically to different operating and environmental conditions [85]. In problems related to vibration suppression, the transducers' signals are often used in

the feedback control loops analysis involved in the design of active vibration controllers.

The objective of damping structures with peaks of resonance at low frequencies, results in an interesting problem, particularly for the smart structures which have lightly damped modes with closely spaced resonance frequencies.

Due to the fact that a flexible beam is a test-bench available in many labs, it allows the experimental implementation of the proposed control techniques.

The flexible beam is modelled using Finite Element Analysis (FEA) associated with modal analysis that allows to get a multivariable model (MIMO) describing the structure's behavior among all inputs and all outputs, as can be seen in the state-space realization. After the modelling techniques with the Finite Element Method (FEM), the flexible structures (in this case the flexible beam and the flexible membrane) hold a linear time-invariant model, with the same features, inputs and the same outputs.

A reduced-order model in state-space form, is derived from the analysis model and it is used here for the synthesis of the controllers. It can be obtained through a truncation technique, as long as consistency with the static gains of the analysis model be provided.

The input-output frequency response through a high-order and accurate model in state-space form, where according to the presence of direct feedthrough matrices or not, will be considered henceforward either as the synthesis model or as the analysis model, respectively.

The state-space model includes $2n_c = 24$ ill-damped poles, with a damping factor $\xi_i = 1 \times 10^{-3}$, which is not enough for vibration damping applications, that need to deal with these perturbations, and to damp them properly, as fast as possible.

3.6.2 Transfer function representation of the flexible beam

Engineering problems are prone to be complicated. It is valuable to understand the challenges of a problem well enough to be able to specify the nature of its solutions. This is done using the formal language of engineering, mathematics, science and problem solving. In most engineering analysis this is done through developping and studying mathematical models (of varying precision) to predict the behavior of physical systems. The way to describe these physical systems is through differential equations due to their time dependance. All real systems are non-linear, and without generalizing, they can

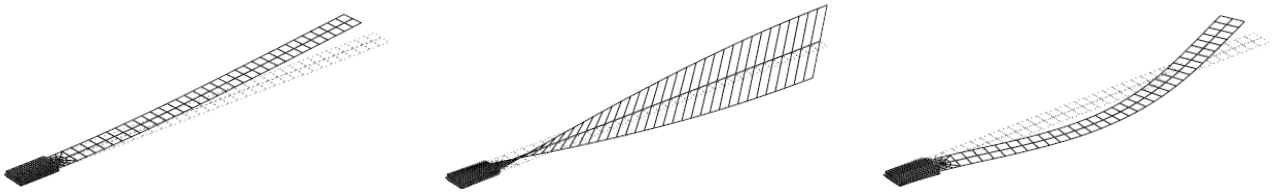

(a) Mode 2 at $230.51\,\mathrm{Hz}$. (b) Mode 6 at $1,373.02\,\mathrm{Hz}$. (c) Mode 7 at $1,406.64\,\mathrm{Hz}$.

Figure 3.7. Uncontrollable and unobservable modes in the range of frequency of interest.

be approximated by linear systems in a given set-point, with the association that superposition characteristics are true to some extent [108, Ch. 13] w.r.t. some variables.

Mathematically, the resulting differential equations are not only linear, but they also have constant coefficients. For example, the description of a single vibration mode is given by the second order equation as follows

$$\ddot{x}(t) + 2\,\zeta\,\omega_n\,\dot{x}(t) + \omega_n^2\,x(t) = f(t) \tag{3.12}$$

where $x(t)$ is the dependent variable or physical phenomenon to control (displacement, voltage, etc.), $f(t)$ is a forcing function (force, voltage, etc.), and ζ and ω_n are the damping factor and the natural frequency, respectively, whose values depend on the size and interconnections of the individual physical components that form the system (spring/stiffness constants, inductance values, etc.).

The Equation (3.12) is a second-order differential equations, also called 'linear constant coefficient ordinary differential of 2$^{\text{nd}}$ order equation' (LCCODE) [184], or simply 'ordinary differential equation' (ODE). The method typically used for solving these kind of equations is the Laplace transform [103].

Though the fact that all the initial conditions of the system must be known for the use of the Laplace transform, an important characteristic of such transformation, is that it transforms ODE into algebraic equations, allowing the problem the use of simple and standard manipulations.

In our systems, from the exogenous perturbation $w(t)$ to the controlled output $z_a(t)$, we have a SISO system. As a wholesome it is composed by the output to be controlled $z_a(t)$, thanks to the model obtained through finite element method, the strain as an output that can be measured through a piezoelectric sensor $y(t)$, the perturbation $w(t)$, and the actuator's control input $u(t)$, as it can be seen in the Equation (3.13). Hence, the transfer function of this SISO's model, with s as the Laplace variable, is written as

$$\mathcal{P}_b \begin{cases} z_a(s) &= \dfrac{Q_{zw}(s)}{\varphi(s)}\,w(s) + \dfrac{Q_{u\,z}(s)}{\varphi(s)}\,u(s), \\ y(s) &= \dfrac{Q_{yw}(s)}{\varphi(s)}\,w(s) + \dfrac{Q_{u\,y}(s)}{\varphi(s)}\,u(s). \end{cases} \tag{3.13}$$

The order for the specified quasipolynomials in equation (3.13) is $2\,n_c$, which differs from the analysis to the synthesis models. We can establish the relations between (3.11) and (3.13) as

$$\begin{aligned} \varphi(s) &= \det(s\mathbb{I} - A), \\ Q_{zw}(s) &= C_z\,B_w + D_{zw}\,\det(s\mathbb{I} - A), \\ Q_{yw}(s) &= C_y\,B_w + D_{yw}\,\det(s\mathbb{I} - A), \\ Q_{zu}(s) &= C_z\,B_u + D_{zu}\,\det(s\mathbb{I} - A), \\ Q_{yu}(s) &= C_y\,B_u + D_{yu}\,\det(s\mathbb{I} - A). \end{aligned}$$

Remark 3.1. *Note that if the measurement of the output $z_a(t)$ is required, we can recover it from an accelerometric sensor at the end of the beam, or through the implementation of a state observer.*

The values of the transfer function coefficients of the synthesis model's polynomials are expressed in Table 3.2, where it is worth mentioning that the denominator $\varphi(s)$ is a monic polynomial.

Table 3.2. Numerical values for the flexible beam's polynomials coefficients in the synthesis model of Equation (3.13).

$Q_{zw}(s) = \sum_{k=0}^{2n_c} q_{zw_k}\, s^k,$	$Q_{zu}(s) = \sum_{k=0}^{2n_c} q_{zu_k}\, s^k,$
$q_{zw_0} = 4.2255 \times 10^{12}$	$q_{zu_0} = -9.3849 \times 10^{10}$
$q_{zw_1} = -2.6316 \times 10^{13}$	$q_{zu_1} = 7.0058 \times 10^{11}$
$q_{zw_2} = -5.7283 \times 10^{13}$	$q_{zu_2} = 1.3460 \times 10^{12}$
$q_{zw_3} = -7.9945 \times 10^{7}$	$q_{zu_3} = 1.5127 \times 10^{6}$
$q_{zw_4} = -1.5930 \times 10^{7}$	$q_{zu_4} = -1.8971 \times 10^{6}$
$q_{zw_5} = -1.4598 \times 10$	$q_{zu_5} = 5.1122$
$q_{zw_6} = -1.2561$	$q_{zu_6} = 4.3989 \times 10^{-1}$
$Q_{yw}(s) = \sum_{k=0}^{2n_c} q_{yw_k}\, s^k,$	$Q_{u\,y}(s) = \sum_{k=0}^{2n_c} q_{y\,u_k}\, s^k,$
$q_{yw_0} = -9.1133 \times 10^{17}$	$q_{yu_0} = 2.02 \times 10^{17}$
$q_{yw_1} = -2.4171 \times 10^{12}$	$q_{yu_1} = 1.8185 \times 10^{12}$
$q_{yw_2} = -2.1924 \times 10^{12}$	$q_{yu_2} = 3.1394 \times 10^{12}$
$q_{yw_3} = -1.729 \times 10^{6}$	$q_{yu_3} = 5.6534 \times 10^{6}$
$q_{yw_4} = -3.184 \times 10^{5}$	$q_{yu_4} = 1.3761 \times 10^{6}$
$q_{yw_5} = -5.0564 \times 10^{-2}$	$q_{yu_5} = 7.4011 \times 10^{-1}$
$q_{yw_6} = -4.3509 \times 10^{-3}$	$q_{yu_6} = 6.3683 \times 10^{-2}$
$\varphi(s) = \sum_{k=0}^{2n_c-1} a_k\, s^k,$	
$a_0 = 2.1983 \times 10^{18}$	$a_1 = 2.2051 \times 10^{13}$
$a_2 = 3.8069 \times 10^{13}$	$a_3 = 7.7528 \times 10^{7}$
$a_4 = 1.8893 \times 10^{7}$	$a_5 = 1.1622 \times 10^{1}$

Remark 3.2. *As a particular remark, we have recalled the modelling of the flexible beam, for its state-space representation and the transfer function equations. The Figure 3.8 shows the frequency responses, where only 6 peaks of resonance can be seen for the analysis model, and only 3 peaks for the synthesis model. These peaks are the modes 1, 3, and 4, with resonant frequencies at $38.82\,\mathrm{Hz}$, $237.38\,\mathrm{Hz}$, and $648.62\,\mathrm{Hz}$, respectively. We notice that the other modes concerned in the whole linear time-invariant system computed from the FEA are not considered. This is because they are non-controllable, non-observable, or neither controllable nor observable.*

The flexible beam is portrayed in the picture of Figure 3.9.

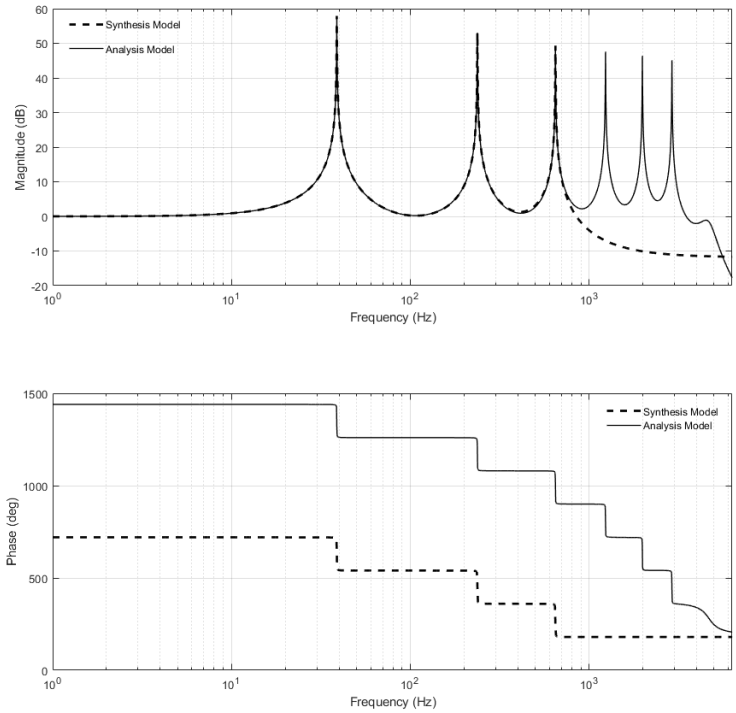

Figure 3.8. Frequency responses of the analysis (-) and synthesis (--) models for the flexible beam.

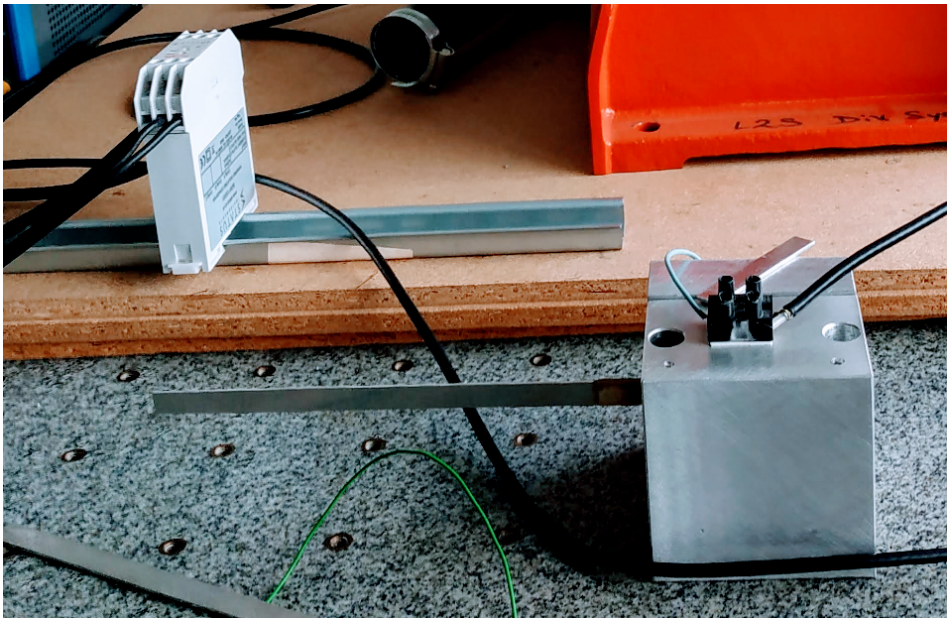

Figure 3.9. Photograph of the flexible beam taken at the L2S.

3.7 Characteristics of the flexible membrane

This section aims to describe the characteristics of the model used for the performance analysis of a flexible axisymmetric membrane against exogenous perturbations. As well as the flexible beam discussed above (Section 3.6.1), two piezoelectric patches are placed, and in this case they are oriented according to its axis of symmetry. For its performance analysis against a perturbation on the z-axis, the structure is fixed on a moving base, whose time response can be shaped as a rectangular signal, pushing the membrane with an acceleration, noted $w(t)$. In [174] where the FEM model of this membrane has been considered before.

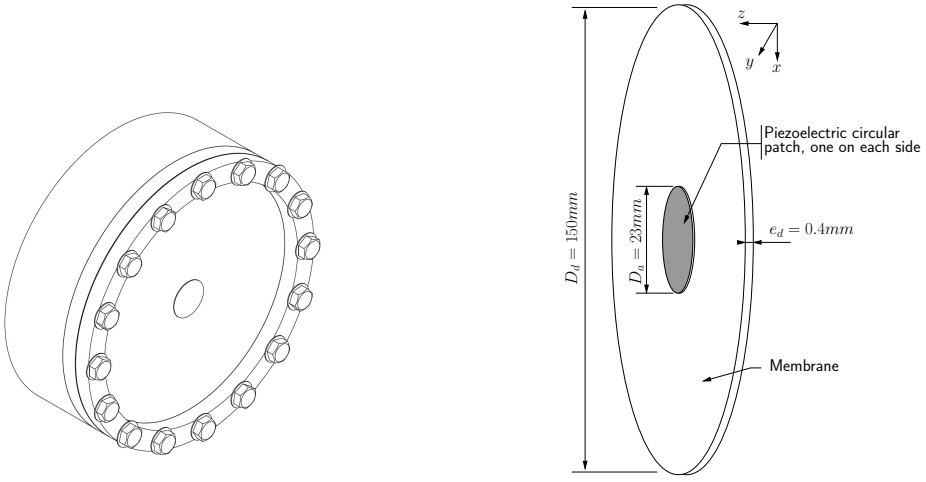

Figure 3.10. Flexible axisymmetric membrane (dimensions on the right) inserted in the device which is subjected to vibrations (Computer Aided Design figure on the left)

The mathematical modeling of the dynamical behavior for such flexible mechanical structures is based on several coupled partial differential equations (PDEs) in space and time-dependant variables. The non-linear system of a similar circular membrane is discussed in [192], where the discussion on a second-order partial differential equation modelling of a damaged membrane for the analysis of its mechanical vibration is carried on. Such equations, that are of infinite dimensional ones, are usually addressed through numerical methods like the Finite Element Modeling (FEM) [139]. This method leads to a set of Ordinary Differential Equations (ODEs) that are linear but with a very great number of variables. Because of the numerical feature of this method, it is worth at mentioning that the physical parameters of the PDEs are dissolved within numerical coefficients of the corresponding ODEs.

An accurate model in state-space form is derived from the set of ODEs from the FEM thanks to a model reduction method called *modal analysis*. It describes the inputs-to-outputs dynamical behavior in the bandwidth of interest, say $[0 - 4000Hz]$ for our system. In contrast to the flexible beam's model described above, this model depicts the first 42 vibration modes plus 2 static modes that account for both inputs (control law u and perturbation w), adding up to $n_c = 44$ vibration modes, and piezoelectric input-output interfaces, given by 1 actuator and 1 sensor, respectively. This model is

the *analysis model* and it is of order $2n_c = 88$, which includes only controllable and observable modes. A low-order model, dedicated to the controller design, is obtained from the analysis one thanks to a reduction method based on state-variable truncation [4]. It is called the *synthesis model*. It is of order 6 and it includes the first three vibration modes that are controllable and observable. Let $x \in \mathbb{R}^{2n_c}$ be the state vector of the system, with $n_c = 44$ in the case of the analysis model and with $n_c = 3$ for the synthesis model. Both models can be described by the linear state-space model in (3.14), denoted as $\mathcal{P}_m$. Note that, in the case of the synthesis model, there are non-zero feedthrough terms between the inputs w and u and the outputs z and y, whereas these feedthrough terms are equal to zero in the case of the analysis model.

The piezoelectric sensor's patch has a thickness of $0.7\,\mathrm{mm}$, and the piezoelectric actuator's patch has a thickness of $0.4\,\mathrm{mm}$. As can be seen, the thickness of the piezoelectric actuator has to be smaller than the piezoelectric sensor, and a discernement about it can be found in [171].

These piezoelectric patches are rigidly bounded each side of the disk and centered according to its axis of symmetry. The problem of vibrations measured through a piezoelectric sensor within a moving membrane has been treated in [49] and [174]. This system is shown in the Figure 3.10.

The controlled signal (input), noted $u(t)$, is the voltage applied across the piezoelectric actuator. The measured output, noted $y(t)$, is the electric voltage delivered by the piezoelectric sensor. The disturbance input $w(t)$ is the total acceleration applied to the clamped circular edge of the structure. The controlled output that is consider in this manuscript, noted $z_a(t)$, is the z component (see Figure 3.10) of the acceleration of a point located at the center of the disc and on the upper side of the piezoelectric chip used as a sensor.

The flexible axysimmetric membrane, is shown in the left of Figure 3.10. The important dimensions of this membrane can be described with the diameters' distances (i.e. $D_d = 150\,\mathrm{mm}$ for the outer disk, and $D_a = 23\,\mathrm{mm}$ for the inner disk), and its thickness (i.e. $e_d = 0.4\,\mathrm{mm}$). They can be observed in the right of the Figure 3.10.

3.7.1 State-space representation of the flexible membrane

The mathematical modeling of the dynamical behavior for such mechanical structures is based on several coupled partial differential equations in space and time-dependant variables. See for example [63] for more details that are out of the scope of this dissertation. Such equations, that are of infinite dimension, are usually addressed through numerical methods like the Finite Element Modeling (FEM) [99]. It allows to obtain a set of several ordinary differential equations that are more tractable, but which occult several physical distributed parameters behind numerical coefficients.

The finite element analysis associated with modal analysis permit to get a high-order and accurate model, in state-space form (3.14), which is devoted to simulation analysis. A low-order one, dedicated to the controller synthesis, is also available and differs from (3.14) especially by the presence of feedthrough terms between the inputs w and u and the outputs z and y, whereas no feedthrough term is present in the analysis model. In our case, the analysis model is of order 10 after eliminating the uncontrollable and unobservable modes. It describes the inputs-to-outputs dynamical behavior

in the bandwidth $[0 - 4000Hz]$. In the current work, the analysis model is composed of 44 oscillating vibration modes making up a model of 88 states, but it contains 38 uncontrollable and unobservable modes. The low-order model is of order 6, containing the first 3 controllable and observable vibration modes. The reduced one is of order 6, including the first three vibration modes. All the kept modes are controllable and observable. Let $x \in \mathbb{R}^{2n_p}$ be the state vector of the system, with $n_p = 44$ vibration modes in the case of the analysis model and with $n_p = 3$ vibration modes for the synthesis model. The shapes of the first vibration modes are shown in the Figure 3.12.

$$\mathcal{P}_m \begin{cases} \dot{x}_p(t) = Ax_p(t) + B_w w(t) + B_u u(t) \\ z_{a1}(t) = C_z x_p(t) + D_{zw} w(t) + D_{zu} u(t) \\ y(t) = C_y x_p(t) \ (+ \ D_{yw} w(t) + D_{yu} u(t)) \end{cases} \tag{3.14}$$

where the structural difference between the analysis model and the synthesis one, is the presence of feedforward matrices

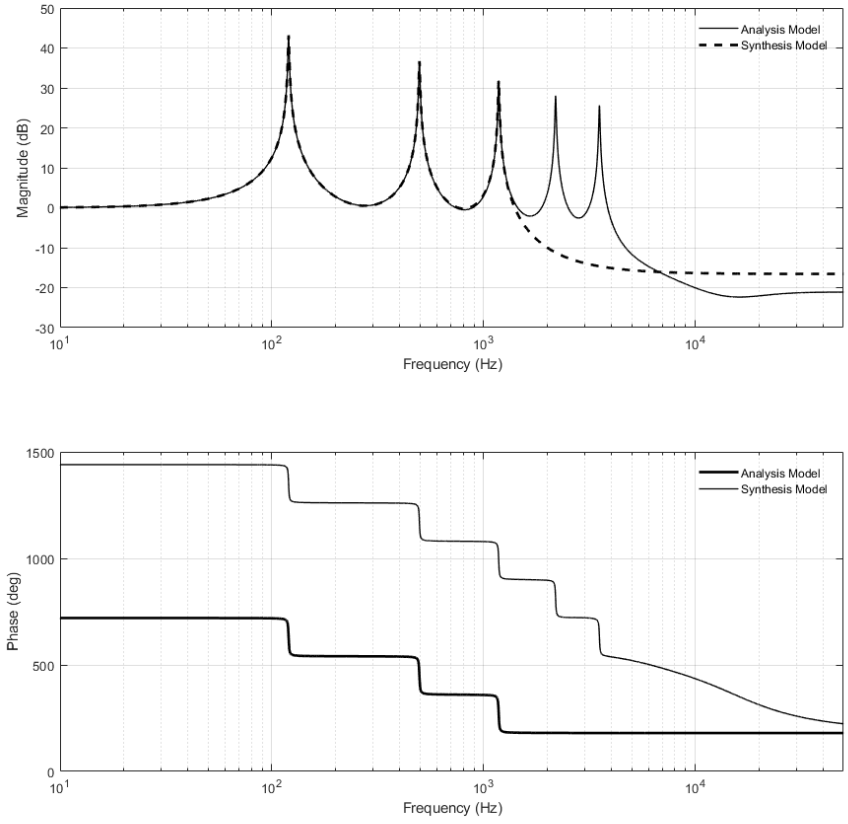

Figure 3.11. Frequency responses of the analysis (-) and synthesis (--) models for the flexible membrane.

in the measured output, given as $y(t) = C_y x_p(t) + D_{yw} w(t) + D_{yu} u(t)$. The piezo-actuated membrane is a SISO system, i.e. with only one actuator, driven by the controlled electrical voltage u, and only one measured output signal corresponding

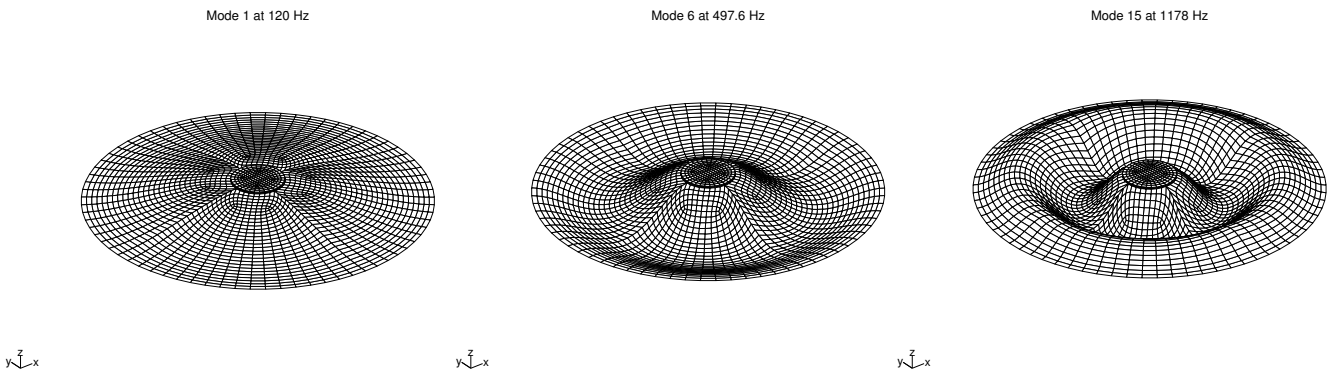

Figure 3.12. First three controllable and observable vibration modes.

to the electrical voltage y. The disturbance input w is the total acceleration applied to the clamped edge of the structure. The vertical total acceleration of the membrane center is our controlled output z.

3.7.2 Transfer function representation of the flexible axisymmetric membrane

In order to talk about the different model's representations of the two flexible structures used in this work, we finish specifying the transfer function model of the flexible axisymmetric membrane, derived from the data of the state-space one.

In the sequel, the transfer functions based model is used for the delay-based control design instead of the state-space form. It is derived from (3.14) by applying to it the Laplace transform. It is given by

$$\mathcal{P}_m \begin{cases} z(s) &= \dfrac{Q_{zw}(s)}{\varphi(s)} w(s) + \dfrac{Q_{zu}(s)}{\varphi(s)} u(s) \\ y(s) &= \dfrac{Q_{yw}(s)}{\varphi(s)} w(s) + \dfrac{Q_{yu}(s)}{\varphi(s)} u(s) \end{cases} \tag{3.15}$$

where s denotes the Laplace variable.

These polynomials are written as

$$\begin{aligned} Q_{zw}(s) &:= \sum_{k=0}^{2n_c} q_{zw_k}\, s^k, \qquad Q_{zu}(s) := \sum_{k=0}^{2n_c} q_{zu_k}\, s^k, \\ Q_{yw}(s) &:= \sum_{k=0}^{2n_c} q_{yw_k}\, s^k, \qquad Q_{yu}(s) := \sum_{k=0}^{2n_c} q_{yu_k}\, s^k \end{aligned}$$

$$\text{and} \quad \varphi(s) := \sum_{k=0}^{2n_c} a_k\, s^k$$

where $a_{n_p} = 1$ is imposed for simplicity. The numerical values of the polynomials' coefficients for the synthesis model in (3.15) are given in Table 3.3.

Table 3.3. Numerical values for the polynomials' coefficients in the case of the axisymmetric membrane's synthesis model.

$Q_{zw}(s) = \sum_{k=0}^{2n_c} q_{zw_k}\, s^k,$	$Q_{zu}(s) = \sum_{k=0}^{2n_c} q_{zu_k}\, s^k,$
$q_{zw_0} = 5.30488 \times 10^{14}$	$q_{zu_0} = -1.01734 \times 10^{20}$
$q_{zw_1} = -5.31674 \times 10^{15}$	$q_{zu_1} = -2.38029 \times 10^{15}$
$q_{zw_2} = -7.53046 \times 10^{14}$	$q_{zu_2} = -2.21049 \times 10^{14}$
$q_{zw_3} = -3.05369 \times 10^{9}$	$q_{zu_3} = -2.00512 \times 10^{9}$
$q_{zw_4} = -5.92403 \times 10^{7}$	$q_{zu_4} = -4.12495 \times 10^{7}$
$q_{zw_5} = -1.29576 \times 10^{2}$	$q_{zu_5} = -1.22644 \times 10^{2}$
$q_{zw_6} = -1.14827$	$q_{zu_6} = -1.08684$
$Q_{yw}(s) = \sum_{k=0}^{2n_c} q_{yw_k}\, s^k,$	$Q_{y\,u}(s) = \sum_{k=0}^{2n_c} q_{u\,y_k}\, s^k,$
$q_{yw_0} = 1.71742 \times 10^{19}$	$q_{yu_0} = 2.93494 \times 10^{19}$
$q_{yw_1} = 4.69023 \times 10^{13}$	$q_{yu_1} = 5.08699 \times 10^{14}$
$q_{yw_2} = -3.20992 \times 10^{12}$	$q_{yu_2} = 5.40386 \times 10^{13}$
$q_{yw_3} = -1.12431 \times 10^{6}$	$q_{yu_3} = 2.67285 \times 10^{8}$
$q_{yw_4} = 7.50731 \times 10^{4}$	$q_{yu_4} = 5.85451 \times 10^{6}$
$q_{yw_5} = -1.68094 \times 10^{-1}$	$q_{yu_5} = 9.45916$
$q_{yw_6} = -1.48961 \times 10^{-3}$	$q_{yu_6} = 8.38248 \times 10^{-2}$
$\varphi(s) = \sum_{k=0}^{2n_c-1} a_k\, s^k,$	
$a_0 = 3.04635 \times 10^{20}$	$a_1 = 5.42594 \times 10^{15}$
$a_2 = 5.72533 \times 10^{14}$	$a_3 = 2.98444 \times 10^{9}$
$a_4 = 6.51670 \times 10^{7}$	$a_5 = 1.12844 \times 10^{2}$

Remark 3.3. *In this section we have reviewed the modelling of the flexible axisymmetric membrane, in state-space and transfer function realizations. We see that the frequency responses are shown in the Figure 3.11, where only 6 peaks of resonance can be seen for the analysis model, and only 3 peaks for the synthesis model. These peaks are the modes* 1, 6, *and* 15, *with resonant frequencies at* $120\,\mathrm{Hz}$, $497.6\,\mathrm{Hz}$, *and* $1178\,\mathrm{Hz}$, *respectively. The other modes are not considered due to the fact that they are not neither controllable, nor observable ones.*

3.8 Chapter summary

In this chapter a general presentation of the flexible structures under consideration is given. The flexible structures included the flexible beam and the flexible axisymmetric membrane. Its behavior involving PDE renders it as an infinite-dimensional system. The physical characteristics were described. The description of its controllable and observable modes as well as

its uncontrollable and unobservable modes were shown. The flexible beam's numerical model was given and it state-space realization was well deployed. Considering the uncontrolled bode plots of the Figure 3.8 and the Figure 3.11, we see the modes that we intend to damp. To avoid that when an input signal with a frequency close to the resonant frequencies produce an output with an high amplitude, we should use an active vibration control technique. The techniques treated in subsequent chapters involve the quasipolynomial-based control technique (Chapter 5), as well as the optimal $\mathcal{H}_\infty$ technique (Chapter 4). Finally, properties on the flexible structures modelling were shown where we can say that, after applying the FEA techniques for the flexible structures, we then get a linear time-invariant system with similar inputs and similar outputs, with different resonant frequencies for the vibration modes, and static gains.

Chapter 4

Optimal $\mathcal{H}_\infty$ controller design

Recalling the purpose of the present work is to explore new control techniques that can be used for the active vibration control problem, specifically in flexible systems. The following method is based on the principle of the $\mathcal{H}_\infty$ control, its robustness properties, as well as its controller synthesis.

This chapter is based on the $\mathcal{H}_\infty$ control techniques used for flexible structures and it deals with the basic results and fundaments on the system's performance regarding regulation, tracking, or disturbance rejection. It is divided into seven sections. In Section 4.1, we discuss the $\mathcal{H}_\infty$ norm and its application in control theory. In Section 2.2.1, we introduce pole placement techniques and explain how they can be used for control design. In Section 4.2, we discuss the objective of the $\mathcal{H}_\infty$ controller and how it can be used to achieve robust performance. In Section 4.3, we discuss unstructured uncertainties and their impact on control design. In Sections 4.4 and 4.5, we present the optimal $\mathcal{H}_\infty$ control design for the flexible beam and axisymmetric membrane, respectively. We discuss the design process and the resulting control laws. Finally, in Section 4.6, we provide concluding remarks, summarizing the main contributions of the chapter.

Contents

4.1 $\mathcal{H}_\infty$ norm

Considering a system with a dynamic given as $y = G(s)\,u$. We can measure its performance according to the next definition

Definition 4.1. *The $\mathcal{H}_\infty$ norm of the transfer function T_{zw}, from the input w to the output z_a is*

$$\|T_{zw}\|_\infty = \sup_{\substack{w\in\mathcal{L}_2,\\ w\neq 0}} \frac{\|z_a\|_2}{\|w\|_2}. \tag{4.1}$$

So, going again with the transfer function G, and using the Fourier transform and the maximum singular value we have

$$\|G\|_\infty = \sup_{\omega\in\mathbb{R}} \sigma_{\max}\big(G(j\omega)\big) \tag{4.2}$$

for every stable rational function G.

The definition 4.1 can be seen as the energy gain $\|G(s)\|_\infty$ from the input w to the output z, i.e. :

$$\|G(s)\|_\infty = \max_{u(t)\neq 0} \frac{\int_0^\infty y^T(t)\,y(t)\,dt}{\int_0^\infty u^T(t)\,u(t)dt}$$

where $y \in \mathbb{R}^n$ and $u \in \mathbb{R}^m$.

Next, the characterization of a system's $\mathcal{H}_\infty$ norm according to its state-space realization (i.e. its A, B, C and D matrices) is addressed using the Bounded Real Lemma.

Lemma 4.1.1 (Bounded Real Lemma)**.** *Let $(A,\,B,\,C,\,D)$ be the $G(s)$ stable transfer function's state-space realization, and let a constant $\gamma > 0$. The $\mathcal{H}_\infty$ norm $\|G(s)\|_\infty < \gamma$ if and only if there exists a positive definite symmetric matrix $X = X^T > 0$ such that*

$$\begin{bmatrix} X\,A + A^T\,X & X\,B & C^T \\ B^T\,X & -\gamma\,I & D^T \\ C & D & -\gamma\,I \end{bmatrix} < 0. \tag{4.3}$$

4.2 Objective of the $\mathcal{H}_\infty$ controller

Out there, there are many different techniques that proove their utility when designing linear multivariable analog controllers, and pole placement is a very attractive technique. The pole placement technique implies to assemble a subset of the open loop poles in specific regions inside the stability region. It consists on specifying a performance function and then optimize it. The most popular norms to perform optimization techniques are the $\mathcal{H}_2$ and the $\mathcal{H}_\infty$ norms. In the $\mathcal{H}_\infty$

control case, such performance function is the norm of the closed-loop transfer matrix, suitably weighted.

The controller structure used here is adequate for systems where we intend to minimise the $\mathcal{L}_2$-norm from an unknown perturbation, say white or colored noise, to the controlled output of interest. Likewise, the synthesis problem of providing robustness to the controller's design against the unstructured modes is essential. Nonetheless, the design objective includes minimising the $\mathcal{H}_\infty$ norm as well as provide damping of the first three vibrating modes through the robustness of the regional pole placement with a full-order dynamic controller (4.5).

The $\mathcal{H}_\infty$ controller is a type of robust control that seeks to achieve several key control objectives. Firstly, the objective of robust stability is achieved by designing the controller to ensure that the closed-loop system is stable, even in the presence of disturbances and uncertainties. This is achieved by minimizing the maximum singular value of the closed-loop transfer function, which corresponds to the largest amplification of the system's sensitivity to disturbances [91, Chap. 3]. Secondly, the performance improvement objective is achieved by reducing the effect of disturbances on the system's response and improving the tracking accuracy. This results in a smoother and more accurate response to changes on the set-point, and reduces the sensitivity of the system to external disturbances. Thirdly, the disturbance rejection is achieved by reducing the effect of disturbances on the system's response, so that the desired performance is maintained despite the presence of external disturbances. This is particularly useful in applications where the system is sensitive to disturbances, such as in process control [157]. Fourthly, the $\mathcal{L}_2$ norm constraint in $\mathcal{H}_\infty$ control design provides a guarantee on the energy of the control input, making it useful in systems where control effort is a concern. This constraint ensures that the control input has a limited energy, making it suitable for systems where high control efforts may cause actuator saturation or other undesirable effects. Finally, $\mathcal{H}_\infty$ control provides robustness against modeling errors by considering the worst-case scenario of the system behavior in the presence of uncertainties. This is particularly useful in situations where the system model is uncertain or incomplete, as it ensures that the control system will remain stable even in the presence of modeling errors. Overall, $\mathcal{H}_\infty$ control is a useful tool for achieving a range of control objectives, including stability, performance improvement, disturbance rejection, guaranteed L_2 norm performance, and robustness against modeling errors.

Among the different synthesis methods of $\mathcal{H}_\infty$ controllers, here we consider the controllers formulated with the help of linear matrix inequalities (LMI). These controllers may be synthetized succesfully with the help of computational tools related to the semi-definitie programming (SDP). This approach based on LMIs allows bigger flexibility and affordability to treat a more specific class of systems, e.g. linear time invariant (LTI) systems, large-scale systems, among others [34, 96].

The robust pole placement technique in LMI regions is a method for designing robust controllers for linear systems that achieves a desired closed-loop pole placement in a region defined by linear matrix inequalities (LMIs) [40]. In this technique, the objective is to design a controller that stabilizes the system and places the closed-loop poles at specified locations, while also ensuring that the system remains robust to uncertainty and disturbances. The design problem is formulated as a convex optimization problem, where the LMI constraints define the region in which the desired poles must be placed. These methodologies can produce controllers with orders comparable with the order of the system. Therefore, techniques to reduce the orders of these controllers have to be used.

Here we use a methodology proposed in [40] for a multiobjective problem through an LMI-based approach introduced in [58].

This methodology is followed using the low-order model for synthesis purposes, in order to compute this low-order controller capable of meeting the multiobjective purpose, as well as its correct implementation into a real-time computer. A robust $\mathcal{D}$-stable controller is computed if a matrix $X > 0$ exists, such that

$$\begin{bmatrix} M_{\mathcal{D}}(A_{c\ell}, X) & M_1^T \bigotimes (X\, B_{c\ell}) & M_2^T \bigotimes C_{c\ell}^T \\ M_1 \bigotimes (B_{c\ell}^T\, X) & -\gamma\, \mathbb{I} & \mathbb{I} \bigotimes D_{c\ell}^T \\ M_2 \bigotimes C_{c\ell} & \mathbb{I} \bigotimes D_{c\ell} & -\gamma\, \mathbb{I} \end{bmatrix} < 0, \tag{4.4}$$

where $M_1^T\, M_2 = M$ is a full-rank factorization of M, $\mathbb{I}$ is the identity matrix of appropriate sizes, $A_{c\ell}$, $B_{c\ell}$, $C_{c\ell}$ and $D_{c\ell}$ are the closed-loop matrices, given by

$$A_{c\ell} := \begin{bmatrix} A + B_u\, D_K\, C_y & B_u\, C_K \\ B_K\, C_y & A_K \end{bmatrix},$$

$$B_{c\ell} := \begin{bmatrix} B_\Delta + B_u\, D_K\, D_{y\Delta} \\ B_K\, D_{y\Delta} \end{bmatrix},$$

$$C_{c\ell} := \begin{bmatrix} C_\Delta + D_{\Delta u}\, D_K\, C_y & D_{\Delta u}\, C_K \end{bmatrix},$$

$$D_{c\ell} := D_{\Delta\Delta} + D_{\Delta u}\, D_K\, D_{y\Delta}.$$

The dynamical output-feedback controller is given as:

$$K \begin{cases} \dot{\eta} &= A_K\, \eta + B_K\, y, \\ u &= C_K\, \eta + D_K\, y. \end{cases} \tag{4.5}$$

Theorem 9. *([40, Thm 5.1]) There exists a full-order output-feedback controller K and a matrix $X > 0$ such that (4.4) holds, if and only if there exist two $n \times n$ symmetric matrices R and S, and matrices $\mathcal{A}_k$, $\mathcal{B}_K$, $\mathcal{C}_K$ and D_K such that*

$$\Lambda_1 := \begin{bmatrix} R & \mathbb{I} \\ \mathbb{I} & S \end{bmatrix} > 0, \tag{4.6}$$

$$\Lambda_2 = \begin{bmatrix} L \bigotimes \Lambda_1 + M \bigotimes \Phi_A + M^T \bigotimes \Phi_A^T & M_1^T \bigotimes \Phi_B & M_2^T \bigotimes \Phi_C^T \\ M_1 \bigotimes \Phi_B^T & -\gamma\, \mathbb{I} & \mathbb{I} \bigotimes \Phi_D^T \\ M_2 \bigotimes \Phi_C & \mathbb{I} \bigotimes \Phi_D & -\gamma\, \mathbb{I} \end{bmatrix} < 0, \tag{4.7}$$

where

$$\Phi_A = \begin{bmatrix} A\,R + B_u\,\mathcal{C}_K & A + B_u\,D_K\,C_y \\ \mathcal{A}_K & S\,A + \mathcal{B}_K\,C_y \end{bmatrix},$$

$$\Phi_B = \begin{bmatrix} B_\Delta + B_u\,D_K\,D_{y\Delta} \\ S\,B_\Delta + \mathcal{B}_K\,D_{y\Delta} \end{bmatrix},$$

$$\Phi_C = \begin{bmatrix} C_\Delta\,R + D_{\Delta u}\,\mathcal{C}_K \\ C_\Delta + D_{\Delta u}\,D_K\,C_y \end{bmatrix}^T,$$

$$\Phi_D = D_{\Delta\Delta} + D_{\Delta u}\,D_K\,D_{y\Delta}.$$

If these LMIs are feasible, then a n^{th}-order controller that robustly assigns the closed-loop poles in $\mathcal{D}$ is

$$K(s) = D_K + C_K\,(s\,\mathbb{I} - A_K)^{-1}\,B_K,$$

with the matrices A_K, B_K and C_K derived as follows:

- *We perform the singular value decomposition of $\mathbb{I} - R\,S$, producing a diagonal matrix S_v containing the singular values and two unitary matrices U and V, such that $U\,S_v\,V = \mathbb{I} - R\,S$.*

- *We compute square matrices $\hat{M}$, $\hat{N} \in \mathbb{R}^{n\times n}$ such that $\hat{M} = U\,S_v^{1/2}$ and $\hat{N} = S_v^{1/2}\,V$.*

- *We solve the following linear equations*

$$\left.\begin{aligned} \mathcal{A}_K &= \hat{N}\,A_K\,\hat{M}^T + \hat{N}\,B_K\,C_y\,R + S\,B_u\,C_K\,\hat{M}^T + S\,(A + B_u\,D_K\,C_y)\,R, \\ \mathcal{B}_K &= \hat{N}\,B_K + S\,B_u\,D_K, \\ \mathcal{C}_K &= C_K\,\hat{M}^T + D_K\,C_y\,R. \end{aligned}\right\} \tag{4.8}$$

  for B_K, C_K and A_K.

4.3 Unstructured Uncertainties

The designing of control laws for different systems' models, often conveys the involvement of uncertainties that have to be taken into account. These uncertainties can come from model differences, i.e. differences between the mathematical model and the actual system; from parameteric uncertainties, which can be produced due to measurement erros or changes in the operating conditions; from exogenous inputs, these are external inputs that affect the system's behavior; or from unmodeled dynamics that have to be neglected during the modelization process for control purposes. By robust control theory, we intend to control a system, i.e. to render it stable, even under the presence of the uncertainties and disturbances.

In this thesis project, we consider this last class of uncertainties. As these unmodeled dynamics uncertainties are assumed static because they do not change over time, they can be modeled as constant matrices.

Consider the uncertain linear system given as

$$\begin{aligned} \dot{x} &= A(\Delta)\, x, \\ A(\Delta) &:= A + B\,(\mathbb{I} - \Delta D)^{-1}\,\Delta C, \end{aligned} \tag{4.9}$$

where the state matrix $A(\Delta) \in \mathbb{R}^{n\times n}$ depends on the uncertainty matrix, which is bounded as

$$\sigma_{\max}(\Delta) \leq \gamma^{-1}$$

with $\Delta \in \mathbb{C}^{m\times m}$, and let $G(s) := D + C\,(s\,\mathbb{I} - A)^{-1}\,B$ be the closed-loop of the system without uncertainties. The nominal value of this system corresponds to the case when the uncertainty matrix, $\Delta = 0$. The parameter γ defines the level of uncertainty measured through the $\mathcal{H}_\infty$ norm by

$$\|G(s)\|_\infty < \gamma$$

Consider the next LMI given by

$$\mathcal{D} = \{z \in \mathbb{C} : f_{\mathcal{D}}(z) = L + z\,M + \bar{z}\,M^T < 0\} \tag{4.10}$$

which defines the generic LMI region in the complex plane. To say that the matrix $A(\Delta)$ is $\mathcal{D}$-stable it is required that the closed-loop poles remain in $\mathcal{D}$ for all Δ. Therefore, given some uncertainty level γ, we need to manage to place all the eigenvalues of $A(\Delta)$ in $\mathcal{D}$.

The robust $\mathcal{H}_\infty$ controller is represented by the block diagram in Figure (4.1). This is the linear fractional transformed model. The $\mathcal{H}_\infty$ norm of the synthesis model interconnected with the computed controller has to be less than one, but to

deal with the neglected vibration modes, or unstructured uncertainties, we choose the weight filter W_3 such that [176]:

$$\|W_3(s)\,\Delta(s)\|_\infty \leq 1.$$

To isolate low-frequency modes in the case of the flexible beam from the high-frequency modes belonging to unstructured uncertainties, we choose the weighting filter W_1 as a low-pass filter to only allow frequencies below a certain cutoff frequency to pass through. In the other hand, the weighting filter W_2 is a low-pass filter used to penalize high-frequencies of resonant peaks in the accelerometric frequency response $z_a(s)$. Besides W_3 is selected as a high-pass filter to capture the behaviour of the system at high-frequencies to provide robustness to the $\mathcal{H}_\infty$ controller.

4.4 Optimal control for the flexible beam

The application we are considering in this section is focused in the active vibration control of a flexible beam equipped with piezoactuated patches. Here we lay out the way we implement a linear $\mathcal{H}_\infty$ control synthesis for computing a linear controller that allows us to afford a good performance in closed-loop.

The Figure 4.3 exhibits the closed-loop frequency response of the acceleration at the end of the beam, overlapping with the uncontrolled response. In the Subfigure 4.3a is shown the synthesis model of the flexible beam system, which describes the first three vibration modes, which are the modes 1, 3 and 4. To its right, we find the analysis model, which displays the first six controllable and observable modes that we found in the beam's model frequency response is shown in the Figure 4.3b. One can note the reduction of at least 20dB on each targeted peak of resonance. This corroborates the previous analysis of the $\mathcal{H}_\infty$ costs.

A way of dealing with the design problems can be the construction of a Nichols chart, which involves the construction of a plane plotting the logaritmic magnitude versus the phase of the closed-loop system with the low-order optimal $\mathcal{H}_\infty$ controller, which is of order 8. The Nichols chart of the closed-loop system's analysis and synthesis model with the

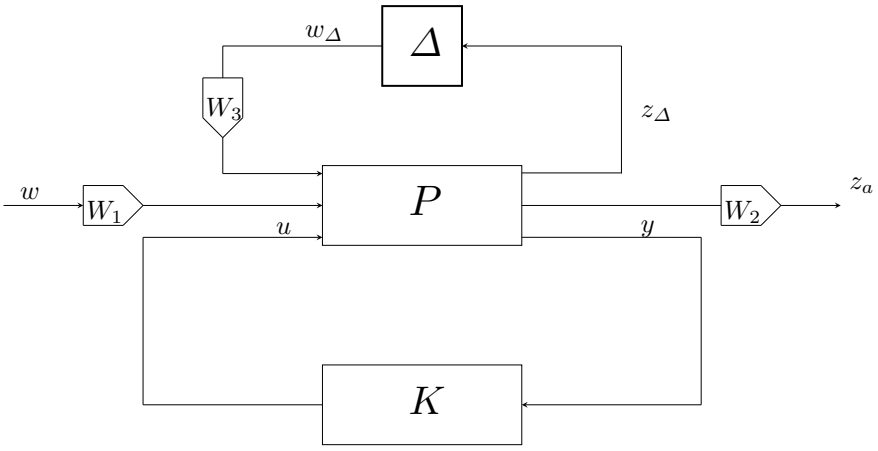

Figure 4.1. Synthesis structure.

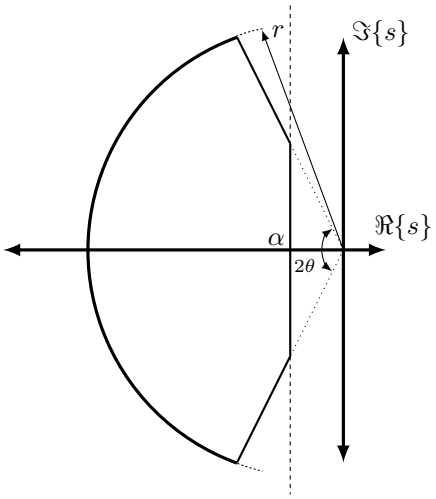

Figure 4.2. Convex cluster sector described by LMI regions, located in the open left-half of the complex plane.

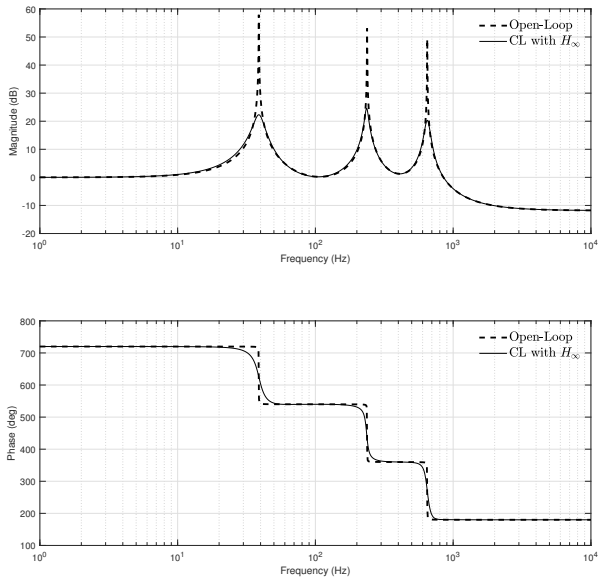

(a) Bode plot responses in closed-loop of the flexible beam's synthesis model.

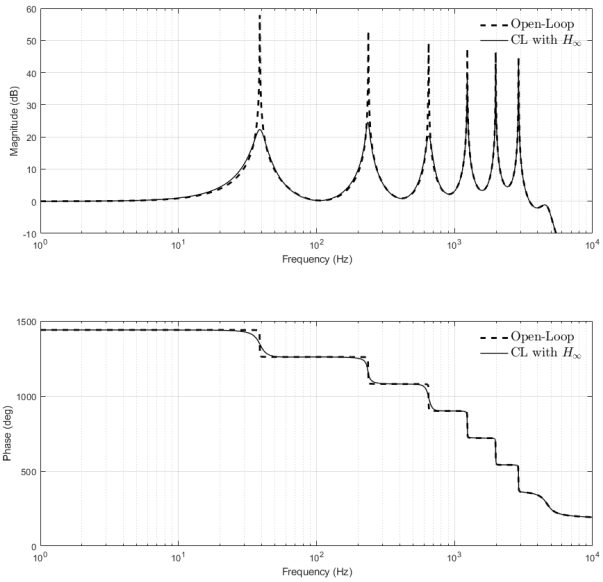

(b) Bode plot responses in closed-loop of the flexible beam's analysis model.

Figure 4.3. Bode plot responses of the synthesis and analysis model's of the flexible beam system in closed-loop with the low-order optimal LMI-based $\mathcal{H}_\infty$ controller. We can see that beyond the third vibration mode, the damping effect is similar to the FRF of the undamped system. In dashed line we have the uncontrolled response. In solid line we find the closed-loop response with the $\mathcal{H}_\infty$ controller.

low-order controller of order 8 can be beheld in the Figure 4.6, where solid lines represent the analysis model, and the dashed lines represent the synthesis model. It gives the gain characteristics and the phase characteristics of the closed-loop transfer function at the same time [135]. The $\mathcal{H}_\infty$ controller computed is effective in damping the first three vibration modes. Moreover, the order size of this controller is reduced through implicit balancing techniques. These techniques are methods for reducing the order of a LTI system while preserving its dynamical properties, producing a lower-order system

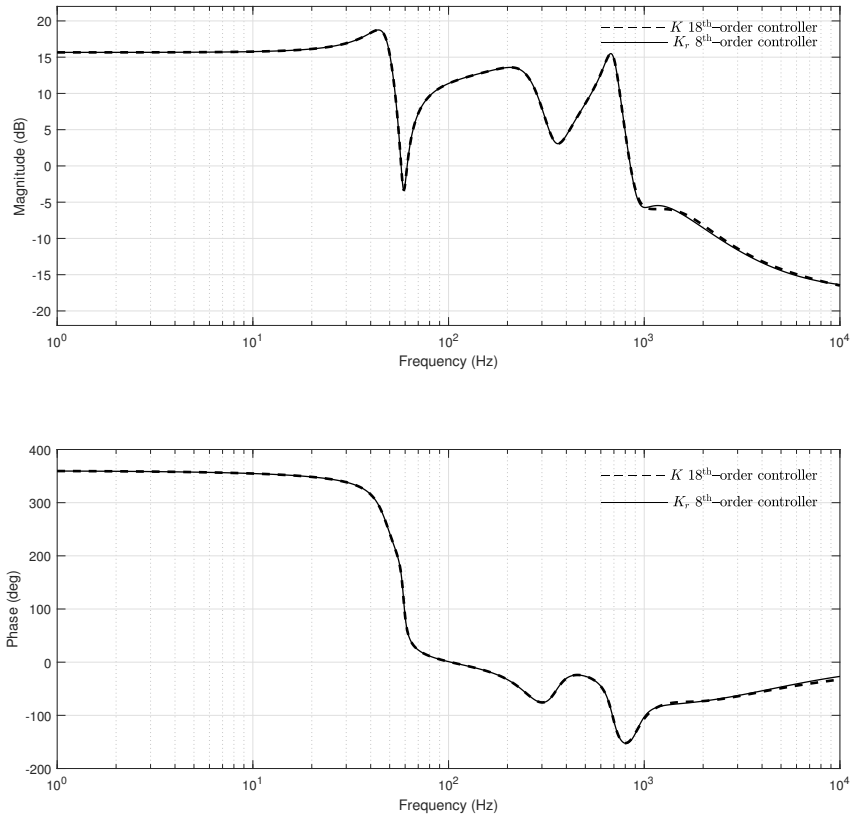

Figure 4.4. Bode plot responses in magnitude (up) and phase(down) for the flexible beam's optimal LMI-based $\mathcal{H}_\infty$ controller. In dashed line we have the full-order synthesized controller of 18 states. In solid line we find the low-order controller of 8 states.

that approximates the behaviour of the original system as closely as possible. The Bode diagrams of the closed-loop system with the computed low-order controller from Equation (4.11), are given in the Figure 4.3a, where above we find the gain margin (above) and the phase margin (below), with the original high-order controller K first computed of 18$^{\text{th}}$ order in dashed black-line, and the consequent reduced low-order controller K_r of 8$^{\text{th}}$ order, shown in solid black-line.

The method treated here has been tailored for linear systems particularly. Robust regional pole placement has been succesfully applied in [177] to a plate like flexible structure. The theoretical background for this problem can be found in [40]. In what follows we specify its application for this smart structure.

Three filters are used for weighting the signals with a good trade-off. The first filter $W_1(s)$ is chosen as an order 1 low-pass filter, with a cut-off frequency $f_{c1} = 950\,\text{Hz}$ at the disturbance input-signal to characterize the power spectral density of this irregular signal. The filter $W_2(s)$ is a penalizing filter, which is designed with $f_{c2} = 950\,\text{Hz}$ and placed at the controlled output-signal $z_a(t)$. Filter $W_3(s)$ is designed as an order 10 Butterworth high-pass filter, with a cut-off frequency $f_{c3} = 5,654\,\text{Hz}$.

The prescribed LMI-region was chosen as the intersection of three LMI regions, as seen in the Figure 4.2. These

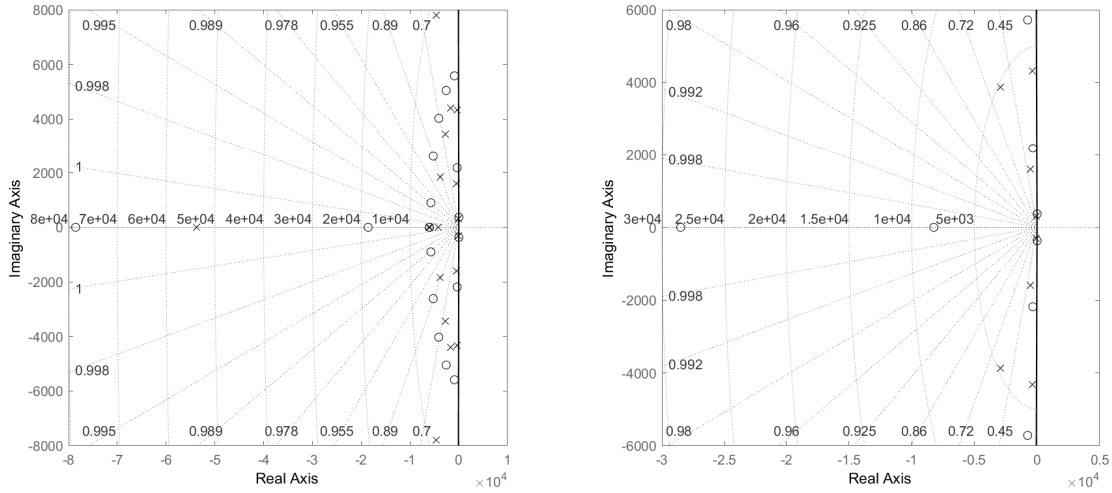

Figure 4.5. Poles and zeros of the flexible beam's optimal $\mathcal{H}_\infty$ LMI-based controller. (Left) The full-order controller of 18 states. (Right) Low-order controller of 8 states.

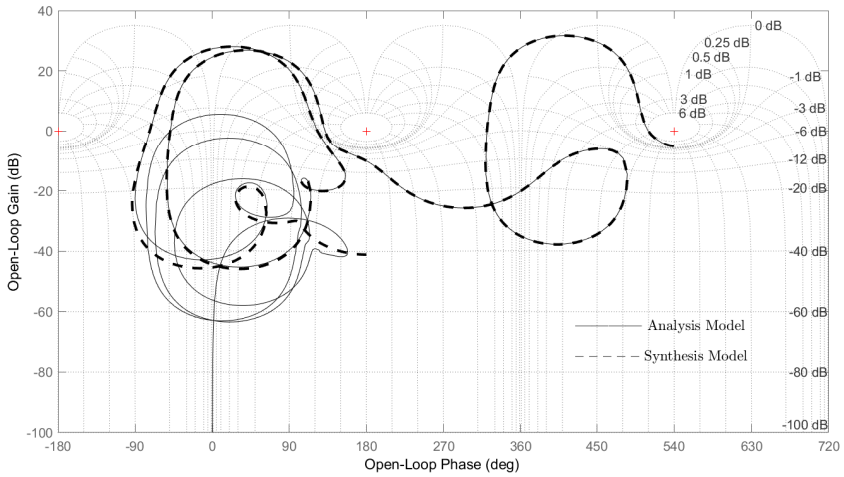

Figure 4.6. Nichols chart of the flexible beam's analysis and synthesis models.

constraints are defined by the shifted open left-half plane, a disk centered at the origin and a conic sector with apex at the origin defined by the numerical values of $\alpha = -15$, radius $r = 1e5$ and $\theta = 89.4°$. This LMI region is chosen to achieve a good trade-off between robustness, speed of response, control performance, and a bigger damping ratio for the high-frequency modes of the system.

Besides, the magnitude Bode diagram of the 18 states full-order controller and the 8 states low-order controller is shown in Figure 4.4. The transfer function of the low-order controller is written in equation (4.11), where the coefficients' values of the numerator and the denominator of this linear transfer function can be found in table 4.1. The low-order dynamic controller in state-space representation is obtained in a canonical state-space realization, with a modal decomposition where the state matrix A is block-diagonal, with each block corresponding to a cluster of nearby modes, using the MATLAB

`canon` command [89]. It's corresponding continuous transfer function in frequency domain is given by equation (4.11) with its coefficients given in the Table 4.1.

$$K_{\mathcal{H}_\infty}(s) = \frac{N_b(s)}{D_b(s)} \tag{4.11}$$

4.5 Optimal control for the axisymmetric membrane

In this section, we carry on with the conundrum of active vibration control using an optimal $\mathcal{H}_\infty$ controller for a different flexible structure. The flexible structure taken into consideration is a thin circular membrane equipped with piezoelectric patches, fixed on each side, and centered according to their axis of symmetry. The final goal of this controller keeps being the vibration damping of several of its vibration modes. We analyse these specific modes through a model reduction technique which looks upon neglecting the non observable modes, and the modes out of the bandwidth of interest. We evaluate the model's performance throughout several numerical simulations which will be useful for assessing the results obtained from our main cotribution, given in the next chapters.

As has been said above, this membrane is a thin fabric composite structure which is used in different applications, such as to predict the elastic performance of woven fabric composites [92, 130], or homogenisation techniques for membrane structures based on repeating unit cell geometry [44].

The biggest challenge for the current technique is to compute a controller which is able to damp the specified vibrating modes in a low frequency bandwidth. Robustness against vibrating modes outside the range of frequency is desired, in order to avoid the "spillover" phenomenon [22]. The behavior of these flexible structures when they are studied and linearized in a specific range of frequency, can be controlled thanks to linear control techniques [80].

The computed continuous-time axisymmetric membrane's optimal $\mathcal{H}_\infty$ controller in frequency domain is given by equation (4.12), and its corresponding coefficients are in table 4.2.

$$\mathcal{K}_{\mathcal{H}_\infty}(s) = \frac{N_m(s)}{D_m(s)}. \tag{4.12}$$

The Figure 4.7 illustrates the closed-loop accelerometric frequency response overlapped with the uncontrolled response. In the Subfigure 4.7a we have the synthesis model describing up to the first three vibration modes, composed of the modes 1, 6 and 15. And the analysis model, which includes the first five controllable and observable modes that we found in the membrane model frequency response is shown in the Figure 4.7b. Also, we can see the frequency response of the stable low-order optimal $\mathcal{H}_\infty$ controller function given in the Figure 4.9, which overlaps the frequency response of the former high-order controller, and the latter low-order controller.

In the Figure 4.10 we seeand that the order reduction is adequate with the open-loop gains in decibels and in degrees for the reduced-order model, as well as the full-order model. One can note the reduction of at least 20dB on each targeted

Table 4.1. Coefficients of the continuous controller's transfer function of the flexible beam given by (4.11).

$N_b(s) = \sum_{k=0}^{8} n_i\, s^i,$	$D_b(s) = \sum_{k=0}^{8} n_i\, s^i,$
$n_0 = 7.168\times10^{26}$	$d_0 = 1.182\times10^{26}$
$n_1 = 1.207\times10^{23}$	$d_1 = 1.854\times10^{23}$
$n_2 = 5.396\times10^{21}$	$d_2 = 1.399\times10^{21}$
$n_3 = 1.786\times10^{18}$	$d_3 = 8.962\times10^{17}$
$n_4 = 1.437\times10^{15}$	$d_4 = 7.323\times10^{14}$
$n_5 = 2.718\times10^{11}$	$d_5 = 2.012\times10^{11}$
$n_6 = 4.855\times10^{7}$	$d_6 = 5.737\times10^{7}$
$n_7 = 5346$	$d_7 = 7747$
$n_8 = 0.1374$	$d_8 = 1$

Table 4.2. Coefficients of the controller's transfer function of the axisymmetric membrane given by (4.12).

$N_m(s) = \sum_{k=0}^{8} n_i\, s^i,$	$D_m(s) = \sum_{k=0}^{8} n_i\, s^i,$
$n_0 = 2.112\times10^{33}$	$d_0 = 7.443\times10^{32}$
$n_1 = 1.521\times10^{30}$	$d_1 = 3.508\times10^{29}$
$n_2 = 6.984\times10^{26}$	$d_2 = 1.154\times10^{27}$
$n_3 = 2.421\times10^{23}$	$d_3 = 1.908\times10^{23}$
$n_4 = 3.118\times10^{19}$	$d_4 = 1.408\times10^{20}$
$n_5 = 6.045\times10^{15}$	$d_5 = 1.62\times10^{16}$
$n_6 = 2.643\times10^{11}$	$d_6 = 3.235\times10^{12}$
$n_7 = 2.106\times10^{7}$	$d_7 = 2.8\times10^{8}$
$n_8 = 421.6$	$d_8 = 1.807\times10^{4}$
$n_9 = 0.00652$	$d_9 = 1$

peak of resonance. This corroborates the previous analysis of the $\mathcal{H}_\infty$ costs.

4.6 Concluding remarks

The problem of the active damping control technique of an infinite-dimensional systems with a robust linear controller, with a proper model order reduction has been tackled using a finite dimensional technique. We have emphasized the fact that, computing a controller with a order reduced model of the plant accentuates the interest in avoiding the spillover phenomenon, which occurs when high-frequency disturbances are present in the system, and they can "spill over" into the reduced-order model and cause significant errors in the system's response. We have considered two flexible systems, such as the flexible beam and the flexible axisymmetric membrane. We have shown how, despite using different flexible

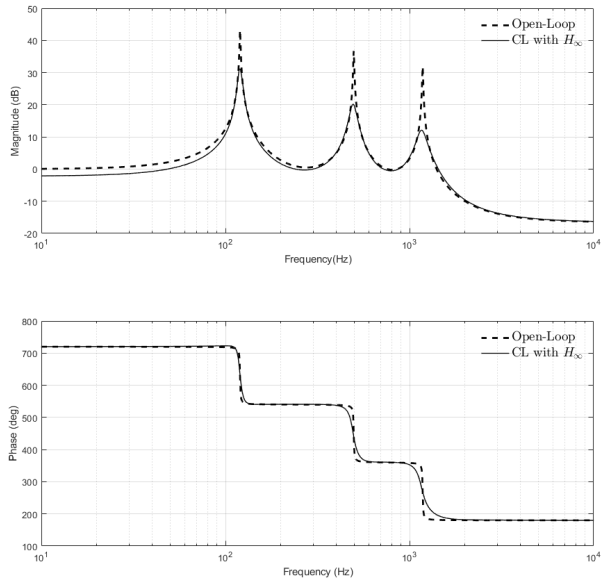

(a) Bode plot responses in magnitude (up) and phase(down) in closed-loop for the flexible axisymmetric membrane's synthesis model.

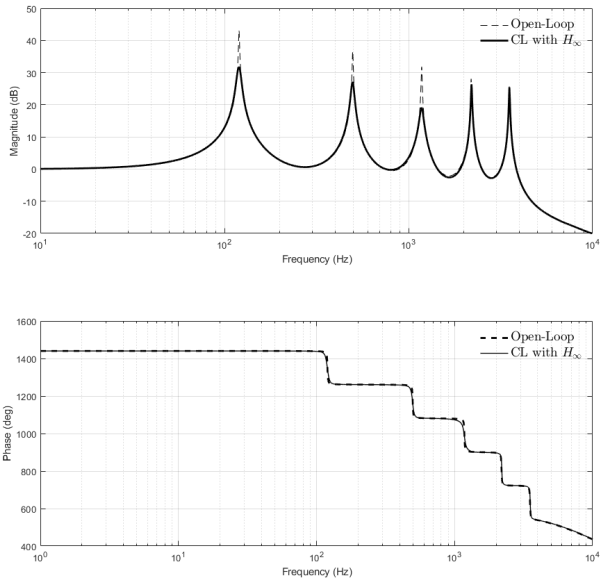

(b) Bode plot responses in magnitude (up) and phase(down) in closed-loop of the flexible axisymmetric membrane's analysis model.

Figure 4.7. Bode plot response of the axisymmetric membrane's analysis and synthesis models with the optimal LMI-based $\mathcal{H}_\infty$ controller. In dashed line we have the open-loop response. In solid line we find the closed-loop response with the $\mathcal{H}_\infty$ controller.

structures we can accurately be controlled through the $\mathcal{H}_\infty$ controller, accomplishing robustness and control performance in the presence of uncertainties, including modeling errors and disturbances. The importance of achieving a low-order controller is emphasized. Overall, we have designed an efficient control method through the FEM technique, weighting filters and the optimal $\mathcal{H}_\infty$ technique based on LMIs. Then, some details concerning the discretization of the controller for its consequent study in a sampled-data system is shown.

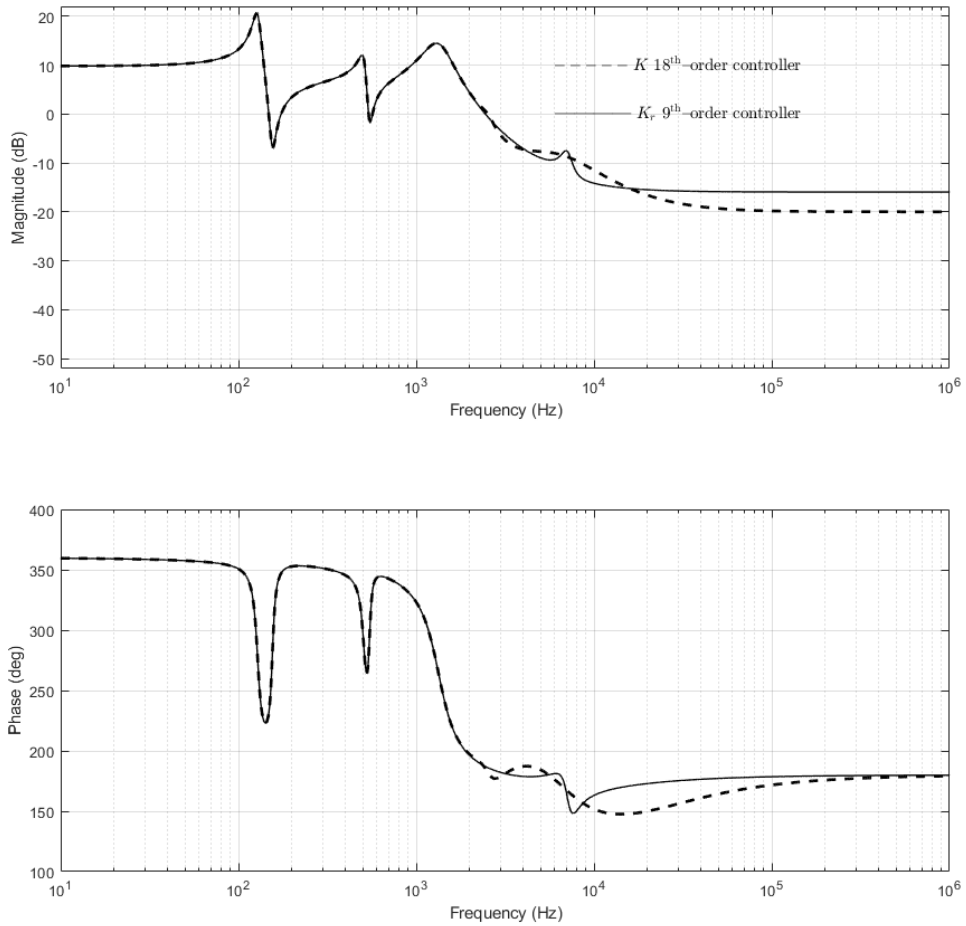

Figure 4.8. Bode plot responses in magnitude (up) and phase(down) for the axisymmetric membrane's optimal LMI-based $\mathcal{H}_\infty$ controller. In dashed line we have the full-order synthesized controller of 18 states. In solid line we find the low-order controller of 8 states.

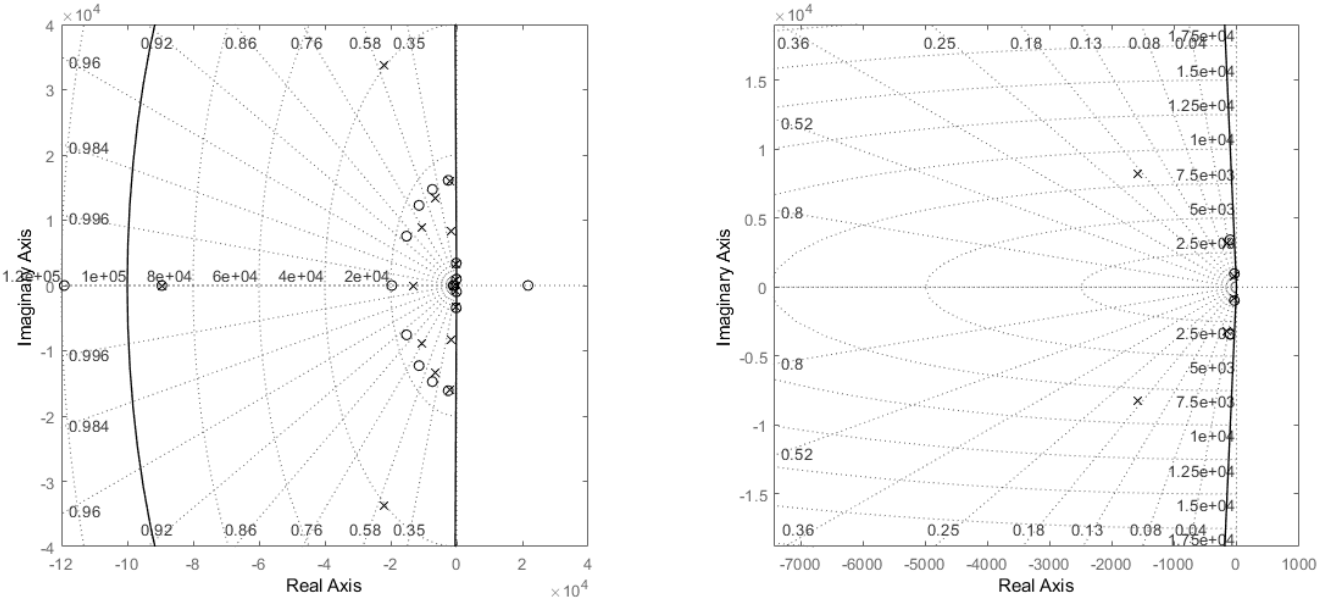

Figure 4.9. Poles and zeros of the flexible axisymmetric membrane's optimal $\mathcal{H}_\infty$ LMI-based controller. (Left) The full-order controller of 18 states. (Right) Low-order controller of 9 states.

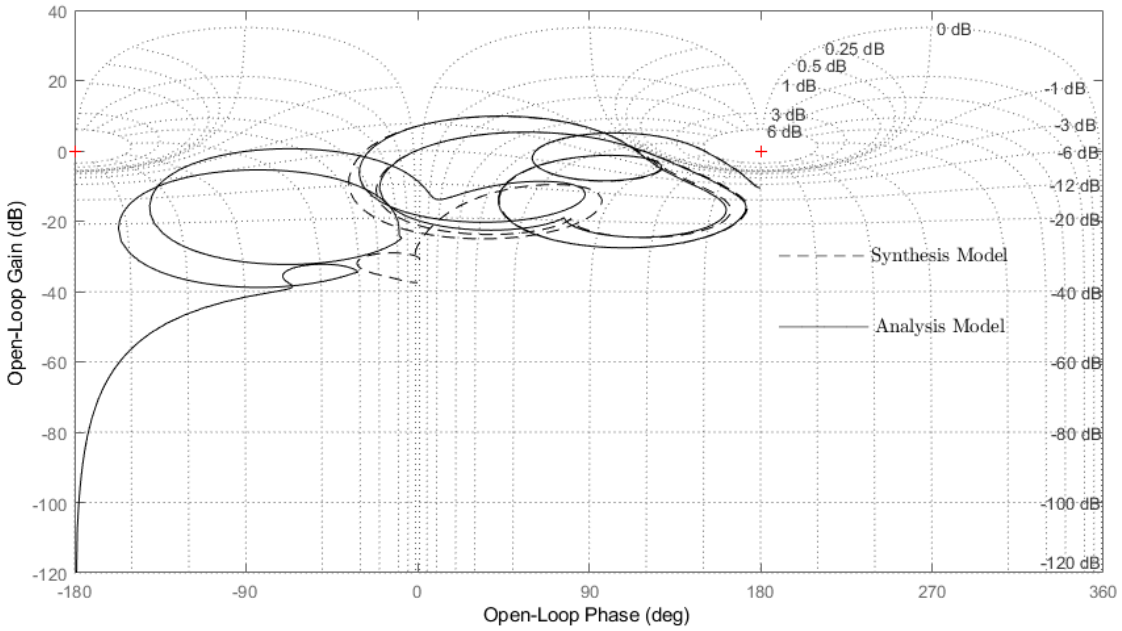

Figure 4.10. Nichols chart of the flexible axisymmetric membrane's analysis and synthesis models.

Chapter 5

Quasi-polynomial Based Control Design

This chapter focus its attention into a class of time-delay systems, whose application lies in the partial pole-placement (PPP) of some poles of the spectrum into the negative real axis of the complex plane.

The chapter is structured as follows. First some general remarks about time-delay systems for a continuous domain are considered for an overview of time-delay systems in Section 5.1. Then, the objective of a Quasi-Polynomial Based (QPB) controller is considered in Section 5.2. Then some characteristics about the controller design based on delayed-differential characteristic functions, or QPB controller design, is discussed in Section 5.3. The Section 5.4 includes the results obtained through several simulations for the previously modelled flexible structures, i.e. the flexible equipped beam and the flexible axisymmetric membrane. And finally, Section 5.5 summarizes the chapter with some brief remarks.

Contents

5.1 Introduction

The time between when a control signal is sent, when it is received and acted upon it is what we consider a time-delay in control theory. The control applications which send and receive signals constantly, and as they do, they are vulnerable to many factors and affect areas such as mobile devices networks [124], lagrangian systems [132], robot manipulators [61] and active damping of flexible structures [31].

The main objective in this chapter is to investigate an approach based on the stabilization properties that time-delay systems can bear when correctly used for an output-feedback controller. This output-feedback is applied in such a way that we solve with its parameters' values the problem of correctly assigning partial poles of the spectrum distribution into the negative real-axis of the complex plane. This is a property related with time-delay systems which is reviewed in this chapter. It has been treated in recent studies, and it is called QPB control [179, 6]. Besides, novel properties related to time-delay systems have been studied before, see for instance [32], where an interesting property sought through the feedback control of these system is called Multiplicity Induced Dominancy (MID).

The type of linear time-delay systems considered for the Quasi-Polynomial Based (QPB) control is infinite dimensional with constant delays, given as

$$\dot{x}(t) = \sum_{k=0}^{N} A_k \, x(t - \tau_k) \tag{5.1}$$

where the state-vector $x = \begin{bmatrix} x_1 & x_2 & \cdots & x_n \end{bmatrix}^T \in \mathbb{R}^n$, and the according initial conditions belong to the Banach space of continuous functions $\mathcal{C}([-\tau_N, 0], \mathbb{R}^n)$. The time-delays, given by $\tau_N > \tau_{N-1} > \cdots > \tau_1 > \tau_0 = 0$ are strictly increasing positive constant delays, and the matrices $A_k \in \mathcal{M}_n(\mathbb{R}$, where $\mathcal{M}_n(\mathbb{R})$ denotes the $n \times n$-dimensional matrices with real numbers denoted by the set $\mathbb{R}$. The stability of the solutions of the system (5.1) can be defined by the location of the zeros of the characteristic quasipolynomial, which is given by

$$\Delta(s, \tau) = \det(s\mathbb{I} - A_0 - \sum_{k=1}^{N} A_k \, e^{-\tau_k s}). \tag{5.2}$$

We emphasize the fact that the characteristic quasipolynomial of the characteristic equation, which is given in the way of (5.2), involves an infinite number of roots, while for pure linear and time-invariant differential equations there are only a finite number of roots [18, p. 55]. We recall that systems described by retarded differential equations is found in most of the applications, because they are found in systems with a feedback subjected to a time-delay [18].

We show that an upper-bound for multiple coexisting negative real roots of time-delay systems is given. It is also shown that the codimension of roots in the origin of the complex plane can be characterized with an appropriate functional Birkhoff matrix [25], instead of using the argument principle, as done in [140].

The dominant properties of multiple roots is the fact that makes the time-delay controllers of utility for a control synthesis technique. Through the use of scalar delay equations, the dominant property of a multiple root is shown in [28].

Next, such a property was considered for second-order systems controlled by a delayed proportional controller as proposed in [31, 29] where its applicability in active vibration damping for a piezo-actuated beam is shown. An extension to the delayed proportional-derivative controller case is studied in [26, 30] where the dominancy property is parametrically characterized and proven using the argument principle. Besides, the reader can see [30, 26], where an analytical proof for the dominancy of the spectral value with maximal multiplicity for second- order systems controlled via a delayed proportional-derivative controller is discussed. Recently, in [3] it was shown that under appropriate conditions, the coexistence of distinct negative zeros of the quasipolynomial of reduced degree, bounded by the admissible multiplicity given by the Polya-Szegö bound [140, p. 144] of exactly B_{PS} spectral values, guarantees the asymptotic stability of the trivial solution of the corresponding time-delay system through assigning B_{PS} real spectral values which make them the rightmost roots of the corresponding quasipolynomial. The dominancy of such real spectral values is shown using an extended factorization technique which generalizes the one proposed in [3]. More precisely, an analytical characterization of the spectral abscissa for the low-order retarded time-delay system with real spectral values which are not necessarily multiple is explored, see also [17]. The effect of the coexistence of such non oscillatory modes on the asymptotic stability of the trivial solution is then exploited. In particular, the method Coexistence of Real Roots Induce Dominancy (CRRID) of B_{PS}-order real spectral values makes them rightmost-roots of the corresponding quasipolynomial. These results give rise to a new control approach for the design of output feedback controllers based on delayed actions, that is based in a PPP method, which pointwise assign locations in the negative real axis of the complex plane to specific dominant poles in the spectrum distribution. These methods are based on the adequate manipulation of the quasipolynomial obtained from the system in closed-loop, and therefore we call this method CRRID or MID, combined with QPB controller.

Furthermore, if the number of coexistent real spectral values reaches the B_{PS}, then a necessary and sufficient condition for the asymptotic stability is provided (which is equivalent to the exponential stability [98, p. 79]), see also [127] for an estimate of the exponential decay rate for stable linear delay systems. Notice also that the proposed constructive approach, which consists in providing an appropriate factorization of a given quasipolynomial function and then to focus on the location of zeros of one of its factors, gives further insights on such a qualitative property. Namely, it furnishes the exact exponential decay rate rather than just counting the number of the quasipolynomial roots on the left-half plane as may be done by using the principle argument, see for instance [164].

Moreover, it was stressed in [133] that, in some cases, time-delay has a *stabilizing effect* in the control design. Indeed, the closed-loop stability is guaranteed precisely by the existence of the delay. A control law of the form $\sum_{k=1}^{m} \gamma_k \, y(t-\tau_k)$ results interesting from the practical point of view, avoiding complicated control laws and giving a straightforward way to apply the control law.

Thus, the problems considered through these time-delay systems lead to methods that provide an asymptotic stability characterized by the coefficients which multiply the output of the systems, plus a scale and delayed value of the same output and the control input. We need to recall that assigning pointwise values of the roots to specific points in the complex plane has been treated before [19, 36]. For instance, in [19] a method for poles assignment through the closed-

loop system with terms affected by a bounded time-delay is proposed. In [114] is shown how systems that are affected by time-delays in the states outputs and the control input, and with the purpose of designing a stabilizing output-feedback, can be converted into systems with time-delays in the states only. It is valuable to consider that the feedback law includes past values of itself.

In [112], a similar finite pole placement for time-delay systems with commensurate delays is proposed. Other analytical/numerical placement methods for retarded time-delay systems are proposed in [121, 126], see also [207] for further insights on pole-placement methods for retarded time-delays systems with proportional-integral-derivative controller-design.

In this thesis, we further aim at experimenting the methodology described in [3] in order to perform the damping of the main vibration modes for flexible structures, modelled by the Finite Element method. These flexible structures are the flexible beam, whose state of the art related to its distributed sensing and control through piezoelectric materials was reviewed in [144], and for the flexible membrane in [41], where several approaches using membranes are considered.

5.2 Objective

The main goal of the sought controller is to reduce the peaks of resonance for the first three controllable and observable modes, by using an *output feedback controller*, without making unstable the vibration modes that are not in the synthesis model. By using the same kind of output feedback controller as in [179], the considered system is inserted in the output feedback control structure of the Figure 5.1, where the reference signal is always equal to zero. A rectangular impulse signal is used for the disturbance input $w(t)$. The control problem consists in reducing the vibrations generated by the first three modes when the mobile support imposes a shock to the whole flexible membrane.

The transfer function model of the exogenous perturbation $w(t)$ to the controlled output $z_a(t)$ is composed by a linear and time-invariant system. Its transfer functions are given by equation (5.3). This equation contains the piezoelectric sensor's voltage output $y(t)$ and possesses a single input, given by the control signal $u(t)$, that corresponds to the voltage accross the piezoelectric actuator which behaves as a strain actuator and s represents the Laplace variable.

$$\begin{cases} z_a(s) &= \dfrac{Q_{zw}(s)}{\varphi(s)}\, w(s) + \dfrac{Q_{zu}(s)}{\varphi(s)}\, u(s), \\ y(s) &= \dfrac{Q_{yw}(s)}{\varphi(s)}\, w(s) + \dfrac{Q_{yu}(s)}{\varphi(s)}\, u(s). \end{cases} \tag{5.3}$$

There is a bound B_{PS} on the number of real roots that can be placed in the negative real-axis of the complex-plane. It is possible to obtain this bound thanks to the next theorem:

Theorem 10. *([140, p. 144]) Let $\tau_1, \tau_2, \ldots, \tau_N$ denote real numbers such that*

$$\tau_1 < \tau_2 < \cdots < \tau_N$$

and let $m_1, m_2, \ldots, m_\ell$ *be positive integers such that*

$$m_1 \geq 1, \ldots, m_\ell \geq 1, \quad m_1 + m_2 + \cdots + m_N = D.$$

Let $f_{i,j}(s) = s^{i-1}\, e^{\tau_j s}$, *for* $1 \leq i \leq d_j$ *and* $1 \leq j \leq N$. *Let* B_{PS} *be the number of zeros of the function*

$$f(s) = \sum_{\substack{1 \leq j \leq N \\ 1 \leq i \leq d_j}} c_{i,j}\, f_{i,j}(s) \tag{5.4}$$

that are contained in the horizontal strip

$$\alpha \leq \Im(s) \leq \beta$$

Assuming that

$$\sum_{1 \leq k \leq d_1} |c_{k,1}| > 0 \quad \textit{and} \quad \sum_{1 \leq k \leq d_n} |c_{k,N}| > 0$$

then

$$\frac{(\tau_N - \tau_1)\,(\beta - \alpha)}{2\,\pi} - D + 1 \leq B_{PS} \leq \frac{(\tau_N - \tau_1)\,(\beta - \alpha)}{2\,\pi} + D + N - 1. \tag{5.5}$$

Setting $\alpha = \beta = 0$, *the above theorem yields* $B_{PS} \leq D + N - 1$ *where* D *stands for the sum of the degrees of the polynomials involved in the quasipolynomial function* $f(s)$ *and* N *denotes the associated number of polynomials.*

This theorem enables us to set an upper-bound in the number of a quasipolynomial's real roots. We proceed with the case of the negative non-oscilating poles' presence for a second-order system's quasipolynomial Δ of the form

$$\Delta(s, \tau) = s^2 + a\, s + b + \alpha\, e^{-\tau s} = 0. \tag{5.6}$$

Theorem 11 ([3, Thm 4]). *The second-order system's quasipolynomial (5.6) has three distinct negative real roots, such that* $s_3 < s_2 < s_1$ *if, and only if, the parameters* a, b, *and* α, *are given by*

$$\begin{aligned}
a(s_1, s_2, s_3, \tau) &= \tfrac{1}{\Phi} \textstyle\sum_{\substack{i,j,k \in \Lambda \\ i<j, i \neq j \neq k}} (-1)^{i+j} (s_i^2 - s_j^2)\, e^{-s_k \tau}, \\
b(s_1, s_2, s_3, \tau) &= -\tfrac{1}{\Phi} \textstyle\sum_{\substack{i,j,k \in \Lambda \\ i<j, i \neq j \neq k}} (-1)^{i+j} s_i\, s_j\, (s_i - s_j)\, e^{-s_k \tau}, \\
\alpha(s_1, s_2, s_3, \tau) &= -\tfrac{1}{\Phi} \textstyle\prod_{\substack{i,j \in \Lambda \\ i<j}} (s_i - s_j)
\end{aligned}$$

where $\Lambda := \{1, 2, 3\}$, *and where*

$$\Phi := \Phi(s_1, s_2, s_3, \tau) = \sum_{\substack{i,j,k \in \Lambda \\ i<j, j \neq i,j}} (-1)^{i+j} (s_i - s_j)\, e^{-s_k \tau}$$

In this case, α *is necessarily negative.*

- *The spectral value* s_1 *is negative if, and only if, there exists a time-delay* $\tau_0 > 0$ *such that*

$$a(s_1, s_2, s_3, \tau_0) + s_2 = 0.$$

  This ensures the asymptotic stability of the system.

- *The root* s_1 *is the spectral abcissa of (5.6).*

Remark 5.1. Thanks to the latter theorem a number of roots in any finite vertical region can be upper-bounded. Moreover, for higher order time-delay systems, it is possible to get conditions on a number N of negative real roots, and we can get an upper-bound by applying the Polya-Szegö Theorem 10 as $N \leq B_{PS}$. The dominancy of the assigned spectral values can be proved using either the principle argument or the quasipolynomial factorization proposed in [28, 3].

5.3 Methodology

In this section, we summarize the procedure for calculating the parameters' values of a quasipolynomial-based controller (for more details on the theory of stabilization of time-delay systems see [119]).

Given the equation (5.1), with a complete set of eigenvalues of A_k, with $k = 0, \ldots, N$, it is possible to construct a subspace of solutions of (5.1) that corresponds to those eigenvalues.

We organize this section in two parts. Firstly, we focus in the parameters to find, which generally involves the computation with the aid of a symbolic algebra package as Mathematica [194], and it is numerically accomplished with its spectral values computation with the help of MATLAB [50]. These are the settings for the calculations to perform. Secondly, we will see how the computations are implemented in the software package Mathematica.

5.3.1 QPB control design method

To solve the control problem posed by a dynamical system, we prefer to consider a controller with a low complexity in its design. The controllers treated here are denominated as quasipolynomial-based (QPB) controllers [179]. The idea of these methods lies in the assignation of poles to a specific point (or points) of the left-half of the complex-plane, which in the active vibration control corresponds to non-oscillating modes.

Recently, two different methods to control dynamical systems involving the analysis of a characteristic equation described by a quasipolynomial have been proposed. These are the multiplicity induced dominancy (MID) and the coexisting real roots inducing dominancy (CRRID). Their properties and their use for feedback stabilization using time-delays has allowed the use of a time-delay as a design parameter. Consider the next definition and proposition.

Definition 5.1. *Let q_0, q_{r_0}, p_0, p_{r_0} be scalar coefficients such that $\tau \in \mathbb{R}_+$, $p_0 \neq 0$, and at least one of the two other numbers q_0 and q_{r_0} is nonzero. Then a generic output feedback QPB controller is defined in the frequency domain by:*

$$\mathcal{K}(s,\tau) := \frac{q_0 + q_{r_0}\, e^{-\tau s}}{p_0 + p_{r_0}\, e^{-\tau s}}, \tag{5.7}$$

thus, it yields to the following continuous-time delay-difference equation:

$$u(t) = -\frac{p_{r_0}}{p_0}\, u(t-\tau) + \frac{q_0}{p_0}\, y(t) + \frac{q_{r_0}}{p_0}\, y(t-\tau). \tag{5.8}$$

Proposition 5.1. *There exists a set of parameters q_0, q_{r_0}, p_0, p_{r_0} and $\tau > 0$ such that the controller (5.10) allows to assign three negative coexisting poles (spectral values) s_1, s_2 and s_3 for the system* (5.12) *in closed-loop with the control law (5.9).*

Proof. The first pronouncement about the existence of four free parameters is related to the quasipolynomial interpolation, i.e., having four free parameters and three constraints, the problem is well-posed since there are more parameters than unknown constraints. Furthermore, the dominancy of the assigned poles is guaranteed through the integral factorization of the quasipolynomial, where the function will have the desired behavior, as previously used in the works of [3, 17] or [179]. □

The above proposition involves that for this specific quasipolynomial with a single time-delay, we can find constant values that assign three negative dominant poles, such that the corresponding synthesis model's resonance peaks are well damped.

Considering a generic quasipolynomial $\Delta(s)$ with $m \leq n$, we force a given negative value $s_0 \in \mathbb{C}_-$ to be a multiple spectral root of the system's closed-loop characteristic function. These controller's parameters can be obtained due to the parametric conditions that show the dominant property of the multiple spectral root [32].

1. Obtain the transfer function from the state-space model computed through the finite element method, which describes the number of vibration modes that we are interested in using for the synthesis model. For this we use the command `ss2tf` in MATLAB [117, pp. 12526-12536], which converts a state-space representation of a system into an equivalent transfer function. We recall that the modal reduced state-space matrices that compose the dynamics of certain

vibration modes of a mechanical system in state-space can be described as

$$A = \begin{bmatrix} \mathbf{0}_{n_c} & \mathbb{1}_{n_c} \\ -\Omega^2 & -2\,Z\,\Omega \end{bmatrix},$$

$$B_w = \begin{bmatrix} \mathbf{0} \\ b_w \end{bmatrix}, \qquad B_u = \begin{bmatrix} \mathbf{0} \\ b_u \end{bmatrix},$$

$$C_y = \begin{bmatrix} c_y & \mathbf{0} \end{bmatrix}, \qquad C_z = \begin{bmatrix} c_z & \mathbf{0} \end{bmatrix}.$$

where $\Omega = \mathrm{diag}(\omega_1^2, \ldots, \omega_{n_c}^2)$, $Z = \mathrm{diag}(2\xi_1\omega_1, \ldots, 2\xi_{n_c}\omega_{n_c})$, n_c is the number of vibration modes, ω_i is the natural frequency of the i^{th} mode, and ξ_i is the damping coefficient of the same i^{th} mode.

2. Get the closed-loop transfer function

Let us define the output feedback control law in the frequency domain by

$$u(s) = \mathcal{K}(s,\tau)\, y(s), \tag{5.9}$$

where $\mathcal{K}(s,\tau)$ stands for the QPB controller. For this purpose, let's define the proportional-delayed output-feedback controller as

$$\mathcal{K}(s,\tau) := \frac{\Delta_q(s,\tau)}{\Delta_p(s,\tau)} \quad \text{where} \quad \begin{cases} \Delta_q(s,\tau) & := \quad q_0 + q_{r_0}\, e^{-\tau s}, \\ \Delta_p(s,\tau) & := \quad p_0 + p_{r_0}\, e^{-\tau s}. \end{cases} \tag{5.10}$$

It can be seen that, after using the Laplace anti-transform on (5.10), we write this control law given in the time-domain as

$$u(t) = \frac{q_0}{p_0}\, y(t) + \frac{q_{r_0}}{p_0}\, y(t-\tau) - \frac{p_{r_0}}{p_0}\, u(t-\tau) \tag{5.11}$$

which is an output feedback control law based on proportional actions plus delayed proportional actions.

We can refer to equation (5.11) as an output-feedback proportional-delayed control law that uses proportional and delayed signals from the output as well as delayed values of the control.

The transfer function between the controlled output $z_a(s)$ and disturbance input-signal $w(s)$ in closed-loop is given by

$$z(s) = \frac{Q_{zw}(s)\,\Delta_p(s,\tau) + Q(s)\,\Delta_q(s,\tau)}{\varphi(s)\,\Delta_p(s,\tau) - Q_{yu}(s)\,\Delta_q(s,\tau)}\, w(s) \tag{5.12}$$

where $Q(s)\,\varphi(s) = Q_{zu}(s)\,Q_{yw}(s) - Q_{zw}(s)\,Q_{yu}(s)$. The characteristic quasipolynomial of this structure's transfer

function in closed loop is given by the denominator of equation (5.12), i.e.

$$\Delta(s,\tau) := \varphi(s)\,\Delta_p(s,\tau) - Q_{u\,y}(s)\,\Delta_q(s,\tau). \tag{5.13}$$

For the sake of future reference, we will call the numerator of (5.12) as

$$\Delta_{num}(s,\tau) := Q_{zw}(s)\,\Delta_p(s,\tau) + Q(s)\,\Delta_q(s,\tau). \tag{5.14}$$

3. Express the function (5.12) as a retarded equation with a normalization of the highest degree monomial. The degree of the non-delayed part

$$P_0(s) = \sum_{i=0}^{2n_c} a_i\, s^i,$$

has to be strictly greater than the degree of the delayed part.

$$P_1(s,\tau) = \sum_{j=0}^{2n_c-1} b_j\, s^j\, e^{-\tau s}.$$

In other words, we have

$$\Delta(s,\tau) = \underbrace{\sum_{i=0}^{2n_c} a_i\, s^i}_{P_0(s)} + \underbrace{\sum_{j=0}^{2n_c-1} b_j\, s^j\, e^{-\tau s}}_{P_1(s)} \tag{5.15}$$

4. Then, depending if it is intended to use a MID method or a CRRID method, the system of equations that is used to find the parameters of equation (5.10) varies, as it is explained below.

Multiplicity Induced Dominancy (MID): To work with a control law given by a multiplicity that defines the rightmost root of the system, we take the characteristic quasipolynomial (5.15) and we derivate w.r.t. the Laplace variable s for each one of the multiple poles. We then, solve the resulting system of equations for the chosen multiple value s_c of the form

$$\begin{cases} \sum_{i=0}^{2n_c} a_i\, s_c^i + \left(\sum_{j=0}^{n_c-1} b_j\, s_c^j\right) e^{-s_c\tau} &= 0, \\ \frac{d}{ds}\left[\sum_{i=0}^{2n_c} a_i\, s_c^i + \left(\sum_{j=0}^{n_c-1} b_j\, s_c^j\right) e^{-s_c\tau}\right] &= 0, \\ \frac{d^2}{ds^2}\left[\sum_{i=0}^{2n_c} a_i\, s_c^i + \left(\sum_{j=0}^{n_c-1} b_j\, s_c^j\right) e^{-s_c\tau}\right] &= 0. \end{cases} \tag{5.16}$$

Coexisting Real Roots Induced Dominancy (CRRID): In order to arrive to a control law that places three co-

existing poles in the negative real axis of the complex-plane, we solve the following system of equations:

$$\begin{cases} \sum_{i=0}^{2n_c} a_i\, s_1^i + \left(\sum_{j=0}^{n_c-1} b_j\, s_1^j\right) e^{-s_1\tau} &= 0, \\ \sum_{i=0}^{2n_c} a_i\, s_2^i + \left(\sum_{j=0}^{n_c-1} b_j\, s_2^j\right) e^{-s_2\tau} &= 0, \\ \sum_{i=0}^{2n_c} a_i\, s_3^i + \left(\sum_{j=0}^{n_c-1} b_j\, s_3^j\right) e^{-s_3\tau} &= 0. \end{cases} \tag{5.17}$$

i.e. the characteristic quasipolynomial $\Delta(s_k, \tau) = 0$ with $k = 1, 2, 3$ [179, Thm 1], and in (5.15) we set $a_{2n_c} = 1$ and $b_{2n_c} = 0$, for solving the parameters given in the control law (5.10), where we are using a time-delay as a design parameter.

Stability of the closed-loop transfer function (5.12), with $w(s)$ considered as a rectangular impulse perturbation of the system, is achieved if and only if all roots of the quasipolynomial (5.15) lie in the left-half of the complex plane.

We are interested in the frequency domain analysis of the transfer function's denominator with some roots aligned in the negative real-axis contained in the left-half of the complex plane.

Nonetheless, we need to ensure that the rightmost root be included in the subset of assigned poles. If all the poles of the function (5.13) have negative real parts, the equilibrium point is BIBO-stable.

Remark 5.2. *For solving the five parameters of the controller equation (5.13) we have to impose five constraints, as it was shown above.*

With the help of the software MATLAB [50], and using the command QPmR introduced in [188], a numerical study of the complex plane allows to see the behavior of our rightmost assigned root s_1 as the spectral abscissa of the system (5.12), whose relation to the other chosen roots is described by the inequalities $0 > s_1 > s_2 > s_3$. Therefore, the behavior of s_1 as the spectral abscissa is verified, in order that our choice of poles renders the complete high-order analysis model BIBO-stable.

Thus, a quasi-polynomial based controller can be calculated and tested for a generic flexible structure, whose model was obtained through the Finite Element Method (FEM) techniques.

5.3.2 Solving the controller's parameters

The computational implementation of the analytical results shown above, will be described in this subsection. The obtention of the Delay-Differential Equation (5.15) will be achieved after the next steps. The transfer function realization of a flexible structure, as shown for our study cases in Equation (3.13) and (3.15) for the flexible beam and the flexible axysimmetric membrane, respectively, is introduced in our symbolic software Mathematica with a sintaxis given as follows:

```
> φ[s_] = s^6 + a5 s^5 + a4 s^4 + a3 s^3 + a2 s^2 + a1 s + a0
```

Where the constants a_5, a_4, a_3, a_2, a_1 and a_0 are considered as indicated in the Table 3.2 for the flexible beam, and

by the Table 3.3 for the flexible axisymmetric membrane. Moreover, the polynomials symbolic representation has to be created with a special syntax for subscripted variables with the *Notation Palette* as shown below,

```
> Needs["Notation`"]
> Symbolize[Q_zu]
> Symbolize[Q_yu]
> Symbolize[Q_zw]
> Symbolize[Q_yw]
```

The values for the coefficients of the polynomials defined above are given by the Table 3.2 for the flexible beam, and by the Table 3.3 for the flexible axisymmetric membrane.

```
> Symbolize[p_0]
> Symbolize[q_0]
> Symbolize[p_r0]
> Symbolize[q_r0]
```

Where the variables p_0, q_0, p_{r0} & q_{r0} are the coefficients of the controller's transfer function, defined as

```
> K[s_,τ_] = (q_0 + q_r0 e^(-τs)) / (p_0 + p_r0 e^(-τs))
```

A definition that considerably simplifies terms in the evaluation of the output signal to be controlled is

```
> Q[s_] = (Q_zu[s] Q_yw[s] - Q_zw[s] Q_yu[s]) / φ[s]
```

After that, we define the controller's numerator and denominator with the variables $\Delta_q(s)$ and $\Delta_p(s)$, respectively, as follows:

```
> Symbolize[Δ_q]
> Symbolize[Δ_p]
> Δ_q[s_ ,τ_] := Numerator[K[s_ ,τ]];
> Δ_p[s_ ,τ_] := Denominator[K[s_ ,τ]];
```

The transfer function of the controlled output of interest is defined as

```
> z[s_] := (Q_zw[s] Δ_p[s,τ] + Q[s] Δ_q[s,τ]) / (φ[s] Δ_p[s,τ] - Q_yu[s] Δ_q[s,τ])
```

From this transfer function, we consider its denominator as the characteristic quasipolynomial with the next instruction:

```
> Δ[s_,τ_] := Denominator[z[s]];
```

We use the next instruction to set constraints on the delayed and non-delayed polynomials that compose the quasipolynomial `Δ[s,τ]`, setting the non-delayed polynomial as a monic polynomial, and the delayed polynomial to the degree $2n_c - 1$, as follows

```
> Collect[Δ[s,τ],{Exp[-s τ],s}]
```

Finally we solve numerically for the 5 parameters of our controller with the instruction `NSolve` :

```
> ns1 = NSolve [ {Δ[s_1,τ] == 0, Δ[s_2,τ] == 0, Δ[s_3,τ] == 0, p_r0 - q_uy6 q_r0 == 0, p_0 - q_uy6 q_0 == 1
}, {p_0,q_0,p_r0,q_r0,τ},Reals ]
```

Where s_1, s_2 and s_3 are the assigned eigenvalues in negative real axis of the complex plane. Nonetheless, it is not clear at this point how to select these pointwise real eigenvalues, but it has been seen that equitable distribution over the real negative axis, can lead to the asymptotic behavior of solutions determined by the real spectral abscissa of the characteristic quasipolynomial (5.15).

Remark 5.3. *It is fundamental to be aware about the dominance property of the assigned real roots. Therefore, to guarantee the dominancy among the assigned spectral values, it is necessary to show it either by using principle argument, or the quasipolynomial factorization. The dominance can be further checked by plotting the spectrum distribution.*

5.4 Simulation results

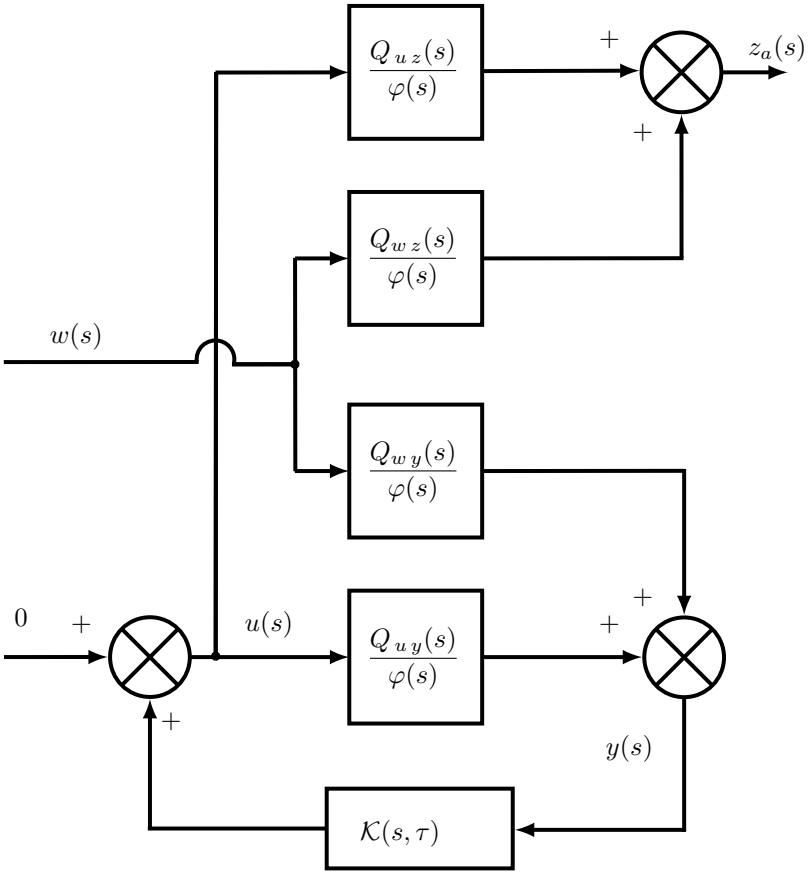

Figure 5.1. Feedback control system.

As it was considered in the former optimal controller design, we intend to damp the first three vibration modes of our systems. The target is to compute a delayed-output feedback controller and to evaluate its performance when the structure is put through a disturbance input $w(t)$ produced by an exogenous perturbation of $1\,\mathrm{m/sec^2}$ and a time length of $t_\ell = 5\times10^{-3}\,\mathrm{sec}$, shaped as a rectangular impulse motion, as it is shown in Figure 5.1. Its robustness features allow to partially place the analysis model's poles, including dominancy over the unmodelled roots of the synthesis model. This is,

to assign precise locations of a few number of poles, whose dominance is proved through the use of the principle argument, or the use of the quasipolynomial factorization proposed in [3].

5.4.1 Flexible beam

By following the controller proposed in (5.10), the numerical values of the controller's parameters in order to damp appropriately the first three vibration modes on the flexible beam are gathered in a clear way in Table 5.1.

We appropriately shape the spectrum of the closed-loop system by assigning a subset of coexisting poles to specific stable locations in the left-half of the complex plane. These poles should be placed sufficiently far from the imaginary axis to guarantee robust stability of the system [122].

Table 5.1. Numerical values of the Quasi-Polynomial Based controller (5.10) for a spectrum assignement given by $s_1 = -1$, $s_2 = -101$ and $s_3 = -201$ in the flexible beam system.

$q_0 = 33.6443$	$q_{r_0} = 1.68338$
$p_0 = 3.14258$	$p_{r_0} = 1.07203 \times 10^{-1}$
$\tau = 7.47849 \times 10^{-3}\,\text{sec}$	

Recoursing to different simulations with subsets of poles varying all along hundreds of units on the negative real-axis, the QPB method gives the following numerical values for the parameters of the controller in (5.10) that assigns $s_1 = -1$, $s_2 = -101$ and $s_3 = -201$ as the dominant roots of the characteristic polynomial for: $p_0 \simeq 3.14258$, $p_{r0} \simeq 1.07203 \times 10^{-1}$, $q_0 \simeq 33.6443, q_{r0} \simeq 1.68338$ and $\tau \simeq 7.47879 \times 10^{-3}\,\text{sec}$.

The roots of the characteristic function of the control law used for the flexible beam system are plotted in the Figure 5.2, which can be used to check graphically the stability of the control law, as well as to get some insights into how the control law will respond to changes in the signals, delays and coefficients that compose it. We recall that in this section we

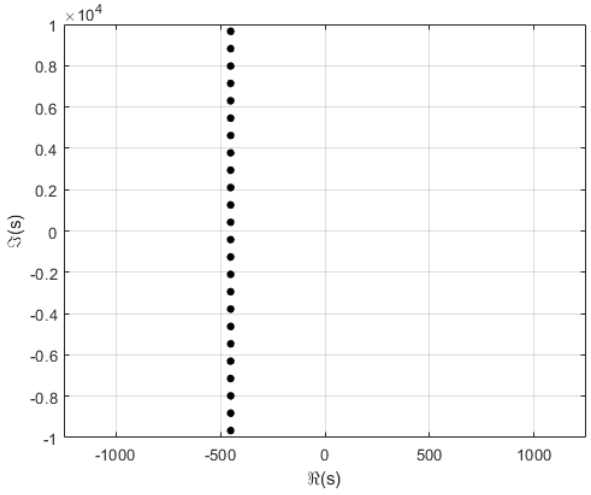

Figure 5.2. Spectrum distribution of the controller's complex plane around the origin.

are interested on the design of a delayed output-feedback controller that will stabilize the system. It is worth to mention that the QPB controller design involves an infinite number of roots, as can be seen in the Figure 5.3.

This quasipolynomial is given by

$$\Delta(s,\tau) = \varphi(s)\,\Delta_P(s,\tau) - Q_{u\,y}(s)\,Q(s,\tau), \tag{5.18}$$

whose terms can be rearranged as the addition of two polynomials, i.e. $\Delta(s,\tau) = P_0(s) + P_1(s)\,e^{-\tau s}$. For the dominant values $s_1 = -1$, $s_2 = -101$ and $s_3 = -201$, these polynomials are given as

Table 5.2. Coefficients a_i and b_i of polynomials $P_0(s) = \sum_0^6 a_i s^i$ and $P_1(s) = \sum_0^6 b_i s^i$

i	a_i	b_i
6	1	0
5	11.6217	-2.24265×10^{-14}
4	1.3075×10^{7}	-291117
3	5.3432×10^{7}	-1.20563×10^{6}
2	1.4011×10^{13}	-1.2037×10^{12}
1	8.11729×10^{12}	-6.97186×10^{11}
0	1.05493×10^{17}	-1.04712×10^{17}

In the figure 5.3 we show the distribution of the closed-loop poles, with a focus around the three assigned poles s_1, s_2 and s_3. We can check the frequency response of the quasipolynomial-based controller in the Figure 5.4, where damping of the first three vibration modes in the analysis model, where the amplitude of the first mode is nearly zero, while the amplitudes of the second and third modes were significantly reduced. The vibration modes neglected during the controller synthesis were the 4^{th}, 5^{th} and 6^{th} modes.

To show the performances of the proposed QPB-controller, the time responses of both signals in open-loop (red) and in closed-loop (blue) for the controlled output $z_a(t)$ of the full-order (analysis) model is depicted in the figure 5.5 where the disturbance $w(t)$ is a rectangular impulse (black), modelling a brief shock imposed to the whole flexible structure.

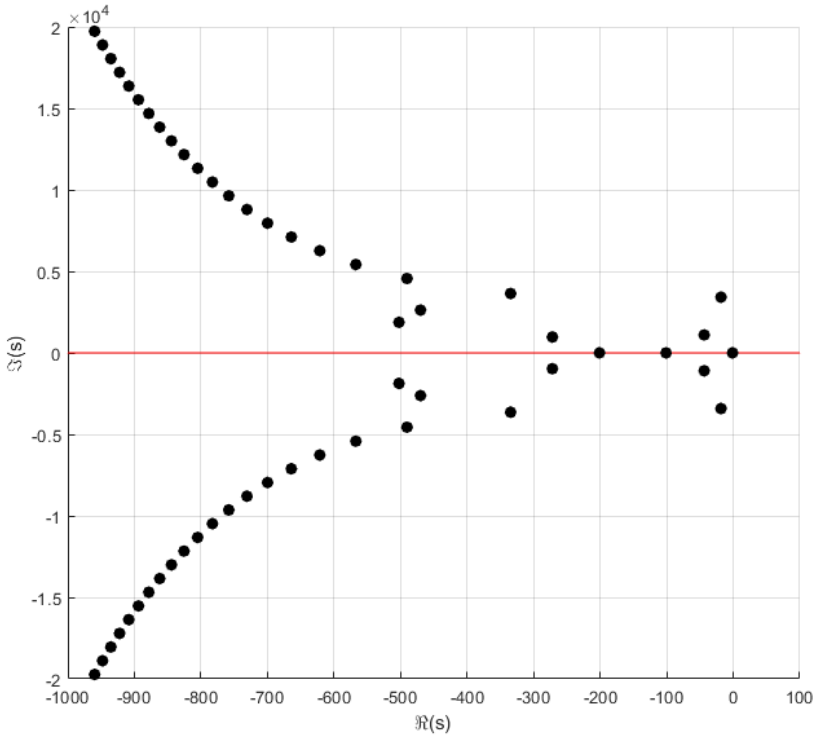

Figure 5.3. Three coexisting real roots of the flexible beam's infinite-dimensional characteristic quasipolynomial in closed-loop with the QPB controller. The parameters' values chosen are $p_0 \simeq 3.14258$, $p_{r0} \simeq 1.07203\times10^{-1}$, $q_0 \simeq 33.6443$, $q_{r0} \simeq 1.68338$ and $\tau \simeq 7.47849\times10^{-3}$ sec.

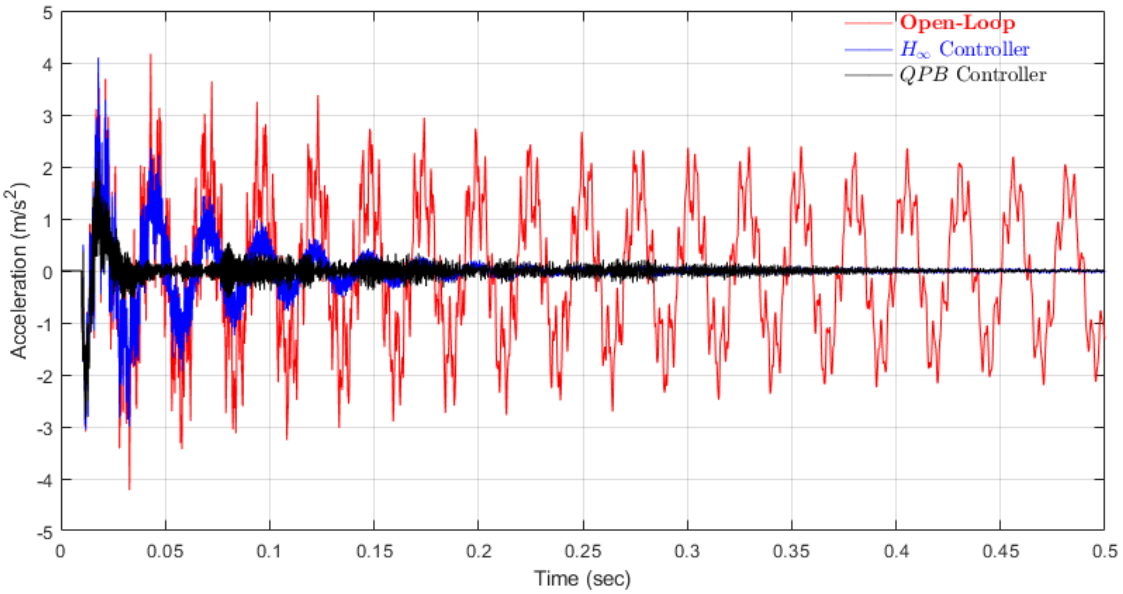

Figure 5.5. Time response of the flexible beam for the case of the controlled output $z_a(t)$ with an exogenous perturbation $w(t)$, which has an amplitude of $1\,\mathrm{m/sec^2}$, and a time length $t_\ell = 5\times10^{-3}\,\mathrm{sec}$. It describes the accelerometric behavior of the tip of the beam. It is possible to see in red color the open-loop response. In blue color is drawn the closed-loop response with the optimal H_∞ controller and in black is the closed-loop response with the QPB controller.

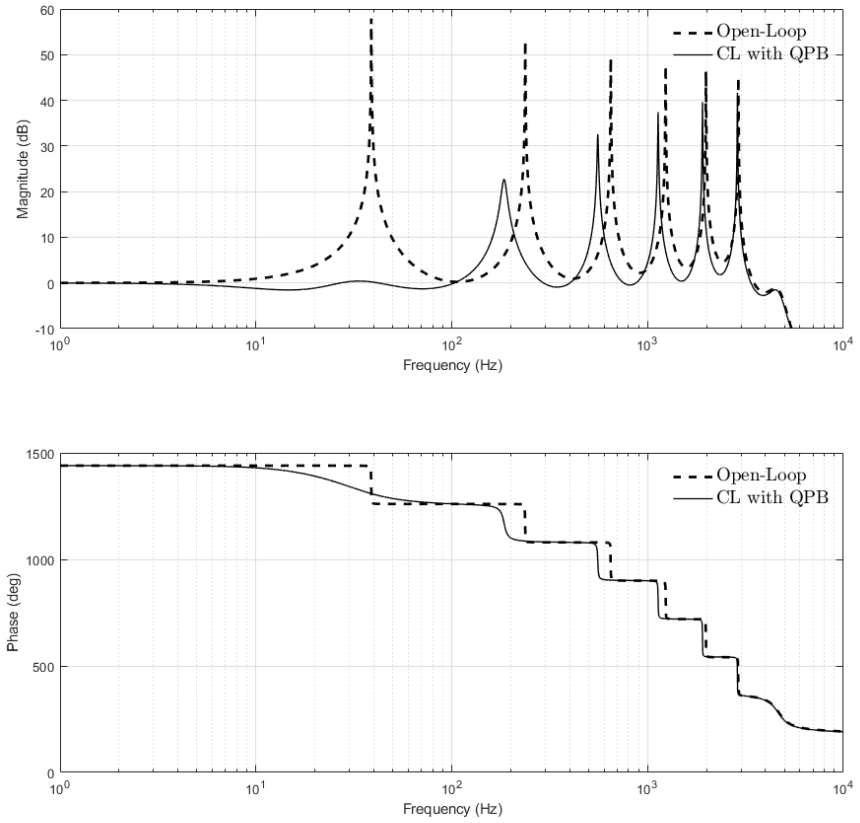

Figure 5.4. Frequency response of the flexible beam's system in closed-loop with the QPB controller. Above is placed the magnitude frequency response, and below is located the phase frequency response. The open-loop system is drawn with dashed lines, and the closed-loop with the QPB controller is with solid lines.

The Figure 5.5 shows the time response of the flexible beam when subjected to an exogenous perturbation with a given amplitude and duration. The plot illustrates the accelerometric behavior of the tip of the beam, with the open-loop response displayed in red, and the closed-loop responses with the optimal H_∞ controller and the QPB controller displayed in blue and black, respectively. The plot provides useful insights into the effectiveness of the different control strategies, and can be used to analyze and optimize the behavior of the system under different conditions.

5.4.2 Flexible axisymmetric membrane

We shape the spectrum of the closed-loop system by assigning a subset of dominant poles to specific stable location in the left-half of the complex plane. Starting with the Multiplicity-Induced Dominance control, we assign three poles far enough from the imaginary axis. This guarantees good and fast control of the output of interest, combined with a small peak in the actuator voltage. Using the MID-based control, we assign $s_c = -600$ as our spectral abscissa of multiplicity 3, getting the parameters as shown in the Table 5.3 for the case of the analysis model.

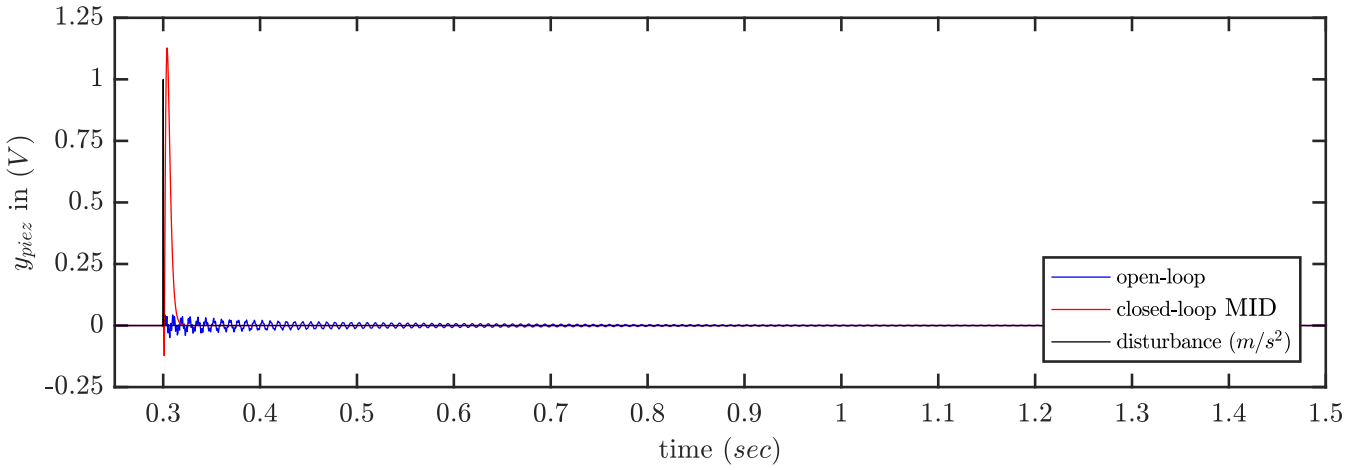

Figure 5.6. Time response of the measured output $y_{piez}(t)$.

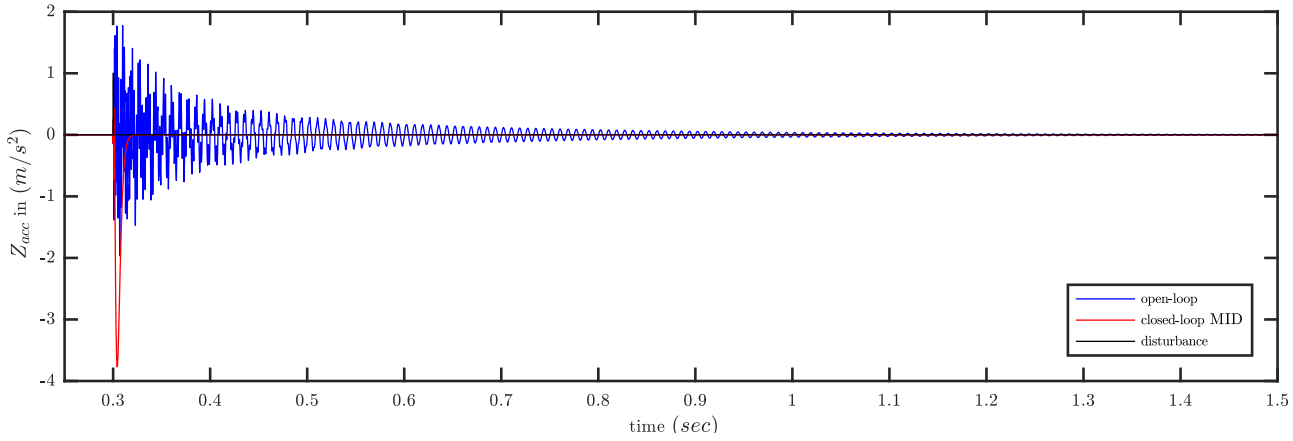

Figure 5.7. Time response of the controlled output $z_a(t)$.

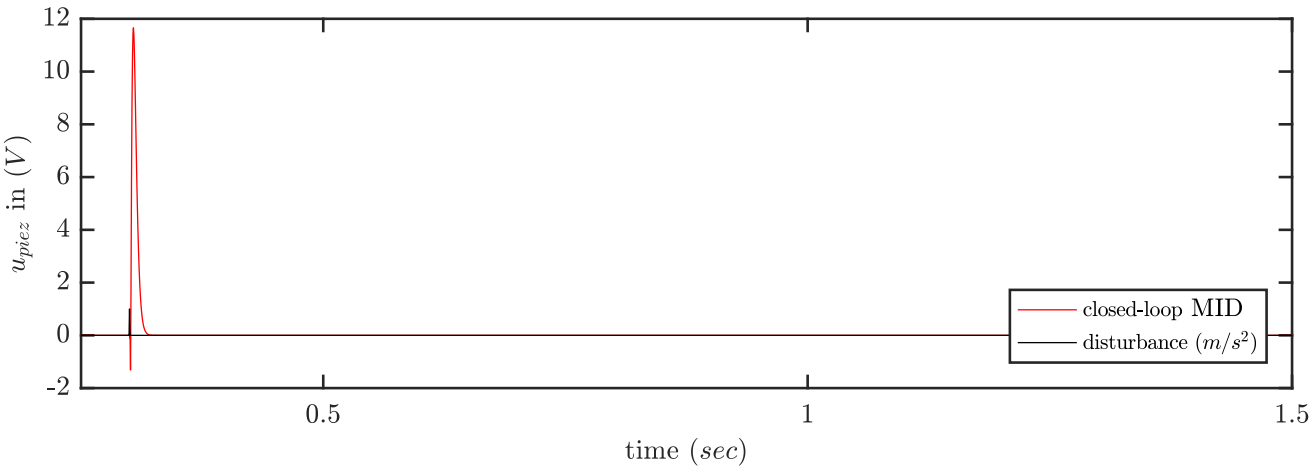

Figure 5.8. Closed-loop control signal $u_{piez}(t)$.

Table 5.3. Parameters' values for the axisymmetric membrane's MID-based control law.

$q_0 \simeq 7.478$	$q_{r_0} \simeq 69.884$
$p_0 \simeq 1.6268$	$p_{r_0} \simeq 5.858$
$\tau = 1.904 \times 10^{-4}\,\text{sec}$	

Table 5.4. Parameters' values for the axisymmetric membrane's CRRID-based control law.

$q_0 \simeq 41.290$	$q_{r_0} \simeq 36.403$
$p_0 \simeq 4.4611$	$p_{r_0} \simeq 3.0515$
$\tau = 3.36 \times 10^{-4}\,\text{sec}$	

In the case of the CRRID approach these poles should be placed sufficiently far from the imaginary axis to guarantee robust stability of the system [122]. Recoursing to different simulations with subsets of poles varying all along hundreds of units on the negative real-axis, the quasipolynomial-based control method gives the following numerical values for the parameters of the controller in (5.10) that assigns $s_1 = -500$, $s_2 = -550$ and $s_3 = -600$ as the coexisting real roots of the characteristic quasipolynomial are given in the Table 5.4.

In the Figure 5.10 we see the controller's poles in the complex plane. It is worth to recall that this is an infinite dimensional controller, due to the fact of the time delay involved in its design.

The latter QPB controller proposed in Equation (5.10) for the flexible axisymmetric membrane is employed with the numerical values of the controller's parameters, which are gathered in a clear way in Table 5.4.

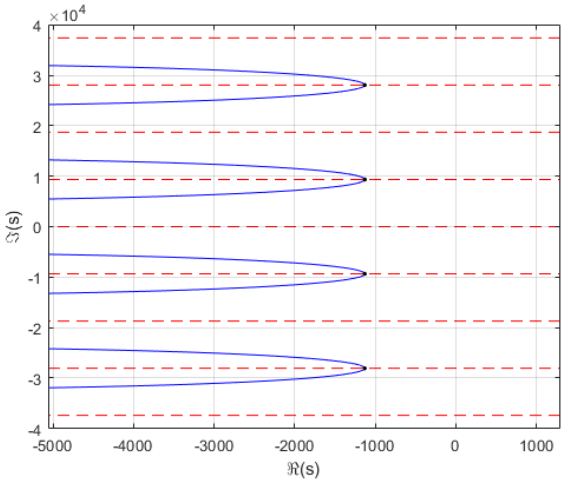

(a) Blue curves are the real parts of the characteristic equation and the red dashed curves are the imaginary parts when both are equal to zero of the QPB controller's characteristic quasipolynomial given by the values in the table 5.4.

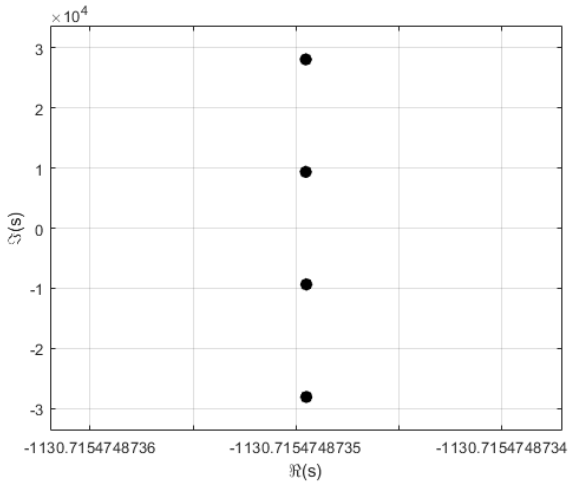

(b) Zeros of the infinite-dimensional controller given by the values in the Table 5.4 with $\Re(s) = -1130.71$.

Figure 5.9. Infinite roots of the controller's characteristic quasipolynomial used for the QPB approach with the flexible axisymmetric membrane. In Subfigure 5.9a, we have the real and imaginary parts in blue and red, respectively. In the Subfigure 5.9b we have the same complex plane with an horizontal zoom to their position.

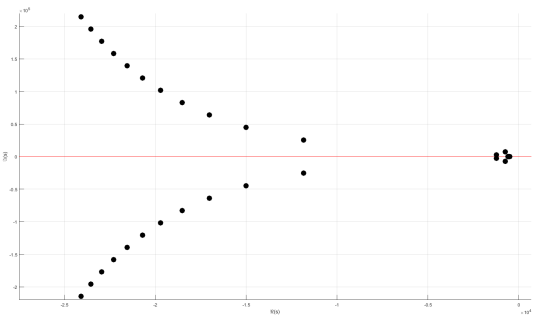

(a) Spectrum distribution of the flexible axisymmetric membrane in closed-loop with QPB controller.

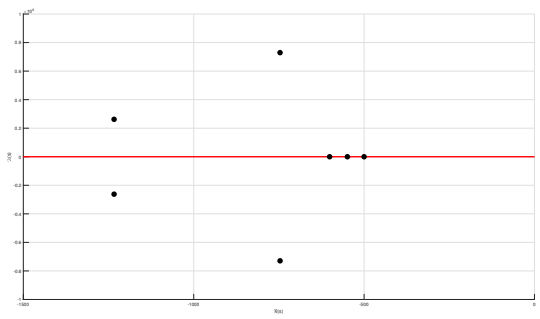

(b) Zoom around the origin of the complex plane of the axisymmetric membrane in closed-loop with the QPB control.

Figure 5.10. The three coexisting real roots in the complex plane for the flexible membrane. The values used in this system are $p_0 \simeq 4.4611$, $p_{r0} \simeq 3.0515$, $q_0 \simeq 41.290$, $q_{r0} \simeq 36.403$, $\tau \simeq 3.360\times10^{-4}\,\mathrm{sec}$. In the Subfigure 5.10a we check graphically the poles' behavior of a quasipolynomial. In the Subfigure 5.10b we do a zoom around the origin to gain insight about how the three assigned real roots in the controller's design include the spectral abcissa.

The quasipolynomial is given by

$$\Delta(s,\tau) = \varphi(s)\,\Delta_p(s,\tau) - Q_{u\,y}(s)\,\Delta_q(s,\tau), \tag{5.19}$$

whose terms can be rearranged as the addition of two polynomials, i.e. $\Delta(s,\tau) = P_0(s) + P_1(s)\,e^{-\tau s}$, given by

$$\begin{aligned} P_0(s) &= s^6 + 112.844\,s^5 + 4.8986\times10^7\,s^4 + 2.2778\times10^9\,s^3 \\ &\quad +3.2288\times10^{14}\,s^2 + 3.2016\times10^{15}\,s + 1.4718\times10^{20}, \\ P_1(s) &= -1.1368\times10^{-13}\,s^5 - 1.4266\times10^7\,s^4 - 6.2302\times10^8\,s^3 \\ &\quad -2.2010\times10^{14}\,s^2 - 1.9611\times10^{15}\,s - 1.3882\times10^{20}. \end{aligned}$$

Figure 5.10 shows the distribution of the closed-loop poles, with a focus around the three assigned poles s_1, s_2 and s_3.

The frequency response of the closed-loop system with the QPB controller, can be seen in the Figure 5.11, where we plotted the frequency response for the uncontrolled system, and the frequency response for the system in closed-loop with a QPB control design approach, in dashed and solid lines, respectively. It shows the magnitude and phase responses of the closed-loop systems as a function of frequency, which is represented on a logarithmic scale in Hertz. We can see that in spite of designing the controller with a synthesis model, which considered only the first three vibration modes, the computed QPB controller brings good damping performance in the five vibration modes included in the analysis model. All the modes are reduced, specially the first three modes. To show the performance of the proposed QPB-controller, we display the time-response of the output to be controlled $z_a(t)$ with the uncontrolled response (red) and the QPB controlled response (blue) in the Figure 5.12, where the disturbance $w(t)$ is a rectangular impulse of an amplitude of $1\,\mathrm{m/sec^2}$, and a time length $t_\ell = 5\times10^{-3}\,\mathrm{sec}$. It models a very brief shock imposed to the whole flexible structure.

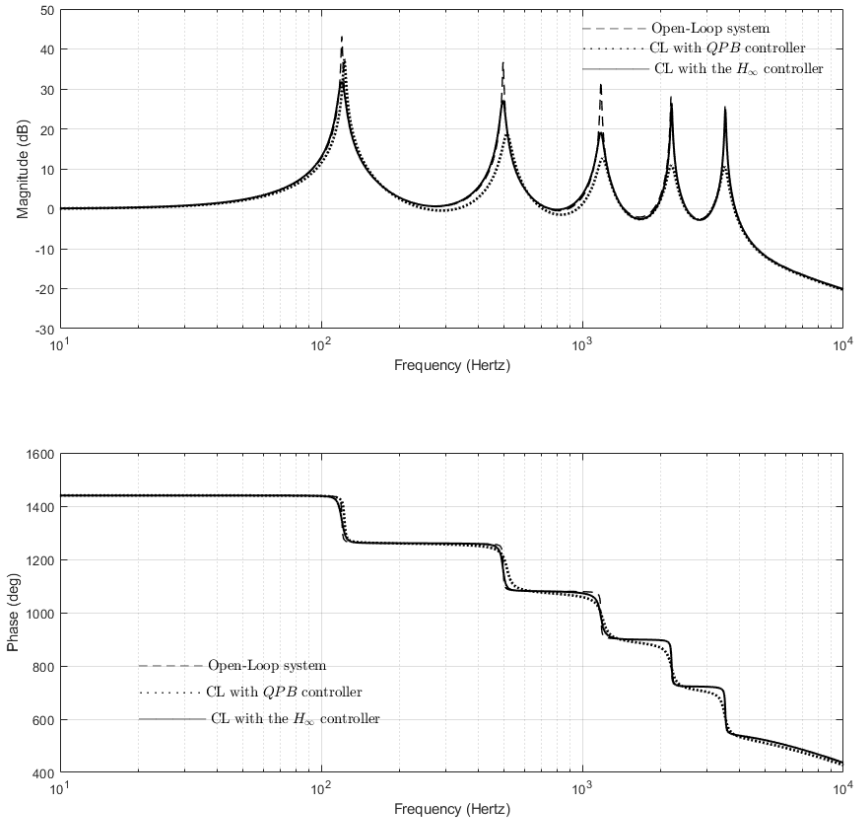

Figure 5.11. Frequency response of the flexible axisymmetric membrane's system in closed-loop with a QPB control design approach. Above is placed the magnitude frequency response, and below is located the phase frequency response. The open-loop system is drawn with dashed lines, and the closed-loop with the QPB controller is with solid lines.

Upon completing the simulations of our control approaches, it becomes crucial to examine the effects of these strategies on the system's behavior. To shed light on these dynamics, we present Table 5.5, which offers a comprehensive comparison within the analysis model. This table provides valuable insights into the excitation frequencies of each vibration mode and reveals subtle variations induced by the implementation of our controllers in the closed-loop system.

Table 5.5. Natural frequencies of 6 Vibration Modes (VM) in the analysis model.

	Frequency (Hz)		
VM	OL	QPB	$\mathcal{H}_\infty$
1	38.8207	45.457	38.95524
2	237.7805	233.247	235.4965
3	648.62584	631.300	647.3163
4	1,236.0549	1,210.8981	1,235.8108
5	1,986.94097	1,965.2276	1,986.5378
6	2,907.37549	2,898.358	2,907.1782

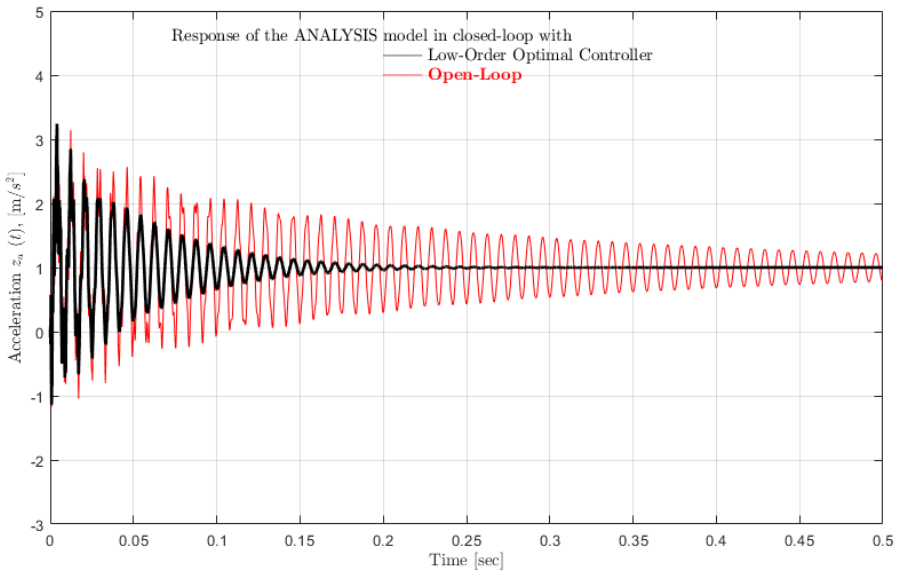

Figure 5.12. Time response of the controlled output $z_a(t)$, against a disturbance $w(t) = 1\,\mathrm{m/sec^2}$ during a time length of $t_\ell = 5\times10^{-3}\,\mathrm{sec}$.

Forthwith, a crucial analysis of the damping characteristics is essential for understanding the stability and performance of the controlled modes. Table 5.6 serves this purpose, presenting the damping factors associated with each mode.

Table 5.6. Damping coefficients of the 6 Vibration Modes (VM) in the analysis model.

	Damping Coefficient		
VM	OL	QPB	$\mathcal{H}_\infty$
1	0.001	0.132	0.0819
2	0.001	0.0.0709	0.0287
3	0.001	0.0232	0.0447
4	0.001	0.009	0.0029
5	0.001	0.0035	0.0017
6	0.001	0.0014	0.0011

Furthermore, to gain a deeper understanding of the system's response, Table 5.7 provides critical information on the exact pole positions corresponding to the non-oscillating modes. These tables collectively contribute to a comprehensive evaluation of the control strategies and their impact on the flexible structure's vibrational behavior.

5.5 Concluding remarks

In this chapter, a basic introduction to time-delay control theory required for developping this work is summarized. The interest in using time-delays as a designer parameter of the controllers is highlighted. We consider to implement this

Table 5.7. Pole locations of the 6 Vibration Modes (VM) in the analysis model.

	Pole Locations		
VM	OL	QPB	$\mathcal{H}_\infty$
1	$-0.2439 \pm \mathrm{i}\,243.9176$	$-37.6468 \pm \mathrm{i}\,283.123$	$-20.0504 \pm \mathrm{i}\,243.9403$
2	$-1.4915 \pm \mathrm{i}\,1491.5048$	$-103.864 \pm \mathrm{i}\,1461.85$	$-42.5827 \pm \mathrm{i}\,1479.0555$
3	$-4.0754 \pm \mathrm{i}\,4075.4342$	$-92.185 \pm \mathrm{i}\,3965.507$	$-181.8802 \pm \mathrm{i}\,4063.1394$
4	$-7.7663 \pm \mathrm{i}\,7766.3578$	$-69.248 \pm \mathrm{i}\,7607.982$	$-22.4875 \pm \mathrm{i}\,7764.7959$
5	$-12.4843 \pm \mathrm{i}\,12484.3120$	$-44.058 \pm \mathrm{i}\,12347.811$	$-21.6714 \pm \mathrm{i}\,12481.7663$
6	$-18.2675 \pm \mathrm{i}\,18267.5698$	$-27.248 \pm \mathrm{i}\,18210.903$	$-20.8727 \pm \mathrm{i}\,18266.3271$

controller in the low-order synthesis model of our flexible structures under consideration, which are the flexible beam and the flexible axisymmetric membrane, which are distributed parameter systems. These synthesis models include only the first three controllable and observable vibration modes. An active vibration damping is achieved through the use of a pointwise pole placement technique with an adequate characteristic quasipolynomial.

This chapter has shown the interest to use time-delay in a controller as a design parameter. The practical applications that we have considered are for flexible structures equipped with a piezoelectric sensor and a piezoelectric actuator in a collocated configuration. For this systems it is expected to achieve an active vibration control thanks to an output feedback controller. This controller has been designed by using a PPP technique through an approach based on the design of a characteristic quasipolynomial that acts as the equation of these closed-loop delayed systems. The possibilities are left open for a proper discretization into a digital system, which will be dealt with on the next chapter. This action is taken in order to ensure the damping of the first three observable and controllable vibrating modes. The output feedback feature opens the possibility to implement such a controller in an experimental test bench.

Chapter 6

The saturation problem, antiwindup compensator design and numerical simulations

The aim of this chapter is to present an approach for designing antiwindup compensators. The chapter begins in the section 6.1 with an introduction to the antiwindup compensators and the windup phenomenon, where their importance in control system design is discussed. Next, in section 6.2 the antiwindup compensator design methodology is treated. The approximation techniques come in section 6.3 which include techniques such as Pade approximation and Thiran approximation. In addition, the implementation of sampled data systems is presented in section 6.4, which is essential for digital control systems. Then, the quasipolynomial-based controller simulation is discussed in section 6.5. Finally, the chapter concludes in section 6.6 with some remarks on the performance of the designed antiwindup compensator and its potential for improving the vibration control of flexible structures.

Contents

6.1 Introduction

A phenomenon that is often overlooked is the fact that neither motors nor actuators are flawless, and therefore, they face saturations as an intrinsec property that can constrain the control laws' designs. Not considering these limitations can lead into undesirable effects. Besides, through balanced reduction techniques, we have followed a methodology for the synthesis of an H_∞ controller, which in turn has been approximated by a lower-order representation that represents faithfully the behavior of the system of interest under the frequency range that concerns us. Also, a QPB controller approach has been considered, and it is in our nature to look for an appropriate real-time implementation of such delayed-controller. Such models' implementation generally involve too many degrees of freedom and they are reduced to produce closed-loop models that involve only a few degrees of freedom (including just the vibration modes of the system).

The windup effect is an event which occurs when a non-linearity comes into account, i.e. the control-input signal saturation [204]. These are due to physical limitations in the devices, particularly the actuators' constraints, they can be considered as limited positions and speeds. Usually this implies a situation where the system suffers a degradation. This was first identified as a common effect on the PID controllers [113, 9, 138]. Several anti-windup schemes were reviewed and a unified framework was formulated in [101]. Then, with the broadening of the anti-windup studies, modern theories [60, 168, 204] identify two areas of methods for the anti-windup design, the Direct Linear Anti-Windup (DLAW) and the Model Recovery Anti-Windup (MRAW), where the DLAW method is used in [90] where a control approach with input saturations is proposed for the control of an autopilot system, and the MRAW method is used in [94] where the PID controller and the Anti-Windup filter are obtained simultaneously.

Considering that saturations can be found in every real system's dynamic, and that they can produce defective and treacherous behaviors, it becomes a paramount concern to avoid reaching such limits. To avoid these scenarios, a first possibility is the design of control laws that do not reach these thresholds of saturating levels, at expense of a potential decrease in the closed-loop performance. But a second possibility involves the tweak (or compensation) of the closed-loop dynamics, and hence avoiding this performance degradation [168]. For the latter possiblity, is necessary to develop and validate a control law for an ideal control input signal free from saturations. This is that, as long as the dynamics of the systems stay below saturation levels, the control input signal behaves as it is originally designed. Then, when saturations are present in the system, is when tweaks in the closed-loop dynamics are carried out through the attachment of another control loop, which will be active only when saturation levels are reached.

And nowadays, controllers are implemented in a digital manner. Nonetheless, there are good reasons to carry out a continuous design and transform the continuous controller into a digital one with appropriate techniques [141]. The time-delays involved in the QPB controller were linearized using the Padé approximation [65, pp. 530-531]. The Thiran approximation was used to digitalize the control laws in order to implement them through the real-time device available at the lab.

The term "anti-windup compensation" appeared in the literature to treat the windup effect seen on the integral action

of a PID controller when it was affected by input saturation, where the value of the state could 'windup' to very high values. However, many linear control systems (not only integral actions) can exhibit unpredictable behavior when they reach saturation in the control signals. The main idea behind these anti-windup compensators is to compensate the bad performance beared by the non-linear saturations.

In [173] a linear anti-windup technique that takes into account the presence of a direct feedthrough term, i.e. $D_{yu} \neq 0$ in the plant's dynamic model is considered to extend the results given in [195] for the strictly proper case (no direct feedthrough term from u to y).

The state of the art related to the problem of the synthesis of compensators has been treated before in several works, such as [190], where the stability and convergence of an adaptive pole placement controller with saturating inputs is analyzed, and in [162], where optimal compensators are designed for discrete-time input-constrained systems. In [79] the synthesis of anti-windup compensators is carried out through a formulation in discrete-time ensuring an upper bound on the $\mathcal{L}_2$ norm in three different cases, full-order (an order equal to the plant's order), static (zeroth order), which bestows a low computational complexity, and low-order cases, which can be outperformed the static compensators [145]. In [167] we find computation strategies that guarantee a specific $\mathcal{L}_2$ performance level and the topic of anti-windup compensators has also been extended to include the synthesis of compensators for discrete-time linear systems with saturating control inputs.

6.2 Antiwindup compensator design

The design of the anti-windup compensator is explained in this section. The design of this anti-windup compensator takes into account systems which are not strictly proper, making this procedure better tailored for flexible systems [175].

Consider that the linear plant of the system is given as

$$\mathcal{P} \begin{cases} \dot{x} &= A\,x + B_w\,w + B_u\,u \\ z &= C_z\,x + D_{zw}\,w + D_{zu}\,u \\ y &= C_y\,x + \underbrace{D_{yw}\,w + D_{yu}\,u}_{\text{feedthrough terms}} \end{cases} \tag{6.1}$$

where $u \in \mathbb{R}^{n_u}$ stands for the control input (often expressed in voltage), $y \in \mathbb{R}^{n_y}$ is the measured output, $w \in \mathbb{R}^{n_w}$ stands for the exogenous input, and $z_a \in \mathbb{R}^{n_z}$ stands for the controlled output of the system. Equation (6.1) represents the synthesis model (smaller order than the analysis model), which was used for the specific controller design.

The stabilizing controller $\mathcal{C}$ when input saturation is ignored is given in state-space form by

$$\mathcal{C}\begin{cases} \dot{x}_c &= A_c\,x_c + B_c\,y + v_1 \\ y_c &= C_c\,x_c + D_c\,y + v_2 \end{cases} \tag{6.2}$$

where $x_c \in \mathbb{R}^{n_c}$ is the vector containing the states of the linear controller, $y_c \in \mathbb{R}^{n_u}$ is the controller output, and $v = [v_1^T\ v_2^T]^T \in \mathbb{R}^{n_v}$, with $v_1 \in \mathbb{R}^{n_c}$ and $v_2 \in \mathbb{R}^{n_u}$, are the additional inputs delivered by the anti-windup compensator. In the case where there is no input saturation, $v = 0 \in \mathbb{R}^{n_c+n_u}$. The purpose of the additional inputs from the anti-windup compensator is to tweak the closed-loop system, such that the dynamics of the system are improved when the control signal is saturated.

The dynamic anti-windup compensator, whose input is given by the deadzone signal $q = \mathrm{dz}(y_c) := y_c - \mathrm{sat}(y_c)$. This last definition may exceed the saturation limits of the actuator. To prevent this, the deadzone signal is constrained by the inequality $|q| < q_{max}$, where q_{max} is the maximum allowable magnitude of the deadzone signal, and its dynamic is established by

$$\mathcal{AW}\begin{cases} \dot{x}_{aw} &= A_{aw}\,x_{aw} + B_{aw}\,q \\ v &= C_{aw}\,x_{aw} + D_{aw}\,q \end{cases} \tag{6.3}$$

with $x_{aw} \in \mathbb{R}^{n_{aw}}$, where its order is the same as the plant's (6.1) order, i.e. $n_{aw} = n_p$.

For the non-strictly proper case, $\widetilde{\mathcal{P}}$ represents the strictly proper plant w.r.t. $u(t)$, which is given by

$$\widetilde{\mathcal{P}}\begin{cases} \dot{x} &= A\,x + B_w\,w + B_u\,u \\ z &= C_z\,x + D_{zw}\,w + D_{zu}\,u \\ \tilde{y} &= C_y\,x + D_{yw}\,w \end{cases} \tag{6.4}$$

and $\widetilde{\mathcal{C}}$ corresponds to the controller the system and is given as

$$\widetilde{\mathcal{C}}\begin{cases} \dot{\tilde{x}}_c &= \widetilde{A}_c\,\tilde{x}_c + \widetilde{B}_c\,\tilde{y} + \widetilde{M}_c\,q + \tilde{v}_1 \\ \tilde{y}_c &= \widetilde{C}_c\,\tilde{x}_c + \widetilde{D}_c\,\tilde{y} + \widetilde{N}_c\,q + \tilde{v}_2 \end{cases} \tag{6.5}$$

where the additional inputs $\tilde{v} = [\tilde{v}_1 \tilde{v}_2]^T$ are computed as

$$\begin{bmatrix} \tilde{v}_1 \\ \tilde{v}_2 \end{bmatrix} = \begin{bmatrix} \mathbb{1}_{n_c} & B_c\,D_{yu}\,\Delta_c^{-1} \\ \mathbf{0}_{n_u\times n_c} & \Delta_c^{-1} \end{bmatrix} \begin{bmatrix} v_1 \\ v_2 \end{bmatrix} \tag{6.6}$$

with $\Delta_c = \mathbb{1}_{n_u} - D_c\,D_{yu}$. The matrices used for the equivalent controller for the strictly proper case $\widetilde{\mathcal{C}}$ in (6.5) are defined

as follows

$$\begin{cases} \widetilde{A}_c &:= A_c + B_c\, D_{yu}\, \Delta_c^{-1}\, C_c, \\ \widetilde{B}_c &:= B_c\, (\mathbb{1}_{n_y} + D_{yu}\, \Delta_c^{-1}\, D_c), \\ \widetilde{C}_c &:= \Delta_c^{-1}\, C_c, \\ \widetilde{D}_c &:= \Delta_c^{-1}\, D_c, \\ \widetilde{M}_c &:= -B_c\, D_{yu}\, (\mathbb{1}_{n_u} + \Delta_c^{-1}\, D_c\, D_{yu}), \\ \widetilde{N}_c &:= -\Delta_c^{-1}\, D_c\, D_{yu} \end{cases} \tag{6.7}$$

The new matrices written as $\widetilde{M}_c$ and $\widetilde{N}_c$ can not be ignored in the anti-windup compensator synthesis, because they are responsible of taking into account the deadzone signal $q = \mathrm{dz}(y_c)$ in the augmented controller state equations $\widetilde{\mathcal{C}}$ in (6.5).

To have a solution for the anti-windup compensator synthesis, we need to consider certain assumptions, where firstly, we assume that the group of matrices $(A,\, B_u,\, C_y)$ are controllable and observable; and secondly, we assume that the closed-loop interconnection of the plant $\mathcal{P}$ and the linear controller $\mathcal{C}$ is stable when there is no saturation, i.e. $u = y_c$, and $v = 0$ [175].

The closed-loop interconnection of the strictly proper plant $\widetilde{\mathcal{P}}$ (6.4) and the corresponding control law $\widetilde{\mathcal{C}}$ (6.5), is represented as

$$\mathcal{G} \begin{cases} \dot{x} &= \widetilde{A}\, x + \widetilde{B}_0\, q + \widetilde{B}_1\, w + \widetilde{B}_2\, v, \\ y_c &= \widetilde{C}_0\, x + \widetilde{D}_{00}\, q + \widetilde{D}_{01}\, w + \widetilde{D}_{02}\, v, \\ z &= \widetilde{C}_1\, x + \widetilde{D}_{10}\, q + \widetilde{D}_{11}\, w + \widetilde{D}_{12}\, v, \\ q &= \mathbb{1}_{n_u}\, q \end{cases} \tag{6.8}$$

where $q = \mathrm{dz}(y_c)$ and $x \in \mathbb{R}^{n_c+n_p}$. These new closed-loop matrices are defined as

$$\begin{cases} \widetilde{A} := \begin{bmatrix} A + B_u\,\widetilde{D}_c\,C_y & B_u\,\widetilde{C}_c \\ \widetilde{B}_c\,C_y & \widetilde{A}_c \end{bmatrix}; \\ \widetilde{B}_0 := \begin{bmatrix} B_u\,(\widetilde{N}_c - \mathbb{1}_{n_u}) \\ \widetilde{M}_c \end{bmatrix}; \qquad \widetilde{C}_0 := [\widetilde{D}_c\,C_y\ \widetilde{C}_c]; \\ \widetilde{B}_1 := \begin{bmatrix} B_w + B_u\,\widetilde{D}_c\,D_{yw} \\ \widetilde{B}_c\,D_{yw} \end{bmatrix}; \qquad \widetilde{D}_{01} := \widetilde{D}_c\,D_{yw}; \\ \widetilde{B}_2 := \begin{bmatrix} 0_{n_p\times n_c} & B_u\,\Delta_c^{-1} \\ \mathbb{1}_{n_c} & B_c\,D_{yu}\,\Delta_c^{-1} \end{bmatrix}; \quad \widetilde{D}_{02} := [0_{n_u\times n_c}\ \Delta_c^{-1}]; \\ \widetilde{C}_1 := [C_z + D_{zu}\,\widetilde{D}_c\,C_y\ D_{zu}\,\widetilde{C}_c]; \\ \widetilde{D}_{10} := D_{zu}\,(\widetilde{N}_c - \mathbb{1}_{n_u}); \qquad \widetilde{D}_{12} := [\mathbf{0}_{n_z\times n_c}\ D_{zu}\,\Delta_c^{-1}]; \\ \widetilde{D}_{11} := D_{zw} + D_{zu}\,\widetilde{D}_c\,D_{yw}; \qquad \widetilde{D}_{00} := \widetilde{N}_c. \end{cases} \tag{6.9}$$

Then, the anti-windup compensator's matrices are collected in the variable Θ, just as

$$\Theta := \begin{bmatrix} A_{aw} & B_{aw} \\ C_{aw} & D_{aw} \end{bmatrix} \in \mathbb{R}^{(n_p+n_c)\times(n_p+n_c)} \tag{6.10}$$

Then, from the above definitions and clarifications, we can continue applying the feasibility theorem as follows:

Theorem 12 ([173, Theorem 2]). *Given a non-strictly proper LTI plant $\mathcal{P}$ and a respective linear controller $\mathcal{C}$, in view of the assumptions referring to controllability, observability, stabilizability of the controller in the absence of saturations (i.e. $u = y_c$), and the equivalent strictly proper plant $\widetilde{\mathcal{P}}$ with its corresponding controller $\widetilde{\mathcal{C}}$, given real scalars $0 < k_i \leq 1$, $i = 1, 2, \ldots, n_u$, and a scalar $\gamma > 0$, a bound on the desired $\mathcal{L}_2$-norm of the closed-loop system from the exogenous input(s) w to the controlled output(s) z_a. Providing the existence of matrices $R_{11} \in \mathbb{S}_+^{n_p\times n_p}$, $S \in \mathbb{S}_+^{n\times n}$, and a diagonal*

matrix $V = \mathrm{diag}\{v_1, v_2, \cdots, v_{n_u}\} > 0$ *which satisfy the inequalities*

$$\begin{bmatrix} \left\{ \begin{matrix} A\,R_{11} + R_{11}\,A^T \\ -B_u\left((\widetilde{N}_c - \mathbb{1}_{n_u})\,V + V(\widetilde{N}_c^T - \mathbb{1}_{n_u})\right)B_u^T \end{matrix} \right\} & \left\{ \begin{matrix} R_{11}\,C_z^T \\ +2\,B_u\,(\mathbb{1}_{n_u} - K^{-1})\,V\,D_{zu}^T \end{matrix} \right\} & B_w \\ \left\{ \begin{matrix} C_z\,R_{11} \\ +2\,D_{zu}\,V\,(\mathbb{1}_{n_u} - K^{-1})\,B_u^T \end{matrix} \right\} & \left\{ \begin{matrix} -\gamma\,\mathbb{1}_{n_z} \\ +2\,D_{zu}\,(\mathbb{1}_{n_u} - K^{-1})\,V\,D_{zu}^T \end{matrix} \right\} & D_{zw} \\ B_w^T & D_{zw}^T & -\gamma\,\mathbb{1}_{n_w} \end{bmatrix} < 0, \tag{6.11}$$

$$\begin{bmatrix} \widetilde{A}^T\,S + S\,\widetilde{A} & S\,\widetilde{B}_1 & \widetilde{C}_1^T \\ \widetilde{B}_1^T\,S & -\gamma\,\mathbb{1}_{n_w} & \widetilde{D}_{11}^T \\ \widetilde{C}_1 & \widetilde{D}_{11} & -\gamma\,\mathbb{1}_{n_z} \end{bmatrix} < 0, \tag{6.12}$$

$$\begin{bmatrix} R_1 1 & [\mathbb{1}_{n_p}\ 0] \\ \begin{bmatrix} \mathbb{1}_{n_p} \\ 0 \end{bmatrix} & S \end{bmatrix} \geq 0 \tag{6.13}$$

then, there exist an anti-windup compensator $\mathcal{AW}$ *of order* $n_{aw} = n_p$ *that robustly stabilizes the closed-loop system* $\mathcal{G}$ *with respect to a sector-bound assumption.*

It should be noted that the design approach proposed in [195] for anti-windup compensators for non-strictly proper systems is different from that for strictly proper systems in that the former approach involves matrices presented in (6.9) that cover almost all the elements, indicating that these matrices represent general conditions applicable to the non-strictly proper case.

The LTI system given in (6.1) will happen to be a strictly proper case when we assume $D_{zw}(t) = 0$. With this said, we define the $\mathcal{L}_2$ gain of the system (6.1) as the value

$$\sup_{\|w\|_2 \neq 0} \frac{\|z\|_2}{\|w\|_2} \tag{6.14}$$

where the supremum is taken over all nonzero trajectories of the system, and $\|u\|_2^2 = \int_0^\infty u^T\,u\,dt$ is the $\mathcal{L}_2$ norm of u.

If there exists a quadratic function $V(\xi) = \xi^T\,P\,\xi$, with $P > 0$ and a positive constant $\gamma > 0$, such that

$$\frac{d}{dt}V(x) + z^T\,z - \gamma^2\,w^T\,w \leq 0 \tag{6.15}$$

and integrating from 0 to T

$$V(x(T)) + \int_0^T (z^T z - \gamma^2 w^T w)\, dt \leq 0 \tag{6.16}$$

with the initial condition $x(0) = 0$ and since $V(x) \geq 0$, then the $\mathcal{L}_2$ gain is smaller than γ, thus it follows that

$$\frac{\|z\|_2}{\|w\|_2} \leq \gamma$$

We can rewrite the inequality (6.15) as a LMI, given by

$$\begin{bmatrix} A^T P + P A + C_z^T C_z & P B_w \\ B_w^T P & -\gamma^2 \mathbb{I} \end{bmatrix} \leq 0 \tag{6.17}$$

where the identity matrix $\mathbb{I}$ is introduced with appropriate dimensions. Then, we can compute the smallest upper bound on the $\mathcal{L}_2$ gain of the LTI system (6.1) through the minimization of the value γ. Assuming that the group $(A,\, B_w,\, C_z)$ is minimal (controllable and observable), this late eigenvalue problem results in the value of the $\mathcal{L}_2$ gain of the LTI system, which follows a narrow relation with the $\mathcal{H}_\infty$ norm of its transfer matrix $\|C_z\,(s\,\mathbb{I} - A)^{-1}\,B_w\|_\infty$ [34, §6.3.2].

Given this close relation between the $\mathcal{L}_2$ gain and the $\mathcal{H}_\infty$ norm, it becomes intriguing the comparison of the strictly proper and the non-strictly proper cases, to accentuate the differences of both approaches. Specifically, for strictly proper systems, the $\mathcal{L}_2$ gain is equal to the $\mathcal{H}_\infty$ norm, and the analysis and design of antiwindup compensators can be based solely on the $\mathcal{L}_2$ gain. However, for non-strictly proper systems, this relation between the $\mathcal{L}_2$ gain and the $\mathcal{H}_\infty$ norm does not hold, and additional considerations are required for the design and analysis of antiwindup compensators.

In practice, when γ is too small, the existence of a solution can not be guaranteed by this methodology. This means that the system must have very good performance, which may not be achievable with the given controller or actuator limitations. Therefore, the optimization problem may not have a feasible solution. However, all the conditions of theorem 12, arrive to the minimum possible value of γ, and given that (6.11)-(6.13) are non-convex with respect to γ, i.e. it can be translated into the following optimization problem

$$\min_{R_{11},S,V} \gamma \text{ subject to } (6.11)\,(6.12)\,(6.13) \tag{6.18}$$

and the condition (6.13) assures that we will get a n_{aw}th-order anti-windup compensator [59], where $n_{aw} = n_p + n_c$. This is because a n_{aw}th-order anti-windup compensator must hold that

$$\begin{bmatrix} R & \mathbb{I}_n \\ \mathbb{I}_n & S \end{bmatrix} \geq 0 \tag{6.19}$$

$$\operatorname{rank}(R - S^{-1}) \leq n_{aw} \tag{6.20}$$

The anti-windup compensator contruction methodology presented below has been used in past works as in [195] and [173].

Theorem 13. *Given the solutions R_{11}, S, γ and V from the feasibility theorem (Theorem 12), let $W = V^{-1}K^{-1} = K^{-1}V^{-1}$, $H^T = [\mathbb{I}_{n_{aw}}\ \mathbf{0}_{n_{aw}\times(n-n_{aw})}]$ and consider the following decomposition $M\,N^T = \mathbb{I}_n - R\,S$ where M, $N \in \mathbb{R}^{n\times n_{aw}}$, $R = \begin{bmatrix} R_{11} & R_{12} \\ R_{12} & R_{22} \end{bmatrix}$ with $R_{12} = [\mathbb{I}_{n_p}\ 0]S^{-1}\begin{bmatrix} 0 \\ \mathbb{I}_{n_c} \end{bmatrix}$, $R_{22} = \begin{bmatrix} \mathbb{I}_{n_c} \\ 0 \end{bmatrix} S^{-1}[0\ \mathbb{I}_{n_c}] = R_{22}^T$. Then, a n_{aw}th-order anti-windup compensator, where $n_{aw} \geq n_p$, can be obtained by using the following method:*

1. *Compute a feasible $\widehat{D}_{aw} \in \mathbb{R}^{n_v\times n_c}$ such that*

$$\underbrace{\begin{bmatrix} \left\{\begin{array}{l} W\,K\,(\tilde{D}_{00} + \tilde{D}_{02}\,\widehat{D}_{aw}) - 2\,W \\ \\ +(\tilde{D}_{00}^T + \widehat{D}_{aw}^T\,\tilde{D}_{02}^T)\,K\,W \end{array}\right\} & W\,K\,\tilde{D}_{01} & \tilde{D}_{10}^T + \widehat{D}_{aw}^T\,\tilde{D}_{12}^T \\ \tilde{D}_{01}^T\,K\,W & -\gamma\,\mathbb{I}_{n_w} & \tilde{D}_{11}^T \\ \tilde{D}_{10} + \tilde{D}_{12}\,\widehat{D}_{aw} & \tilde{D}_{11} & -\gamma\,\mathbb{I}_{n_z} \end{bmatrix}}_{-\Pi} < 0 \tag{6.21}$$

2. *Compute the least-square solutions of the following equations for $\widehat{B}_{aw} \in \mathbb{R}^{n\times n_u}$, $\widehat{C}_{aw} \in \mathbb{R}^{n_v\times n_{aw}}$*

$$\left[\begin{array}{c|ccc} 0 & \mathbb{I}_{n_u} & 0 & 0 \\ \hline \mathbb{I}_{n_u} & & & \\ 0 & & -\Pi & \\ 0 & & & \end{array}\right]\left[\begin{array}{c} \widehat{B}_{aw} \\ \hline \\ ? \\ \\ \end{array}\right] = \left[\begin{array}{c} 0_{n_u\times n} \\ \hline \\ \tilde{B}_0^T\,S + W\,K\,\tilde{C}_0 \\ \tilde{B}_1^T\,S \\ \tilde{C}_1\,S \end{array}\right] \tag{6.22}$$

$$\left[\begin{array}{c|ccc} 0 & \tilde{D}_{02}^T\,K\,W & 0 & \tilde{D}_{12}^T \\ \hline W\,K\,\tilde{D}_{02} & & & \\ 0 & & -\Pi & \\ \tilde{D}_{12} & & & \end{array}\right]\left[\begin{array}{c} \widehat{C}_{aw} \\ \hline \\ ? \\ \\ \end{array}\right] = \left[\begin{array}{c} \tilde{B}_2^T\,H \\ \hline W\,K\,C_0\,R\,H + \widehat{D}_{aw}^T\,\tilde{B}_2^T\,H + \tilde{B}_0^T\,H \\ \tilde{B}_1^T\,H \\ \tilde{C}_1\,R\,H \end{array}\right] \tag{6.23}$$

and the matrix $\widehat{A}_{aw} \in \mathbb{R}^{n\times n_{aw}}$ as

$$\widehat{A}_{aw} = -\tilde{A}^T\,H - X\left(\widehat{B}_{aw}\right)\,\Pi^{-1}\,Y\left(\widehat{C}_{aw}, \widehat{D}_{aw}\right) \tag{6.24}$$

where

$$X\left(\widehat{B}_{aw}\right) := \begin{bmatrix} S\,\tilde{B}_0 + \widehat{B}_{aw} + \tilde{C}_0^T\,K\,W & S\,\tilde{B}_1 & \tilde{C}_1^T \end{bmatrix} \tag{6.25}$$

$$Y\left(\widehat{C}_{aw}, \widehat{D}_{aw}\right) := \begin{bmatrix} \left(\tilde{B}_0^T + \widehat{D}_{aw}^T\,\tilde{B}_2^T\right) H + W\,K\,\tilde{C}_0\,R\,H + W\,K\,\tilde{D}_{02}\,\widehat{C}_{aw} \\ \tilde{B}_1^T\,H \\ \tilde{C}_1\,R\,H + \tilde{D}_{12}\,\widehat{C}_{aw} \end{bmatrix} \tag{6.26}$$

3. *Compute the original matrices of the anti-windup compensator in the variable Θ as in (6.10) with the algebraic relations given by*

$$\begin{bmatrix} A_{aw} & B_{aw} \\ C_{aw} & D_{aw} \end{bmatrix} = \begin{bmatrix} N & S\,\tilde{B}_2 \\ 0_{n_v \times n_{aw}} & \mathbb{I}_{n_v} \end{bmatrix}^{\dagger} \left(\begin{bmatrix} \widehat{A}_{aw} & \widehat{B}_{aw} \\ \widehat{C}_{aw} & \widehat{D}_{aw} \end{bmatrix} - \begin{bmatrix} S\,\tilde{A}\,R\,H & 0_{n \times n_u} \\ 0_{n_v \times n_{aw}} & 0_{n_v \times n_u} \end{bmatrix} \right) \begin{bmatrix} M^T\,H & 0_{n_{aw} \times n_u} \\ 0_{n_u \times n_{aw}} & \mathbb{I}_{n_u} \end{bmatrix}^{\dagger} \tag{6.27}$$

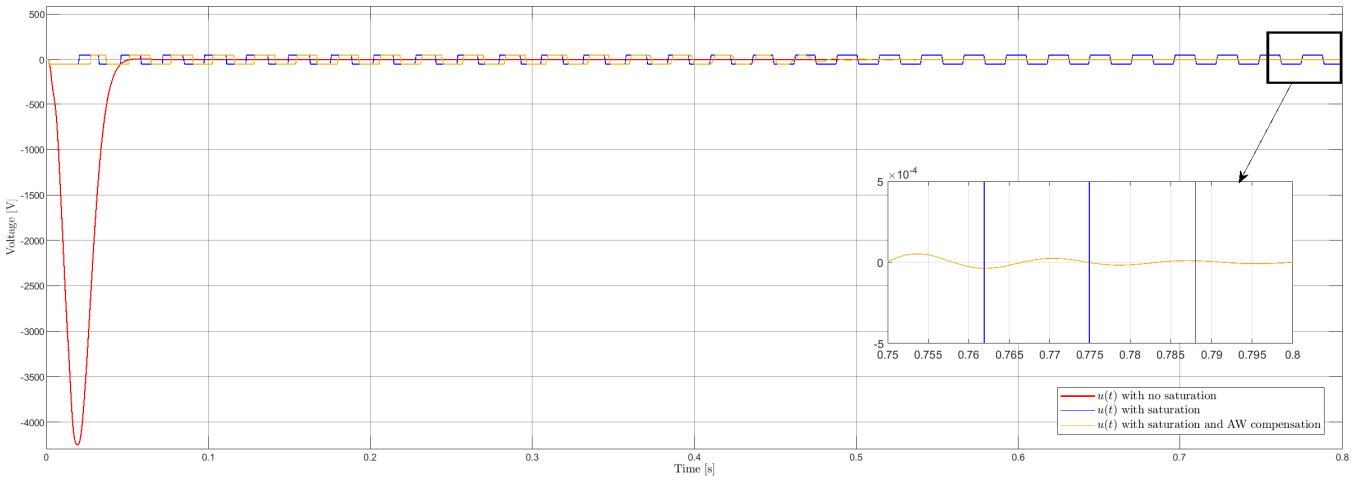

Figure 6.1. Different input signals' responses in the strict proper case for the flexible beam system with a H_∞ control law. In red the closed-loop with no saturation; in blue the system with saturated input without compensation; and in yellow the case with input saturated with anti-windup compensation.

An alternative way to be able to compute the second point of the Theorem 13, provided a solution for $\widehat{D}_{aw}$ from the LMI (6.21) in the first point, lies on the solution of the next BMIs

$$\tilde{A}^T\,S + S\,\tilde{A} + X(\widehat{B}_{aw})\,\Pi^{-1}\,X(\widehat{B}_{aw})^T < 0, \tag{6.28}$$

$$H^T\,(\tilde{A}\,R + R\,\tilde{A}^T)\,H + H^T\,\tilde{B}_2\,\widehat{C}_{aw} + \widehat{C}_{aw}^T\,\tilde{B}_2^T\,H + Y(\widehat{C}_{aw}, \widehat{D}_{aw})^T\,\Pi^{-1}\,Y(\widehat{C}_{aw}, \widehat{D}_{aw}) < 0, \tag{6.29}$$

where the inequalities (6.28) and (6.29) can be solved for the variables $\widehat{B}_{aw}$ and $\widehat{C}_{aw}$, respectively.

With the purpose of showing the benefit of these antiwindup compensators, we have applied such compensators into

the flexible beam, which was described in the section 3.6.1, in closed-loop with an optimal $\mathcal{H}_\infty$ controller, as described in Chapter 4. In the next plots, it is shown how the system is perturbed by a rectangular signal of amplitude $1\,\mathrm{m/sec^2}$ and length of $1\times10^{-3}\,\mathrm{sec}$. The control input responses for the flexible beam can be seen in the Figure 6.1, where we appreciate a peak at the beginning of the control action in the red signal, which represents the closed-loop system without saturation, in blue is the system with saturation, which takes a long time to control, and in yellow we see the saturated control input with the antiwindup compensator, which does not saturate the actuator; the controlled output responses are seen in the Figure 6.2, where once more we find in red the closed-loop response without saturation, in blue we see the closed-loop response with saturation, and in yellow the closed-loop response with the antiwindup compensator, which is able to damp the vibration in less than $0.5\,\mathrm{sec}$.

In the Figure 6.3, the performance of the non-strict proper case with the H_∞ control law is seen in the saturated input signal demanded by the system in yellow, where the unsaturated control input is seen in blue, and their comparison to the non-saturated control input, in red, is an unrealistic due to its voltage peak close to $4000\,\mathrm{V}$. The non-strictly proper case of the anti-windup compensator with the $\mathcal{H}_\infty$ control law outperforms its non-saturated counterpart by significantly reducing the peak value in the actuator signal. The latter exhibits an excessive high peak that can lead to actuator saturation and degrade the overall system performance. The Figure 6.4 shows the controlled output of the flexible beam, where in red the closed-loop with no input saturation; in blue the system with saturated input and without compensation; and in yellow the case with input saturated with anti-windup compensation. The system with antiwindup compensation stabilizes in around $0.8\,\mathrm{sec}$, while the saturated system without compensation looks like an open-loop response. Despite

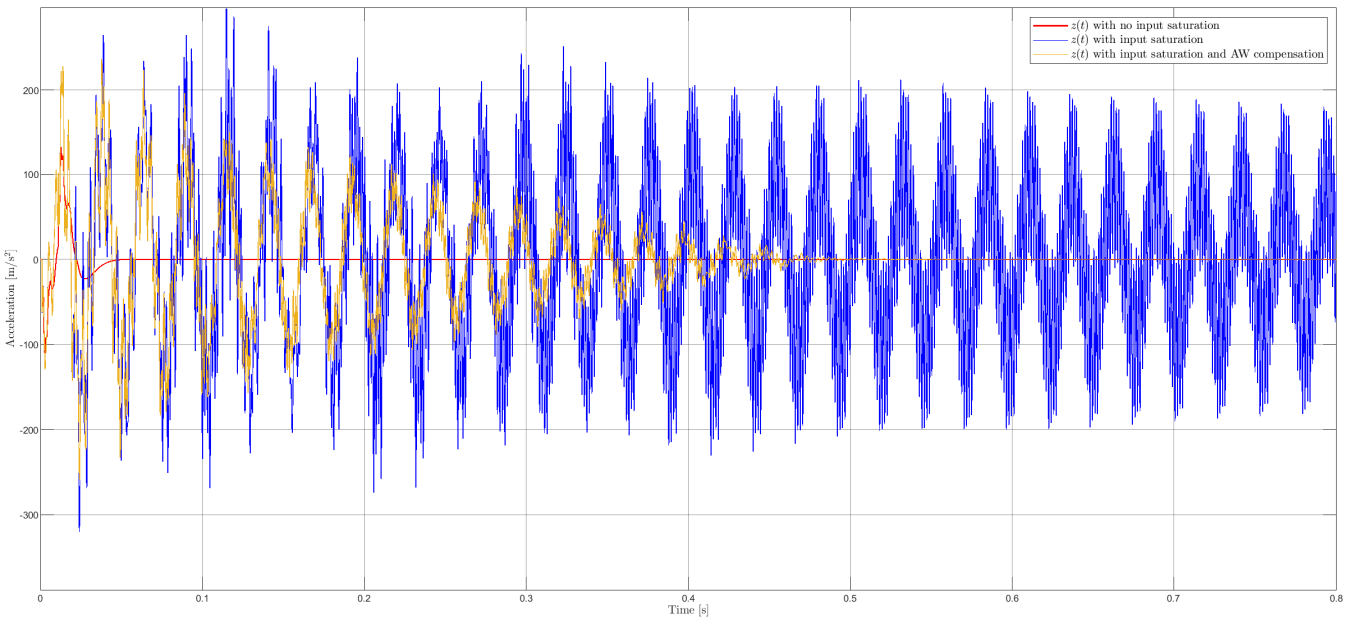

Figure 6.2. Different controlled outputs' responses in the strict proper case for the flexible beam system with a H_∞ control law. In red the closed-loop with no input saturation; in blue the system with saturated input and without compensation; and in yellow the case with input saturated with anti-windup compensation.

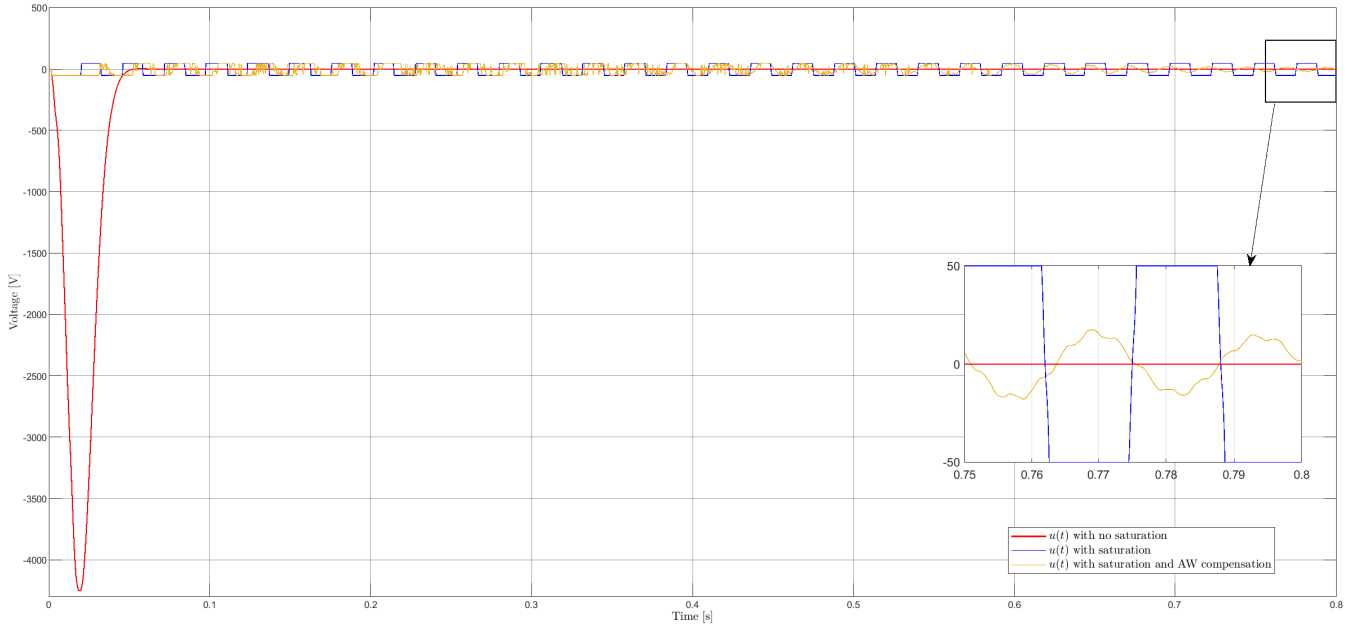

Figure 6.3. Different input signals' responses in the non-strict proper case for the flexible beam system with a H_∞ control law. In red the closed-loop with no saturation; in blue the system with saturated input without compensation; and in yellow the case with input saturated with anti-windup compensation.

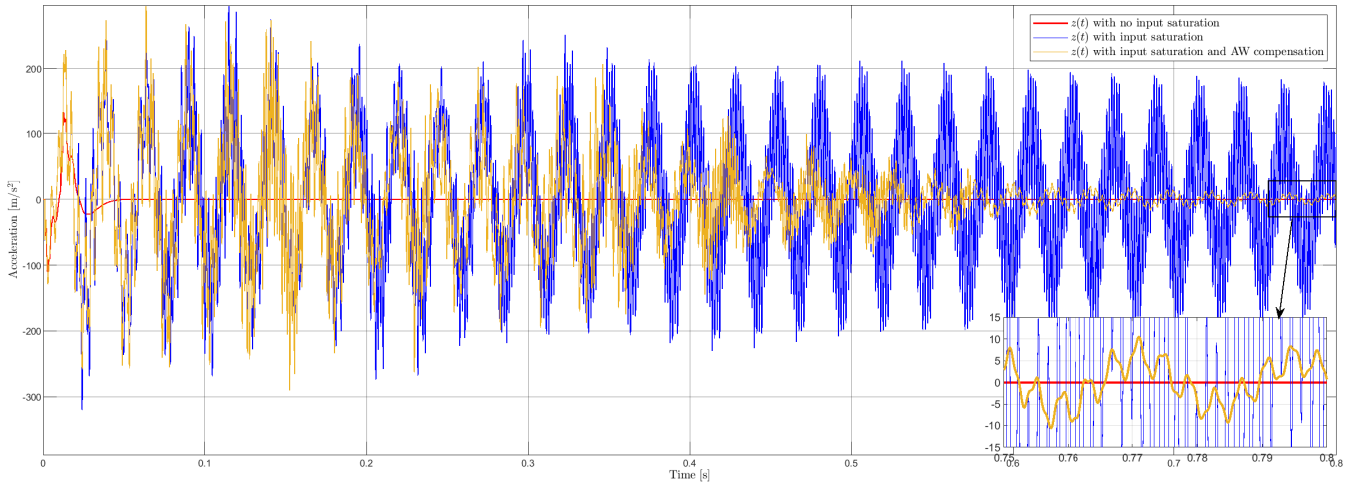

Figure 6.4. Different controlled outputs' responses in the non-strict proper case for the flexible beam system with a H_∞ control law. In red the closed-loop with no input saturation; in blue the system with saturated input and without compensation; and in yellow the case with input saturated with anti-windup compensation.

the unsaturated response is fast, as was mentioned before, it is unrealistic.

6.3 Approximation techniques

In the last chapters, we have shown two interesting and different control approaches to treat the control problem of vibration damping. We have treated a finite dimensional $\mathcal{H}_\infty$ controller, where there exist a $\mathcal{H}_\infty$-norm as a strict upper

bound from signals $w(t)$ to $z_a(t)$ as $\|\mathcal{P}_{zw}(s)\|_\infty < \beta$, where β can be interpreted as a disturbance rejection performance [155] and $\beta \leq 1$. In this case, $\beta = 0.9$ and an $\mathcal{H}_\infty$ LMI-based dynamic controller robust against the neglected modes upperly bounded as $\sigma_{max}(\Delta(s)) \leq \gamma^{-1}$, with $\gamma = 9.28912$.

Also, we have treated a QuasiPolynomial-Based (QPB) controller, where exist a set of parameters p_0, p_{r_0}, q_0, q_{r_0} and τ such that the proportional-delayed output-feedback controller (5.10) that in the structure's closed-loop equation (5.12) pointwise places three negative non-oscillating poles in the left-half side of the complex plane.

To illustrate the results mentioned above, the impulse response has been computed using the digital controllers counterparts of the computed controllers so far, whose structure is described by the equation (6.33), and the analysis and synthesis models.

In the Figure 6.5 the low-order synthesis model is observed, where the proportional-delayed approach in closed-loop, whose time-delays were approximated through the 1st order Padé approximation in Simulink, we get attenuations in the first, second and third vibration modes of $45.97\,\mathrm{dB}$, $36.93\,\mathrm{dB}$ and $26.17\,\mathrm{dB}$, respectively. In the other hand, suppressions of $35.61\,\mathrm{dB}$, $28.46\,\mathrm{dB}$ and $29.02\,\mathrm{dB}$ are obtained against the same amplitude peaks with the optimal $\mathcal{H}_\infty$ LMI-based approach. Robustness issues w.r.t. neglected modes in the synthesis model are well tackled, plus some vibration modes that are slightly damped outside of the frequency range of interest, which are shown in Figure 6.6.

To approximate the time-delays into LTI systems, we use two different approaches, the Padé approximation for continuous time systems and the Thiran approximation for discrete time systems.

6.3.1 Pade approximation

In the context of discrete systems and the Padé approximation, we can define a linear time-delay system as a rational function $N(s)/D(s)$, where $N(s)$ and $D(s)$ are polynomials of degrees p and q, respectively. The Padé approximation aims to approximate this rational function by a truncated power series that matches the first $p+q$ coefficients of the Taylor series expansion of the function around zero, while preserving its essential singularities. This allows us to approximate the exponential term of the function with a polynomial of degree $p+q$.

These systems with time-delays are described with a transfer function of the form

$$G(s) = \frac{N_0(s) + \sum_{i=0}^{M} N_i(s) \cdot e^{-\tau_i s}}{D_0(s) + \sum_{j=0}^{N} D_j(s) \cdot e^{-\tau_j s}} \tag{6.30}$$

where $N_0(s)$ and $D_0(s)$ are polynomials of degress p and q, respectively, $N_i(s)$ and $\tau_i > 0$ are a polynomial and a positive time-delay, respectively, for $i = 1, 2, \ldots, M$, and $D_j(s)$ and $\tau_j > 0$ are another polynomial and another positive time-delay, respectively, for $j = 1, 2, \ldots, N$.

H. Padé in his thesis, elaborated the properties of his approximants with special emphasis on the example of the exponential function: it is a beautiful example of how the approximants work in an ideal situation [10].

Theorem 14. *([136], [10], [143, p. 122]) Let $(p, q) \in \mathbb{N}$, where $\mathbb{N}$ is the set of integer numbers. Let $n_{p,q} \in \mathbb{Q}$ and $d_{q,p} \in \mathbb{Q}$, where $\mathbb{Q}$ is the set of all rational numbers, such that,*

$$N_{p,q}(s) := \sum_{i=0}^{p} \frac{p!}{(p-i)!} \cdot \frac{(p+q-i)!}{(p+q)!} \cdot \frac{s^i}{i!},$$

$$D_{p,q}(s) := \sum_{j=0}^{q} (-1)^j \frac{q!}{(q-j)!} \cdot \frac{(p+q-j)!}{(p+q)!} \cdot \frac{s^j}{j!}.$$

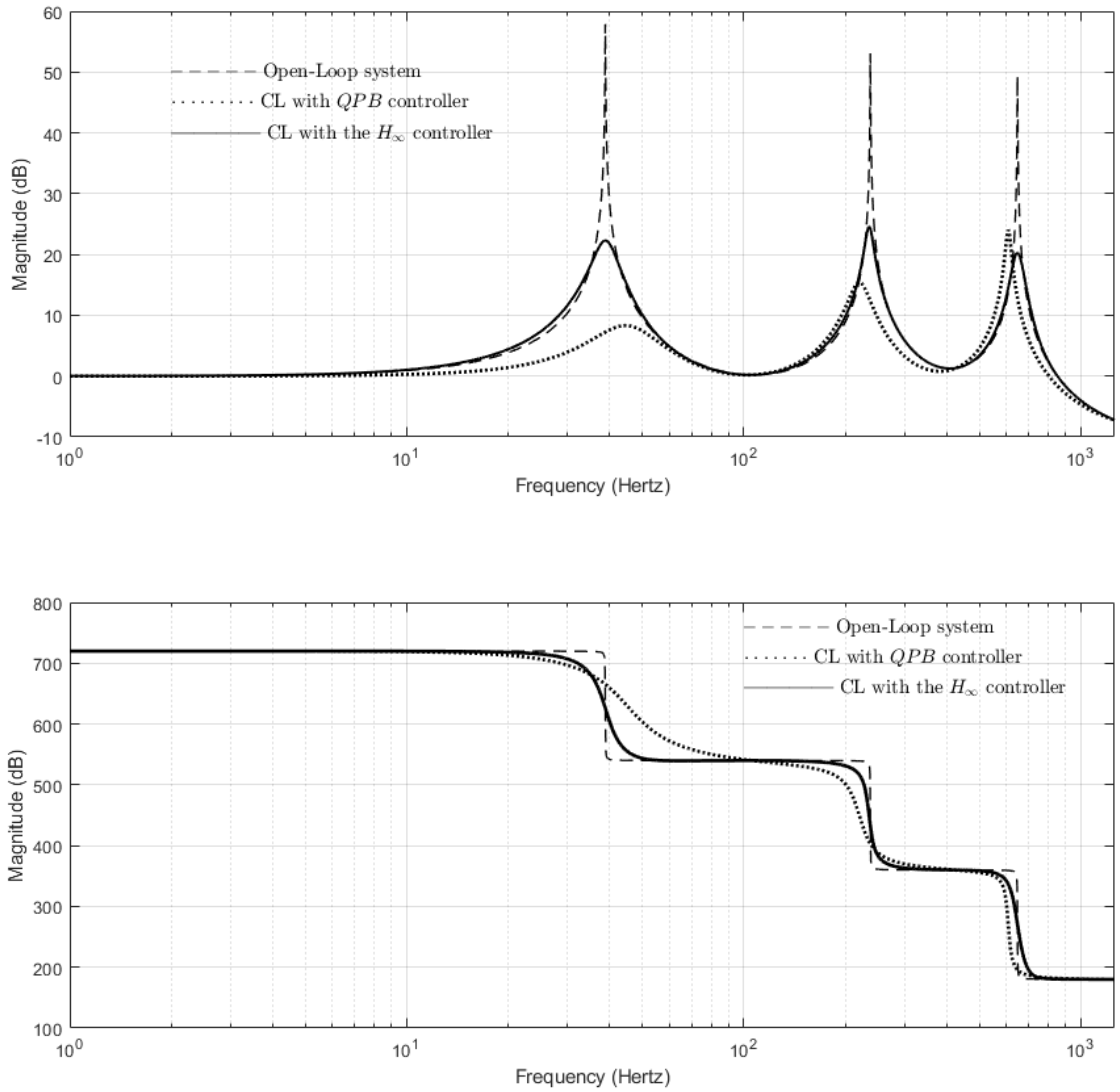

Figure 6.5. Comparison among the implemented controllers with the low-order synthesis model. The open-loop (dashed), the $\mathcal{H}_\infty$ LMI-based controller (solid) and the proportional-delayed controller (dotted).

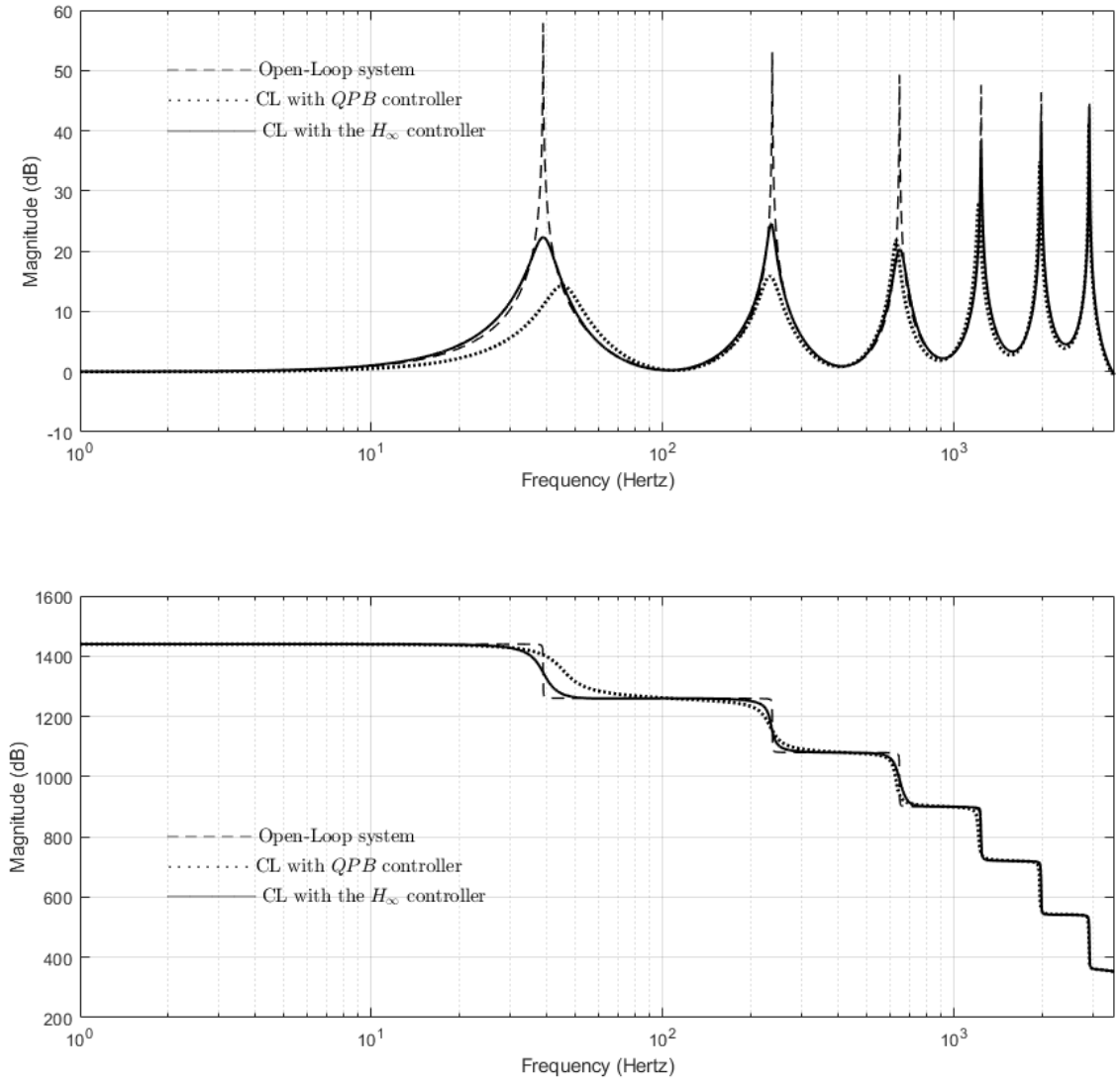

Figure 6.6. Comparison among the implemented controllers with the full-order analysis model. The open-loop (dashed), the $\mathcal{H}_\infty$ LMI-based controller (solid) and the proportional-delayed controller (dotted).

Then, e^s is approximated by

$$e^s \simeq \frac{N_{p,q}(s)}{D_{p,q}(s)},$$

which is called "Pade approximation".

6.3.2 Thiran approximation

The filter design technique developped forthwith is the Thiran approximation, whose main difference with the Pade approximation is that it generates a better phase matching.

Historically, in 1971, Thiran published a solution for a lowpass filter with maximally flat group delay response at the zero frequency [170].

Several applications in numerous fields of signal processing (communications, array processing, speech processing and music technology) use the fractional delay filters as a device for bandlimited interpolation between samples. Generally, recursive digital filters can meet the same frequency-domain specifications with a smaller number of multiplications than a FIR filter. However, a notorious limitation of such filter is its lack of linear phase characteristics, getting only constant group delays approximations. Designing Finite Impulse Response (FIR) filters is simplified because the filter coefficients correspond to the samples of the filter impulse response. As a result, the frequency domain specifications can be converted to the "coefficient domain" through the inverse discrete time Fourier transform. And this is not possible with the recursive filters [106].

The solution for the all-pass filter coefficients approximating the delay τ_D is

$$a_k = (-1)^k \begin{pmatrix} N \\ k \end{pmatrix} \prod_{n=0}^{N} \frac{\tau_D - N + n}{\tau_D - N + k + n} \tag{6.31}$$

for $k = 0, 1, \ldots, N$, where $\begin{pmatrix} N \\ k \end{pmatrix} = \frac{N!}{k!\,(N-k)!}$ is a binomial coefficient. As it always holds that $a_0 = 1$ the polynomial can be scaled as desired. Consequently, an N-th order all-pass filter thiran fractional delay filter has the form

$$\begin{aligned} F(z) &= \frac{z^{-N}\, D(z^{-1})}{D(z)}, \\ &= \frac{a_N\, z^N + a_{n-1}\, z^{-1} + \cdots + a_1\, z^{-(N-1)} + z^{-N}}{1 + a_1\, z^{-1} + \cdots + a_{N-1}\, z^{-(N-1)} + a_n\, z^{-N}} \end{aligned} \tag{6.32}$$

where $\tau_D = \frac{\tau}{T_s}$, with T_s denoting the time sample, $N = \mathrm{ceil}(D)$ being the filter order, z is a complex variable, and the numerator polynomial is a mirrored version of the denominator $D(z)$.

6.4 Sampled-data system implementation

The fact that many of the industrial controllers are digital provides a strong motivation for adapting or extending already known controllers design techniques. Usually, the signals of interest inside control systems are continuous-time signals, altogether with the performance specifications, whose properties are formulated in continuous-time. Modern control systems often use digital technology for controllers and sensors. Then, modern control systems involve both, continuous and discrete-time signals, in a continuous-time framework [38].

The fundamental operation of sampling is taken from continuous physical signals, such as position, velocity, or temper-

ature, and these values are used in order to compute the appropriate control action to be applied. Systems where discrete signals appear in some places and continuous signals occur in other parts are called sampled-data systems. In many ways the analysis of either a pure continuous-time system or a discrete-time system is simpler than that of a sampled-data system [55].

In the real world, the phenomena behaviour occurs in continuous-time and the whole computer operations occur on discrete electrical signals and, in order to properly study and analyse the system response against exogenous signals, it is necessary to consider the behaviour of the plant among the sampling instants.

The flexible cantilevered beam interconnection with the controller can be modelled in Simulink as it is shown in the diagram on Figure 6.7, where black- colored elements represent continuous time operations and signals, the green-colored blocks represent discrete-time manipulations with a time sampling $T_s = 50\mu\,\mathrm{sec}$, and the red-colored blocks represent the scopes of the model with a period of $500\,\mathrm{nsec}$; a low-pass filter is placed after the zero-order hold block, with a corner frequency $f_c = 1,000\ \mathrm{Hz}$ and a quantizer block is used to discretize the signal using a quantization algorithm that uses a round-to- nearest method to map signal values to quantized values at the output. At the output, the signal takes an stair-step shape. Mathematically this operation can be computed in Matlab/Simulink as `y = q * round(u/q)`, where `y` is the quantized output, `u` is the input signal, and `q` is the quantization interval. We used a quantization interval `q = 0.01` seconds.

The sampling and holding process takes place from a physical signal, say a position or velocity magnitude, we need a sensor to produce a voltage, typically in a linear characteristic way [84], and an analog-to-digital converter (commonly known as ADC or A/D) that converts the voltage into a digital number [189]. In order to provide the system with an accurate signal of the control law we use a sample-and-hold block (analogously, we have a physical sample-and-hold circuit) [202].

A lot of care has been devoted to the set up of this model in order to allow Simulink to execute it in an adequate and accurate way. This numeric scheme is based on two feedback loops that simulate the interaction between the host mechanical system and the discrete-time controllers. In the Figure 6.8, we see the sampled-data system, which embeds a discrete system into the real world, represented by a continuous-time.

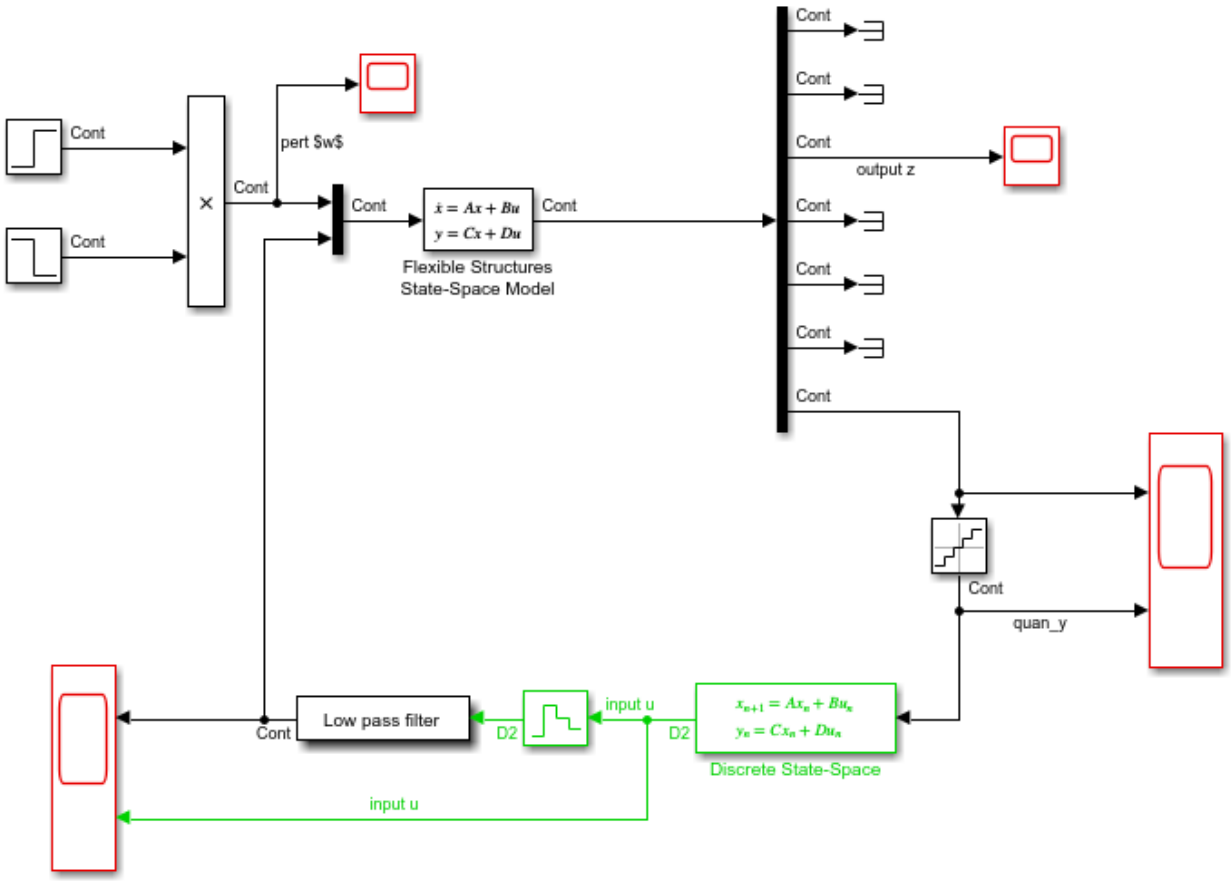

Figure 6.7. Sample-data system built on Simulink.

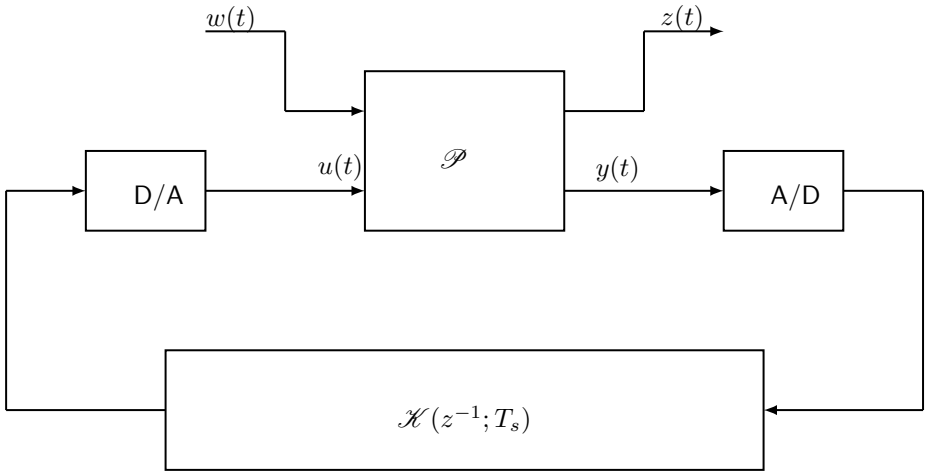

Figure 6.8. Block diagram of a discrete control as a sampled-data system.

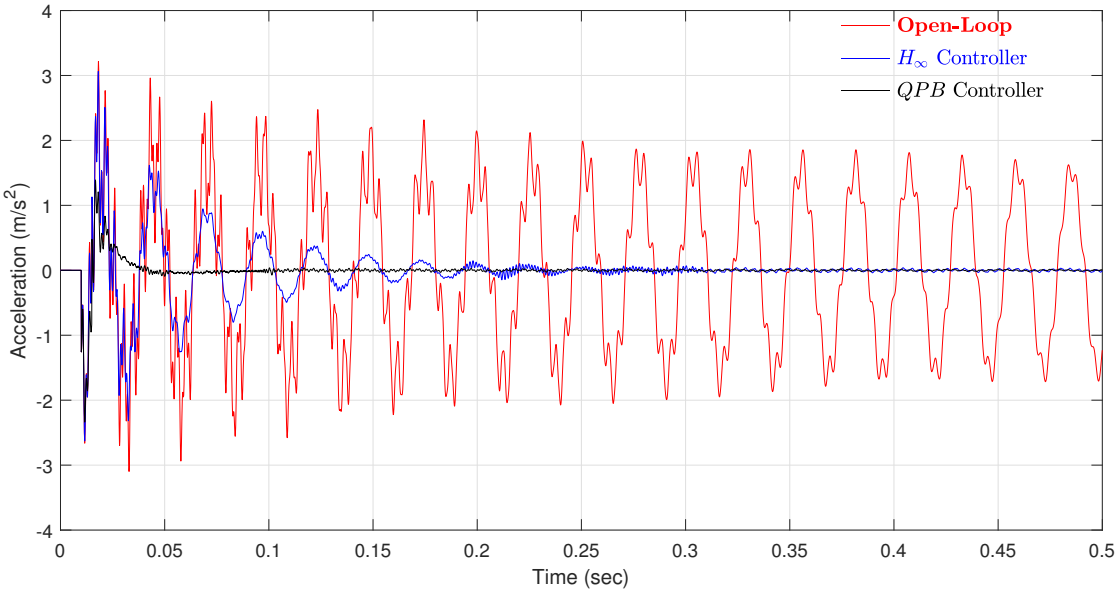

Figure 6.9. Impulse response to a perturbation $w = 1\,\mathrm{m/sec^2}$ to the flexible beam's synthesis model. The open-loop (red), the $\mathcal{H}_\infty$ LMI-based controller (blue) and the QPB controller (black).

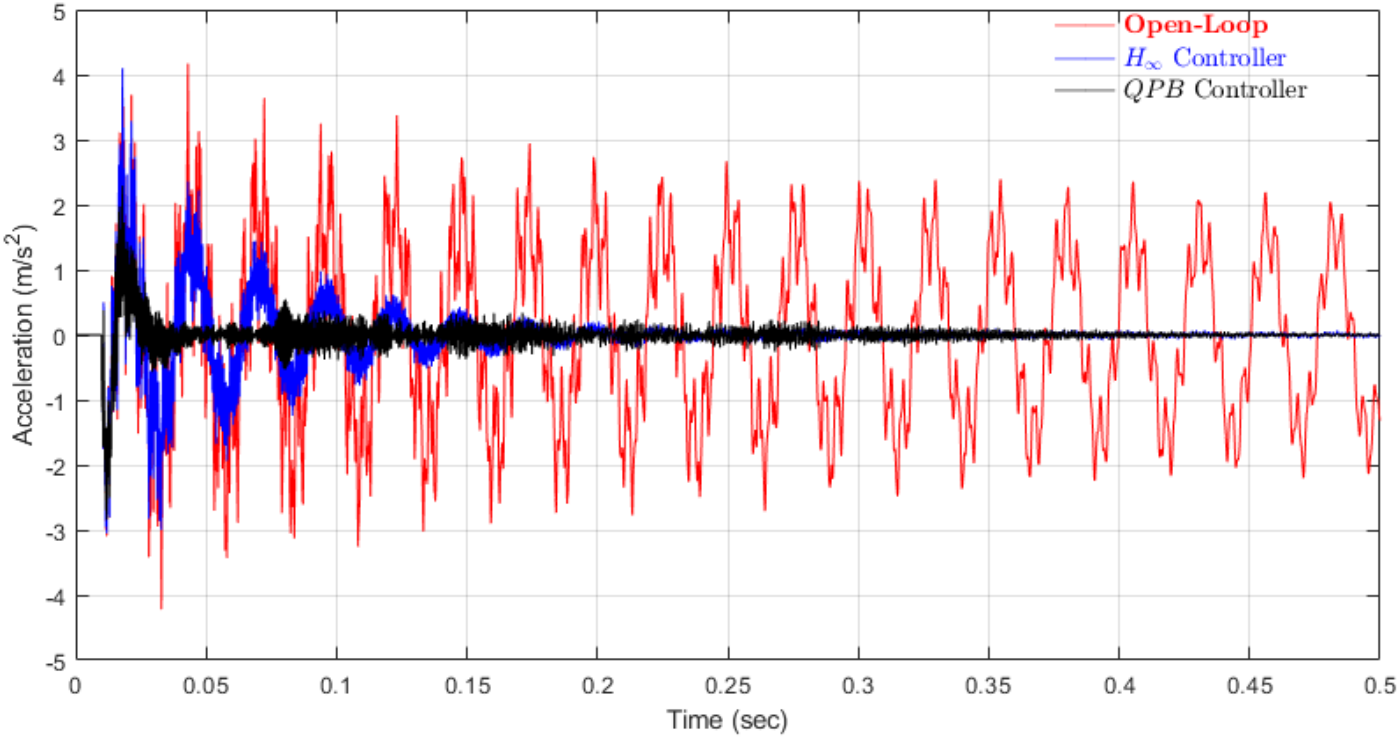

Figure 6.10. Impulse response to a perturbation $w = 1\,\mathrm{m/sec^2}$ to the flexible beam's analysis model. The open-loop (red), the $\mathcal{H}_\infty$ LMI-based controller (blue) and the QPB controller (black).

6.5 QPB Controller Simulation

The proportional-delayed controller was emulated through the tool Simulink of the software Matlab-R2019b, where the time-delay expressed in equation (5.10) is approximated using Thiran's method. The structure of the digital functions of

the controller can be appreciated in equation (6.33).

$$\mathcal{K}^*(z) = \frac{\Delta_q^*(z)}{\Delta_p^*(z)} = \frac{\sum_{k=0}^{\text{ceil}(\tau/T_{s_2})} \delta_{q_k}\, z^{-k}}{\sum_{k=0}^{\text{ceil}(\tau/T_{s_2})} \delta_{p_k}\, z^{-k}}. \tag{6.33}$$

The Figure 6.9 shows the impulse response of the synthesis model, where the open-loop, $\mathcal{H}_\infty$ and the QPB controllers are plotted in red, blue and black colors, respectively. With the $\mathcal{H}_\infty$ controller, an error $|e(t)| < 0.1\,\text{m/sec}^2$, implying a significant vibration reduction, can be checked after $0.22\,\text{sec}$, though with the QPB controller, a significant vibration reduction can be appreciated after $0.04\,\text{sec}$. The full-order (analysis) model, with the open-loop response, $\mathcal{H}_\infty$ and QPB closed-loop responses, in red, blue and black, respectively, are plotted in the Figure 6.10. The same error reference used before can be verified after $0.29\,\text{sec}$ and $0.175\,\text{sec}$, for the $\mathcal{H}_\infty$ and QPB controllers, separately.

6.6 Concluding remarks

This chapter treated the importance of the anti-windup compensators design over systems affected by control input saturations. Results on the numerical implementation of dynamic anti-windup compensators mixed with adequate linear controllers has been handled. To enhance the vibration suppression of a flexible cantilever beam, controlled by an $\mathcal{H}_\infty$ linear control law, a linear dynamic compensator of order 9 is synthetized with the given procedure. Time-domain simulations showed that the chosen configurations improve their impulse-response.

A general presentation of the sampled-data systems was given, as well as a brief explanation of the model's characteristics and the software properties of Simulink that allow us to perform it. These simulations will help us to implement these controllers in the real-time system called flexible cantilevered beam.

Chapter 7

Conclusions and Perspectives

In this work, we have addressed the problem of vibration attenuation in flexible structures, specifically for a flexible beam and a flexible axisymmetric membrane. We successfully applied the delay-stabilizing techniques, using a QPB (quasipolynomial-based) controllers, and demonstrated their effectiveness in reducing vibration. Furthermore, we compared the performance of our QPB controller with an optimal controller based on LMIs and norms minimization, highlighting the robustness attributes of the former. Throughout our study, we used linear finite-dimensional tools, focusing on the compatibility of our results with robustness considerations.

First, in Section 7.1, we present our conclusions based on the findings of our work. We summarize the main contributions of our study, highlighting the effectiveness of the rightmost root assignment technique in reducing vibrations, and discussing the strengths and weaknesses of different control design methods. Secondly, in Section 7.2, we provide perspectives on future work in this area. We identify potential directions for future research, including the application of our findings to other types of flexible structures.

Contents

7.1 Conclusions

In the Chapter 1 we have shown the reasons and the work done up to now, related to the active vibration control of different flexible structures using several approaches, keeping all along a special attention into the dynamic controllers by $\mathcal{H}_\infty$-based controllers applied in SISO systems, and the recent studies and advances related to the quasipolynomial-based controllers, that have been used in several works in SISO models.

In Chapter 2, we have introduced preliminaries of the diverse kind of systems, their mathematical features, and a variety of tools and definitions used throughout the work in the subsequent chapters. It is a brief literature review on analysis and control problems within the finite-dimensional systems.

In Chapter 3 we have introduced the flexible structures used, called "flexible beam" and "axisymmetric membrane", whose models have been studied and approximated through Finite-Element Method techniques, and then reduced accordingly for the controller synthesis, which left us with two different model sizes, the so-called analysis model and the synthesis model. The former used for the approximation of the whole structure including the neglected vibration modes in the controller synthesis, and the latter used for the controllers' synthesis and simulation results.

Chapter 4 serves to present useful results concerning the stabilization and control with an $\mathcal{H}_\infty$ control technique through the use of a theorem involving Linear Matrix Inequalities. Altogether, we present and solve the control problem using a regional pole placement by a region in the complex plane described by the intersection of several LMIs, achieving in this way an adequate vibration control. Furthermore, the discretization and the emulation of the continuous-time system interconnected with the discrete-time dynamic controller is carried-out for the sake of the approximation to the real-time sampled-data system.

In Chapter 5 the QPB controller, which is a PPP (partial pole placement) technique used for placing several non-oscilating poles in the negative real axis of the complex-plane is introduced. The basics about the classical time-delay systems with its corresponding possible approximations, by Padé or Thiran approximations, whose results are appropriate for continuous-time and discrete-time systems, respectively. Also, some final remarks about the frequency-domain representations and the spectrum distribution on time-delays are emphasized before introducing the QPB control technique involving a scalar time-delay.

In the Chapter 6, an exposition of two extensions to the QPB and $\mathcal{H}_\infty$ controller have been exposed. The first extension is the handling of the case where saturation arrives into the actuators, which in practice have upper bounds for the amount of voltage that they can deliver. In this way, despite the system's order is enlarged, antiwindup compensators are developed to avoid the risk of winding-up the closed-loop system. The second extension is the application as a sampled-data system, where the discrete model is used with its corresponding approximation into a discrete-time system with its own interconnection into the continuous-time plant (thus, forming a sampled-data system), with an adequate sampling time, which is smaller than the computed time-delay in the computed QPB controller. Characteristical data analysis in the form of plots in the time-domain is shown.

7.2 Perspectives

The goal of this work is to spread the use of time-delay based control techniques into the control of LTI systems, specifically the active vibration control of flexible structures, presented in Chapter 5, with results shown numerically. The evaluation of the stabilizing capabilities of quasipolynomial-based controllers has resulted attractive for these flexible structures. These systems are infinite dimensional and the Finite Element Method allows us to approximate their models as a finite dimensional system, composed of an appropriate number of vibration modes. With the help of a reduced-order model, we are able to synthetize the desired controllers.

As a second point, this thesis has permitted a better appreciation of these controllers benefits through a comparison of $\mathcal{H}_\infty$-based controlling methods and by the Quasi-Polynomial-based controlling methods. The tools for the calculation and computation of these controllers are well adapted to the characteristics of the system. These calculation tools allow, for example, the trace of plots that represent the evolution of their behavior in the time-domain, as well as the frequency-domain. The simplicity of the quasipolynomial based controllers has been highlighted, and its impact can be spreaded in industrial applications, for which further improvement of their design has to be done.

Addressing the behavior of time-delays and their effect over the flexible structures of distributed parameters is an option to traditional stabilizing controllers, and its simplicity and lower computational complexity make them an appealing method for future researches. The effects of different sampling times for the discrete systems deserves further research.

These results are convincing and reassuring for future extensions of this research. In future works, a subject that deserves to be deeply analysed is the application of these methods for systems with parametric uncertainties and its robustness properties for wider frequency spans, as well as for non-linear systems.

Acknowledgment

Ricardo Falcón-Prado is a doctoral student from l'Ecole Doctorale Sciences et Technologies de l'Information et de la Communication (STIC) and received the fellowship 708010 from CONACYT.

Bibliography

[1] M. K. Al-Solihat and M. Nahon. Flexible multibody dynamic modeling of a floating wind turbine. *International Journal of Mechanical Sciences*, 142:518–529, 2018.

[2] J. P. Amezquita-Sanchez, A. Dominguez-Gonzalez, R. Sedaghati, R. de Jesus Romero-Troncoso, and R. A. Osornio-Rios. Vibration control on smart civil structures: A review. *Mechanics of Advanced Materials and Structures*, 21 (1):23–38, 2014.

[3] S. Amrane, F. Bedouhene, I. Boussaada, and S.-I. Niculescu. On qualitative properties of low-degree quasipolynomials: further remarks on the spectral abscissa and rightmost-roots assignment. *Bulletin mathématique de la Société des Sciences Mathématiques de Roumanie*, 61(4):361–381, 2018.

[4] B. D. Anderson and Y. Liu. Controller reduction: concepts and approaches. In *1987 American Control Conference*, pages 1–9. IEEE, 1987.

[5] R. J. Anderson and M. W. Spong. Bilateral control of teleoperators with time delay. In *Proceedings of the 1988 IEEE International Conference on Systems, Man, and Cybernetics*, volume 1, pages 131–138. IEEE, 1988.

[6] S. Angulo, R. Márquez, and M. Bernal. Quasi-polynomial-based robust stability of time-delay systems can be less conservative than lyapunov–krasovskii approaches. *IEEE Transactions on Automatic Control*, 65(7):3164–3169, 2019.

[7] B. Aruna and R. Devanathan. Necessary and sufficient condition for modified nevanlinna-pick interpolation for closed-loop pole placement. *Control Theory and Technology*, 15(1):58–68, 2017.

[8] H. Arvin. Free vibration analysis of micro rotating beams based on the strain gradient theory using the differential transform method: Timoshenko versus euler-bernoulli beam models. *European Journal of Mechanics-A/Solids*, 65: 336–348, 2017.

[9] K. J. Astrom and L. Rundqwist. Integrator windup and how to avoid it. In *1989 American Control Conference*, pages 1693–1698. IEEE, 1989.

[10] G. A. Baker, G. A. Baker Jr, G. Baker, P. Graves-Morris, and S. S. Baker. *Pade Approximants: Encyclopedia of Mathematics and It's Applications, Vol. 59 George A. Baker, Jr., Peter Graves-Morris*, volume 59. Cambridge University Press, 1996.

[11] W. A. Baker, S. C. Schneider, and E. E. Yaz. Robust regional eigenvalue assignment by dynamic state-feedback control for nonlinear continuous-time systems. In *2015 54th IEEE Conference on Decision and Control (CDC)*, pages 6903–6908. IEEE, 2015.

[12] M. J. Balas. Modal control of certain flexible dynamic systems. *SIAM Journal on Control and Optimization*, 16(3): 450–462, 1978.

[13] S. Barnett. *Polynomials and linear control systems*. Marcel Dekker, Inc., 1983.

[14] H. Baruh and S. Ratan. Damage detection in flexible structures. *Journal of Sound and Vibration*, 166(1):21–30, 1993.

[15] A. Baz, K. Imam, and J. McCoy. Active vibration control of flexible beams using shape memory actuators. *Journal of Sound and Vibration*, 140(3):437–456, 1990.

[16] J. R. Beddington and R. M. May. Time delays are not necessarily destabilizing. *Mathematical Biosciences*, 27(1-2): 109–117, 1975.

[17] F. Bedouhene, I. Boussaada, and S.-I. Niculescu. Real spectral values coexistence and their effect on the stability of time-delay systems: Vandermonde matrices and exponential decay. *Comptes Rendus. Mathématique*, 358(9-10): 1011–1032, 2020.

[18] R. E. Bellman and K. L. Cooke. *Differential-difference Equations, by R: Bellman and Kl Cooke*. Academic Press, 1963.

[19] R. Belotti and D. Richiedei. Pole assignment in vibrating systems with time delay: An approach embedding an a-priori stability condition based on linear matrix inequality. *Mechanical Systems and Signal Processing*, 137:106396, 2020.

[20] B. Bhikkaji, S. R. Moheimani, and I. R. Petersen. Multivariable integral control of resonant structures. In *2008 47th IEEE Conference on Decision and Control*, pages 3743–3748. IEEE, 2008.

[21] F. C. Bolat and S. Sivrioğlu. H2, hinfinity and h2/hinfinity control of elastic beam vibrations using piezoelectric actuator. *International Journal of Applied Mathematics Electronics and Computers*, 5(3):53–61, 2017.

[22] J. Bontsema and R. F. Curtain. A note on spillover and robustness for flexible systems. *IEEE Transactions on Automatic Control*, 33(6):567–569, 1988.

[23] J. Bontsema, R. F. Curtain, and J. M. Schumacher. Comparison of some partial differential equation models of flexible structures. *IFAC Proceedings Volumes*, 20(1):287–292, 1987.

[24] I. Boussaada and S.-I. Niculescu. Tracking the algebraic multiplicity of crossing imaginary roots for generic quasipolynomials: A vandermonde-based approach. *IEEE Transactions on Automatic Control*, 61(6):1601–1606, 2015.

[25] I. Boussaada and S.-I. Niculescu. Characterizing the codimension of zero singularities for time-delay systems. *Acta Applicandae Mathematicae*, 145(1):47–88, 2016.

[26] I. Boussaada and S.-I. Niculescu. On the dominancy of multiple spectral values for time-delay systems with applications. *IFAC-PapersOnLine*, 51(14):55–60, 2018.

[27] I. Boussaada, D. Irofti, and S.-I. Niculescu. Characterizing the multiplicity of spectral values for time-delay systems.

[28] I. Boussaada, H. U. Unal, and S.-I. Niculescu. Multiplicity and stable varieties of time-delay systems: A missing link. In *22nd International Symposium on Mathematical Theory of Networks and Systems (MTNS)*, 2016.

[29] I. Boussaada, S.-I. Niculescu, S. Tliba, and T. Vyhlídal. On the Coalescence of Spectral Values and its Effect on the Stability of Time-Delay Systems: Application to Active Vibration Control. *Procedia IUTAM*, 22:75–82, 2017.

[30] I. Boussaada, S.-I. Niculescu, and K. Trabelsi. Toward a decay rate assignment based design for time-delay systems with multiple spectral values. In *Proceeding of the 23rd International Symposium on Mathematical Theory of Networks and Systems*, pages 864–871, 2018.

[31] I. Boussaada, S. Tliba, S.-I. Niculescu, H. U. Ünal, and T. Vyhlídal. Further remarks on the effect of multiple spectral values on the dynamics of time-delay systems. application to the control of a mechanical system. *Linear Algebra and its Applications*, 542:589–604, 2018.

[32] I. Boussaada, S.-I. Niculescu, A. El Ati, R. Pérez-Ramos, and K. L. Trabelsi. Multiplicity-induced-dominancy in parametric second-order delay differential equations: Analysis and application in control design. *ESAIM: Control, Optimisation and Calculus of Variations*, 2019.

[33] I. Boussaada, G. Mazanti, S.-I. Niculescu, J. Huynh, F. Sim, and M. Thomas. Partial pole placement via delay action: A python software for delayed feedback stabilizing design. In *2020 24th International Conference on System Theory, Control and Computing (ICSTCC)*, pages 196–201. IEEE, 2020.

[34] S. Boyd, L. El Ghaoui, E. Feron, and V. Balakrishnan. *Linear Matrix Inequalities in System and Control Theory*, volume 15. SIAM, 1994.

[35] A. Cavallo, G. De Maria, C. Natale, and S. Pirozzi. An advanced system for vibration control of flexible structures. *IFAC Proceedings Volumes*, 41(2):11841–11846, 2008.

[36] T.-S. Chang and A. N. Gündeş. Mimo pid controller synthesis with closed-loop pole assignment. In *Advances in Computational Algorithms and Data Analysis*, pages 423–437. Springer, 2009.

[37] L. Chen, Y. Yan, C. Mu, and C. Sun. Characteristic model-based discrete-time sliding mode control for spacecraft with variable tilt of flexible structures. *IEEE/CAA Journal of Automatica Sinica*, 3(1):42–50, 2016.

[38] T. Chen and B. A. Francis. *Optimal sampled-data control systems*. Springer Science & Business Media, 2012.

[39] M. Chilali and P. Gahinet. $\mathcal{H}_\infty$ design with pole placement constraints: an LMI approach. *IEEE Transactions on Automatic Control*, 41(3):358–367, 1996.

[40] M. Chilali, P. Gahinet, and P. Apkarian. Robust pole placement in lmi regions. *IEEE transactions on Automatic Control*, 44(12):2257–2270, 1999.

[41] I. Collins, M. Hossain, W. Dettmer, and I. Masters. Flexible membrane structures for wave energy harvesting: A review of the developments, materials and computational modelling approaches. *Renewable and Sustainable Energy Reviews*, 151:111478, 2021.

[42] J. A. Cook and B. K. Powell. Modeling of an internal combustion engine for control analysis. *IEEE Control Systems Magazine*, 8(4):20–26, 1988.

[43] P. Coustal and J.-M. Michelin. Industrial application of an h-infinity design method for flexible structures h/sub/spl infin. *IEEE Control Systems Magazine*, 14(4):49–54, 1994.

[44] A. Dixit and H. S. Mali. Modeling techniques for predicting the mechanical properties of woven-fabric textile composites: a review. *Mechanics of composite Materials*, 49(1):1–20, 2013.

[45] T. Dong and N. H. Kim. Cost-effectiveness of structural health monitoring in fuselage maintenance of the civil aviation industry. *Aerospace*, 5(3):87, 2018.

[46] W. Dunn. *Introduction to instrumentation, sensors, and process control*. Artech, 2005.

[47] P. P. Dyke. *An introduction to Laplace transforms and Fourier series*. Springer, 2014.

[48] Y. Ebihara, D. Peaucelle, and D. Arzelier. *S-variable approach to LMI-based robust control*. Springer, 2015.

[49] M. Ericka, D. Vasic, F. Costa, G. Poulin, and S. Tliba. Energy harvesting from vibration using a piezoelectric membrane. In *Journal de Physique IV (Proceedings)*, volume 128, pages 187–193. EDP sciences, 2005.

[50] D. M. Etter, D. C. Kuncicky, and D. W. Hull. *Introduction to MATLAB*. Prentice Hall, 2002.

[51] R. Falcón-Prado, S. Tliba, I. Boussaada, and S.-I. Niculescu. Active vibration control of axisymmetric membrane through partial pole placement. *IFAC-PapersOnLine*, 54(18):58–63, 2021.

[52] S. Farchaly and M. Shebl. Exact frequency and mode shape formulae for studying vibration and stability of timoshenko beam system. *Journal of sound and vibration*, 180(2):205–227, 1995.

[53] J. Feng, X. He, S. Zhang, and G. Li. Vibration suppression and angle tracking of a fire-rescue ladder. *Nonlinear Dynamics*, 100(3):2365–2380, 2020.

[54] E. Feron, P. Apkarian, and P. Gahinet. Analysis and synthesis of robust control systems via parameter-dependent lyapunov functions. *IEEE Transactions on Automatic Control*, 41(7):1041–1046, 1996.

[55] G. F. Franklin, J. D. Powell, M. L. Workman, et al. *Digital control of dynamic systems*, volume 3. Addison-wesley Reading, MA, 1998.

[56] H. Freedman and Y. Kuang. Stability switches in linear scalar neutral delay equations. *Funkcialaj Ekvacioj*, 34(1): 187–209, 1991.

[57] E. Fridman. *Introduction to time-delay systems: Analysis and control*. Springer, 2014.

[58] P. Gahinet. $\mathcal{H}_\infty$ design with pole placement constraints: An lmi approach. *IEEE Trans. on Auto. Cont.*, 45(3): 358–367, 1996.

[59] P. Gahinet and P. Apkarian. A linear matrix inequality approach to H_∞ control. *International journal of robust and nonlinear control*, 4(4):421–448, 1994.

[60] S. Galeani, S. Tarbouriech, M. Turner, and L. Zaccarian. A tutorial on modern anti-windup design. In *2009 European Control Conference (ECC)*, pages 306–323. IEEE, 2009.

[61] L. Gao. Robot manipulator control using decentralized linear time-invariant time-delayed joint controllers. In *Proceedings., IEEE International Conference on Robotics and Automation*, pages 2070–2075. IEEE, 1990.

[62] W. K. Gawronski. *Advanced structural dynamics and active control of structures*. Springer, 2004.

[63] M. Géradin and D. J. Rixen. *Mechanical vibrations: theory and application to structural dynamics*. John Wiley & Sons, 2014.

[64] F. Golnaraghi and B. C. Kuo. *Automatic control systems*. McGraw-Hill Education, 2017.

[65] G. H. Golub and C. F. Van Loan. *Matrix computations*, volume 3. JHU press, 2013.

[66] M. Green and D. Limebeer. Linear robust control prentice hall. *Englewood Cliffs, New Jersey*, 7632, 1995.

[67] K. Gu and S.-I. Niculescu. Survey on recent results in the stability and control of time-delay systems. *J. Dyn. Sys., Meas., Control*, 125(2):158–165, 2003.

[68] K. Gu, J. Chen, and V. L. Kharitonov. *Stability of time-delay systems*. Springer Science & Business Media, 2003.

[69] R. Güçlü. Active control of seat vibrations of a vehicle model using various suspension alternatives. *Turkish Journal of Engineering and Environmental Sciences*, 27(6):361–374, 2003.

[70] S. Gutman and E. Jury. A general theory for matrix root-clustering in subregions of the complex plane. *IEEE Transactions on Automatic Control*, 26(4):853–863, 1981.

[71] M. S. Hadi, I. Z. Darus, M. H. Ab. Talib, H. M. Yatim, and M. O. Tokhi. Vibration suppression of the horizontal flexible plate using proportional–integral–derivative controller tuned by particle swarm optimization. *Journal of Low Frequency Noise, Vibration and Active Control*, page 1461348420934636, 2021.

[72] J. K. Hale. Functional differential equations. In *Analytic theory of differential equations*, pages 9–22. Springer, 1971.

[73] J. K. Hale and S. M. V. Lunel. *Introduction to functional differential equations*, volume 99. Springer Science & Business Media, 2013.

[74] K. M. Hangos, J. Bokor, and G. Szederkényi. *Analysis and control of nonlinear process systems*. Springer Science & Business Media, 2006.

[75] T. He, G. G. Zhu, S. S.-M. Swei, and W. Su. Smooth-switching lpv control for vibration suppression of a flexible airplane wing. *Aerospace Science and Technology*, 84:895–903, 2019.

[76] W. He and J. Liu. *Active vibration control and stability analysis of flexible beam systems*. Springer, 2019.

[77] W. He, X. Mu, Y. Chen, X. He, and Y. Yu. Modeling and vibration control of the flapping-wing robotic aircraft with output constraint. *Journal of Sound and Vibration*, 423:472–483, 2018.

[78] W. He, W. Xiang, X. He, and G. Li. Boundary vibration control of a floating wind turbine system with mooring lines. *Control Engineering Practice*, 101:104423, 2020.

[79] G. Herrmann, M. C. Turner, and I. Postlethwaite. Discrete-time and sampled-data anti-windup synthesis: stability and performance. *International Journal of Systems Science*, 37(2):91–113, 2006.

[80] J. R. Høgsberg and S. Krenk. Linear control strategies for damping of flexible structures. *Journal of Sound and Vibration*, 293(1-2):59–77, 2006.

[81] A. S. Holland. *Introduction to the theory of entire functions*. Academic Press, 1974.

[82] B. How, S. Ge, and Y. Choo. Active control of flexible marine risers. *Journal of Sound and Vibration*, 320(4-5): 758–776, 2009.

[83] T. Insperger. Stability analysis of periodic delay-differential equations modelling machine tool chatter: Phd dissertation. *Budapest University of Technology and Economics*, 2002.

[84] T. Islam and S. Mukhopadhyay. Linearization of the sensors characteristics: a review. *International Journal on Smart Sensing & Intelligent Systems*, 12(1), 2019.

[85] H. Janocha et al. *Adaptronics and smart structures*. Springer, 1999.

[86] Q. Jian, Y.-s. He, M.-h. Wang, B.-y. LI, and Z. Ji. Numerical study of dynamic behavior of flexible pipes in deep sea mining. *Ocean Engineering*, 19(2):59–64, 2001.

[87] Y.-T. Juang. A fundamental multivariable robustness theorem for robust eigenvalue assignment. *IEEE transactions on automatic control*, 33(10):940–941, 1988.

[88] A. Kaddar and H. T. Alaoui. Hopf bifurcation analysis in a delayed kaldor-kalecki model of business cycle. *Nonlinear Analysis: Modelling and Control*, 13(4):439–449, 2008.

[89] T. Kailath. *Linear systems*, volume 156. Prentice-Hall Englewood Cliffs, NJ, 1980.

[90] M. A. Kakanov, O. I. Borisov, and A. A. Pyrkin. Lmi-based design of output robust controller with static anti-windup. In *2020 International Conference Nonlinearity, Information and Robotics (NIR)*, pages 1–5. IEEE, 2020.

[91] H. R. Karimi. *Vibration Control and Actuation of Large-Scale Systems*. Academic Press, 2020.

[92] M. H. Kashani, A. Hosseini, F. Sassani, F. Ko, and A. Milani. Understanding different types of coupling in mechanical behavior of woven fabric reinforcements: A critical review and analysis. *Composite Structures*, 179:558–567, 2017.

[93] J. Kautsky, N. K. Nichols, and P. Van Dooren. Robust pole assignment in linear state feedback. *International Journal of control*, 41(5):1129–1155, 1985.

[94] K. Kawamura and Y. Ishida. Approach to new model recovery anti-windup scheme with pid controller. In *2015 3rd International Conference on Artificial Intelligence, Modelling and Simulation (AIMS)*, pages 208–212. IEEE, 2015.

[95] S. Khot, N. P. Yelve, R. Tomar, S. Desai, and S. Vittal. Active vibration control of cantilever beam by using pid based output feedback controller. *Journal of Vibration and Control*, 18(3):366–372, 2012.

[96] S. Knorn and B. Besselink. Scalable robustness of interconnected systems subject to structural changes. *IFAC-PapersOnLine*, 53(2):3373–3378, 2020.

[97] V. Kolmanovskii and A. Myshkis. *Introduction to the theory and applications of functional differential equations*, volume 463. Springer Science & Business Media, 2013.

[98] V. B. Kolmanovskii and V. R. Nosov. *Stability of functional differential equations*, volume 180. Elsevier, 1986.

[99] L. Komzsik. *What every engineer should know about computational techniques of finite element analysis*. CRC Press, 2019.

[100] V. A. Koptsik and I. Rez. Pierre curie's works in the field of crystal physics (on the one-hundredth anniversary of the discovery of the piezoelectric effect). *Soviet Physics Uspekhi*, 24(5):426, 1981.

[101] M. V. Kothare, P. J. Campo, M. Morari, and C. N. Nett. A unified framework for the study of anti-windup designs. *Automatica*, 30(12):1869–1883, 1994.

[102] Y. Kuang. *Delay differential equations: with applications in population dynamics*. Academic press, 1993.

[103] P. K. Kuhfittig. *Introduction to the Laplace transform*, volume 8. Springer Science & Business Media, 2013.

[104] S. M. Kuo and D. R. Morgan. Active noise control: a tutorial review. *Proceedings of the IEEE*, 87(6):943–973, 1999.

[105] O. Y. Kushel. Geometric properties of lmi regions. *arXiv e-prints*, pages arXiv–1910, 2019.

[106] T. I. Laakso. Splitting the unit delay. *IEEE signal processing magazine*, 13(1):30–60, 1996.

[107] F. Lacaze, A. Paknejad, D. Remond, and S. Chesne. Improved integral force feedback controllers for lightweight flexible structures. *Journal of Vibration and Control*, page 1077546320974549, 2020.

[108] M. A. Laughton and M. G. Say. *Electrical engineer's reference book*. Elsevier, 2013.

[109] Z. Li, L. Wu, H. Ren, and H. Yu. Kinematic comparison of surgical tendon-driven manipulators and concentric tube manipulators. *Mechanism and machine theory*, 107:148–165, 2017.

[110] G.-R. Liu and S. S. Quek. *The finite element method: a practical course*. Butterworth-Heinemann, 2013.

[111] K. Lochan, B. K. Roy, and B. Subudhi. A review on two-link flexible manipulators. *Annual Reviews in Control*, 42: 346–367, 2016.

[112] J. J. Loiseau. Invariant factors assignment for a class of time-delay systems. *Kybernetika*, 37(3):265–275, 2001.

[113] J. Lozier. A steady state approach to the theory of saturable servo systems. *IRE Transactions on Automatic Control*, 1(1):19–39, 1956.

[114] A. Manitius and A. Olbrot. Finite spectrum assignment problem for systems with delays. *IEEE transactions on Automatic Control*, 24(4):541–552, 1979.

[115] S. R. Marjani and D. Younesian. Suppression of train wheel squeal noise by shunted piezoelectric elements. *International Journal of Structural Stability and Dynamics*, 17(02):1750027, 2017.

[116] M. B. S. Márquez, I. Boussaada, H. Mounier, and S.-I. Niculescu. Neutral-type time-delay systems: Theoretical background. In *Analysis and Control of Oilwell Drilling Vibrations*, pages 57–82. Springer, 2015.

[117] MATLAB. *MATLAB Function Reference (R2021b)*. The MathWorks Inc., Natick, Massachusetts, 2021.

[118] G. Mazanti, I. Boussaada, and S.-I. Niculescu. Multiplicity-induced-dominancy for delay-differential equations of retarded type. *Journal of Differential Equations*, 286:84–118, 2021.

[119] W. Michiels and S.-I. Niculescu. *Stability and stabilization of time-delay systems: an eigenvalue-based approach*. SIAM, 2007.

[120] W. Michiels and S.-I. Niculescu. *Stability, control, and computation for time-delay systems: an eigenvalue-based approach*. SIAM, 2014.

[121] W. Michiels, K. Engelborghs, P. Vansevenant, and D. Roose. Continuous pole placement for delay equations. *Automatica*, 38(5):747–761, 2002.

[122] W. Michiels, T. Vyhlídal, and P. Zítek. Control design for time-delay systems based on quasi-direct pole placement. *Journal of Process Control*, 20(3):337–343, 2010.

[123] D. Miljković. Review of active vibration control. *32nd Int. Conv. on Info. and Comm. Tech., Electronics and Microelectronics*, pages 103–108, 2009.

[124] M. Minea and I. Bădescu. Delay factors modelling for real-time traffic information systems. *WSEAS Transactions on Communications*, page 50, 2013.

[125] S. R. Moheimani. A survey of recent innovations in vibration damping and control using shunted piezoelectric transducers. *IEEE transactions on control systems technology*, 11(4):482–494, 2003.

[126] S. Mondié and J. Loiseau. Finite spectrum assignment for input delay systems. *IFAC Proceedings Volumes*, 34(23): 201–206, 2001.

[127] T. Mori, N. Fukuma, and M. Kuwahara. On an estimate of the decay rate for stable linear delay systems. *International Journal of Control*, 36(1):95–97, 1982.

[128] K. A. Moustafa, E. H. Gad, A. M. El-Moneer, and M. I. Ismail. Modelling and control of overhead cranes with flexible variable-length cable by finite element method. *Transactions of the Institute of Measurement and Control*, 27(1):1–20, 2005.

[129] N. Nadirian, H. Biglari, and M. A. Hamed. Lqg vibration control of sandwich beams with transversely flexible core equipped with piezoelectric patches. *Journal of Computational & Applied Research in Mechanical Engineering (JCARME)*, 7(1):85–97, 2017.

[130] N. Naik and P. Shembekar. Elastic behavior of woven fabric composites: I—lamina analysis. *Journal of composite materials*, 26(15):2196–2225, 1992.

[131] C. Natale, G. Aurilio, and G. De Maria. Modal analysis and vibration control of a fuselage aeronautical panel. *IFAC Proceedings Volumes*, 35(2):117–122, 2002.

[132] K.-D. Nguyen. Uniform continuity and delay robustness of an adaptive controller for lagrangian systems. *IMA Journal of Mathematical Control and Information*, 37(2):559–588, 2020.

[133] S.-I. Niculescu, W. Michiels, K. Gu, and C. T. Abdallah. Delay effects on output feedback control of dynamical systems. In *Complex time-delay systems*, pages 63–84. Springer, 2009.

[134] G. Niemeyer and J.-J. E. Slotine. Telemanipulation with time delays. *The International Journal of Robotics Research*, 23(9):873–890, 2004.

[135] K. Ogata et al. *Modern control engineering*, volume 5. Prentice hall Upper Saddle River, NJ, 2010.

[136] H. Padé. Sur la représentation approchée d'une fonction par des fractions rationnelles. In *Annales scientifiques de l'école Normale Supérieure*, volume 9, pages 3–93, 1892.

[137] A. Pandey, R. Schmid, T. Nguyen, Y. Yang, V. Sima, and A. L. Tits. Performance survey of robust pole placement methods. In *53rd IEEE Conference on Decision and Control*, pages 3186–3191. IEEE, 2014.

[138] Y. Peng, D. Vrancic, and R. Hanus. Anti-windup, bumpless, and conditioned transfer techniques for pid controllers. *IEEE Control systems magazine*, 16(4):48–57, 1996.

[139] M. Petyt. *Introduction to finite element vibration analysis*. Cambridge university press, 2010.

[140] G. Pólya and G. Szegö. *Problems and Theorems in Analysis: Series, integral calculus, theory of functions*. Springer, 1972.

[141] A. Preumont. *Vibration Control of Active Structures: An Introduction*, volume 179. Springer Science & Business Media, 2011.

[142] W. Qian, W. Yang, Y. Zhang, C. R. Bowen, and Y. Yang. Piezoelectric materials for controlling electro-chemical processes. *Nano-Micro Letters*, 12(1):1–39, 2020.

[143] G. Rance. *Commande H∞ paramétrique et application aux viseurs gyrostabilisés*. PhD thesis, Université Paris Saclay (COmUE), 2018.

[144] S. Rao and M. Sunar. Piezoelectricity and its use in disturbance sensing and control of flexible structures: A survey. 1994.

[145] M. Rehan, A. Ahmed, and N. Iqbal. Static and low order anti-windup synthesis for cascade control systems with actuator saturation: an application to temperature-based process control. *ISA transactions*, 49(3):293–301, 2010.

[146] E. I. Rivin. *Passive vibration isolation*. American Society of Mechanical, 2003.

[147] R. Roshin and K. Shihabudheen. Mathematical modeling of flexible beam-a comparative study. In *2013 International conference on control communication and computing (ICCC)*, pages 325–330. IEEE, 2013.

[148] D. Rosinová and I. Holič. Lmi approximation of pole-region for discrete-time linear dynamic systems. In *Proceedings of the 2014 15th International Carpathian Control Conference (ICCC)*, pages 497–502. IEEE, 2014.

[149] D. Rosinová and P. Valach. Switched system robust control: Pole-placement lmi based approach. In *Proceedings of the 2014 15th International Carpathian Control Conference (ICCC)*, pages 491–496. IEEE, 2014.

[150] L. Rouleau, J.-F. Deü, and A. Legay. A comparison of model reduction techniques based on modal projection for structures with frequency-dependent damping. *Mechanical Systems and Signal Processing*, 90:110–125, 2017.

[151] M. R. Roussel. The use of delay differential equations in chemical kinetics. *The journal of physical chemistry*, 100 (20):8323–8330, 1996.

[152] S. Ruan. Delay differential equations in single species dynamics. In *Delay differential equations and applications*, pages 477–517. Springer, 2006.

[153] M. Sabatini, P. Gasbarri, R. Monti, and G. B. Palmerini. Vibration control of a flexible space manipulator during on orbit operations. *Acta astronautica*, 73:109–121, 2012.

[154] J. Sandercock. A dynamic antivibration system. In *1st Intl Conf on Vibration Control in Optics and Metrology*, volume 732, pages 157–165. International Society for Optics and Photonics, 1987.

[155] C. Scherer, P. Gahinet, and M. Chilali. Multiobjective output-feedback control via lmi optimization. *IEEE Transactions on automatic control*, 42(7):896–911, 1997.

[156] J. Schur. Bemerkungen zur theorie der beschränkten bilinearformen mit unendlich vielen veränderlichen. *Journal für die reine und Angewandte Mathematik*, 140:1–28, 1911.

[157] N. Shanmugathasan and R. Johnston. Exploitation of time delays for improved process control. *International Journal of Control*, 48(3):1137–1152, 1988.

[158] N. Shao, J. Cheng, and W. Chen. The reproductive number r0 of covid-19 based on estimate of a statistical time delay dynamical system. *MedRxiv*, 2020.

[159] M. M. Shumafov. Stabilization of linear control systems and pole assignment problem: a survey. *Vestnik St. Petersburg University, Mathematics*, 52(4):349–367, 2019.

[160] A. Siami, H. R. Karimi, A. Cigada, and E. Zappa. Vibration protection of cultural heritage objects. In *Vibration Control and Actuation of Large-Scale Systems*, pages 107–156. Elsevier, 2020.

[161] W. Singhose. Command shaping for flexible systems: A review of the first 50 years. *International journal of precision engineering and manufacturing*, 10(4):153–168, 2009.

[162] M. Sorush, N. Mehranbod, and S. Alaie. Directionality in input-constrained systems: its definition and optimal compensation. In *Proceedings of the 1999 American Control Conference (Cat. No. 99CH36251)*, volume 3, pages 2002–2006. IEEE, 1999.

[163] A. Souza and L. Souza. Design of a controller for a rigid-flexible satellite using the h-infinity method considering the parametric uncertainty. *Mechanical Systems and Signal Processing*, 116:641–650, 2019.

[164] G. Stépán. *Retarded dynamical systems: stability and characteristic functions*. Longman Scientific & Technical, 1989.

[165] I. Suh and Z. Bien. Proportional minus delay controller. *IEEE Transactions on Automatic Control*, 24(2):370–372, 1979.

[166] G. Tallman and O. Smith. Analog study of dead-beat posicast control. *IRE Transactions on Automatic Control*, 4 (1):14–21, 1958.

[167] S. Tarbouriech, J. G. da Silva Jr, and F. Bender. Dynamic anti-windup synthesis for discrete-time linear systems subject to input saturation and l2 disturbances. *IFAC Proceedings Volumes*, 39(9):489–494, 2006.

[168] S. Tarbouriech, G. Garcia, J. M. G. da Silva Jr, and I. Queinnec. *Stability and stabilization of linear systems with saturating actuators*. Springer Science & Business Media, 2011.

[169] S. Thenozhi and W. Yu. Advances in modeling and vibration control of building structures. *Annual Reviews in Control*, 37(2):346–364, 2013.

[170] J.-P. Thiran. Recursive digital filters with maximally flat group delay. *IEEE Transactions on Circuit Theory*, 18(6): 659–664, 1971.

[171] S. Tliba. *Contrôle actif des vibrations dans des structures mécaniques minces instrumentées de transducteurs piézoélectriques*. Thèse de doctorat (in french), École Normale Supérieure de Cachan, Cachan (94), France, Décembre 2004.

[172] S. Tliba. Contrôle actif des vibrations dans des structures mécaniques minces instrumentées de transducteurs piézoélectriques. 2006.

[173] S. Tliba. Anti-windup control design for exponentially unstable lti systems with actuator saturation: the non-strictly proper case. 2011.

[174] S. Tliba. Control of a vibrating axisymmetric membrane using piezoelectric transducers. *IFAC Proceedings Volumes*, 44(1):7713–7718, 2011.

[175] S. Tliba. Vibration damping of a flexible beam with saturated control. In *2012 American Control Conference (ACC)*, pages 5330–5335. IEEE, 2012.

[176] S. Tliba and H. Abou-Kandil. $\mathcal{H}_\infty$ controller design for active vibration damping of a smart flexible structure using piezoelectric transducers. *IFAC Proceedings Volumes*, 36(11):49–54, 2003.

[177] S. Tliba, A. K. Hisham, and C. Prieur. Active vibration damping of a smart flexible structure using piezoelectric transducers: $\mathcal{H}_\infty$ design and experimental results. *IFAC Proceedings Volumes*, 38(1):760–765, 2005.

[178] S. Tliba, M. Varnier, and G. Duc. Anti-windup augmented controller for active vibration control in a smart flexible structure. In *18th Mediterranean Conference on Control and Automation, MED'10*, pages 17–22. IEEE, 2010.

[179] S. Tliba, I. Boussaada, F. Bedouhene, and S.-I. Niculescu. Active vibration control through quasi-polynomial based controller. *IFAC-PapersOnLine*, 52(18):49–54, 2019.

[180] S. Tliba, I. Boussaada, S.-I. Niculescu, and R. Falcon. Delayed control design of a vibrating thin membrane via a partial pole placement. In *ICSTCC 2020-24th International Conference on System Theory, Control and Computing*, pages 196–201, 2020.

[181] S. Tliba, I. Boussaada, S.-I. Niculescu, and R. Falcon Prado. An mid-based control of a vibrating axisymmetric membrane using piezoelectric transducers. In *ENOC 2021-10th European Nonlinear Dynamics Conference*, 2021.

[182] S. Tliba, I. Boussaada, S.-I. Niculescu, and R. F. Prado. Design of quasipolynomial-based controllers with dynamical parameters-application to active vibration damping. *IFAC-PapersOnLine*, 55(36):31–36, 2022.

[183] M. S. Troitsky. *Stiffened plates: bending, stability, and vibrations*. Elsevier Scientific Publishing Company, 1976.

[184] A. Ungar. Addition theorems for solutions to linear homogeneous constant coefficient ordinary differential equations. *aequationes mathematicae*, 26(1):104–112, 1983.

[185] C. Vasques and J. D. Rodrigues. Active vibration control of smart piezoelectric beams: comparison of classical and optimal feedback control strategies. *Computers & structures*, 84(22-23):1402–1414, 2006.

[186] M. Vaz and N. Rizzo. A finite element model for flexible pipe armor wire instability. *Marine Structures*, 24(3): 275–291, 2011.

[187] M. Vijaya. *Piezoelectric materials and devices: applications in engineering and medical sciences*. CRC press, 2012.

[188] T. Vyhlidal and P. Zítek. Mapping based algorithm for large-scale computation of quasi-polynomial zeros. *IEEE Transactions on Automatic Control*, 54(1):171–177, 2009.

[189] R. H. Walden. Analog-to-digital converter survey and analysis. *IEEE Journal on selected areas in communications*, 17(4):539–550, 1999.

[190] K. Walgama and J. Sternby. On the convergence properties of adaptive pole-placement controllers with antiwindup compensators. *IEEE transactions on automatic control*, 38(1):128–132, 1993.

[191] W. Wang, H. E. Stanley, and L. A. Braunstein. Effects of time-delays in the dynamics of social contagions. *New Journal of Physics*, 20(1):013034, 2018.

[192] A. Waszczuk-Młyńska and S. Radkowski. Circular membrane with a centrally-located opening-analytical model using parameterisation of the non-empty torus. *ZAMM-Journal of Applied Mathematics and Mechanics/Zeitschrift für Angewandte Mathematik und Mechanik*, 99(4):e201800167, 2019.

[193] H. WEI. Modeling and control of marine flexible systems. 2011.

[194] P. R. Wellin, R. J. Gaylord, and S. N. Kamin. *An introduction to programming with Mathematica®*. Cambridge University Press, 2005.

[195] F. Wu and B. Lu. Anti-windup control design for exponentially unstable lti systems with actuator saturation. *Systems & Control Letters*, 52(3-4):305–322, 2004.

[196] H. Wu and K. Fan. A survey of resonance frequency detection in robot joint systems. In *2020 IEEE International Conference on Mechatronics and Automation (ICMA)*, pages 496–501. IEEE, 2020.

[197] Y. Wu, W. Zhang, and X. Meng. Compensated positive position feedback for active control of flexible structures. In *International Conference on Engineering Vibration 2017*, 2017.

[198] B. YANG and C. MOTE. On time delay in noncolocated control of flexible mechanical systems. *Journal of dynamic systems, measurement, and control*, 114(3):409–415, 1992.

[199] J. Yang and G. Chen. Experimental study of adaptive fuzzy sliding mode control for vibration of a flexible rectangular plate. *Journal of Aerospace Engineering*, 28(4):04014098, 2015.

[200] L. Yang, Z. Wan, Y. Qu, and N. Wang. Vibration suppression of flexible systems by velocity feedback. In *2019 IEEE 9th Annual International Conference on CYBER Technology in Automation, Control, and Intelligent Systems (CYBER)*, pages 1014–1021. IEEE, 2019.

[201] T. Yang and Q. Cao. Time delay improves beneficial performance of a novel hybrid energy harvester. *Nonlinear Dynamics*, 96(2):1511–1530, 2019.

[202] M. Yousefi, Z. D. KoozeKanani, A. Rostami, J. Sobhi, and M. H. Zarifi. A flexible sample and hold circuit for data converter applications. In *2008 IEEE Region 8 International Conference on Computational Technologies in Electrical and Electronics Engineering*, pages 318–321. IEEE, 2008.

[203] Y. Yuwei, Z. Xinhua, Z. Minglu, M. Guangzhu, and W. Shoujun. Study of dynamic transient stability of a 2-link wheeled-suspended mobile flexible manipulator. In *2011 Third International Conference on Measuring Technology and Mechatronics Automation*, volume 3, pages 397–400. IEEE, 2011.

[204] L. Zaccarian and A. R. Teel. *Modern anti-windup synthesis: control augmentation for actuator saturation*, volume 38. Princeton University Press, 2011.

[205] G. Zames. Feedback and optimal sensitivity: Model reference transformations, multiplicative seminorms, and approximate inverses. *IEEE Transactions on automatic control*, 26(2):301–320, 1981.

[206] F. Zhang. *The Schur complement and its applications*, volume 4. Springer Science & Business Media, 2006.

[207] P. Zítek, J. Fišer, and T. Vyhlídal. Dimensional analysis approach to dominant three-pole placement in delayed pid control loops. *Journal of Process Control*, 23(8):1063–1074, 2013.